ELECTROCHEMICAL GENERATION OF HYDROGEN

A thesis submitted in partial fulfillment of the requirements for the degree of Doctor of Philosophy

By

Syed Khurram Raza

Wolfson Centre for Material Processing
Brunel University London
2014

Supervisor:

Professor Jack Silver

Executive Director

Wolfson Centre for Materials Processing

Brunel University

Uxbridge

UB8 3PH

United Kingdom

University:

Brunel University London

Uxbridge

UB8 3PH

United Kingdom

Rationale

The objective of the research reported in this thesis was to design an on-demand, high performance electrochemical hydrogen generator. The design also considered low cost manufacturing, maintenance, durability and hazard- free production of hydrogen. To produce hydrogen the following four areas were considered in this thesis in order to optimise the objective stated above:

Membrane	:	To find the best possible membrane to keep the generated hydrogen and oxygen separate. Membrane 1010 was found to be the best for this project.
Electrolyte	:	To make the best possible composition of electrolyte material to get a higher ion exchange and optimized performance. The best was found at 30% KOH concentration.
Electrode	:	To find the best electrode material to generate hydrogen. The stainless steel electrode satisfied the requirements relatively with the following attributes:- low cost, long life, low maintenance and high performance.
Device Design	:	To optimise the equipment design to facilitate facile break-up of water molecules into hydrogen and oxygen. The Cell-3 design was found to be the best prototype for hydrogen generation.

In this research an On-Demand Hydrogen Generation cell-3 achieved a 95% hydrogen generation coulombic efficiency, which is about a 49% efficiency improvement, as compared to the stainless steel electrode, and was 22% better than the nano-structured electrode used in the conventional hydrogen generator. The achievement, here, of such high efficiency becomes possible because of pure dedication and by analysing the problem from all directions (device chemistry, physics and the philosophy of the objective).

I started a computer science course during my first year of college and continued until I finished my college studies. Owing to generated interest in computers, I completed my BSc and MSc degrees in computer sciences, which provided me with skills in systems analysis, systems design and logical

design. Thereafter I became a Microsoft and CISCO-certified network administrator and Microsoft-certified network administrator. I also wrote books in computer science for high schools.

I started my business to provide network and software solutions after gaining some experience in teaching and in network administration employment.

The direction towards research was fuelled by my desire to do something for people. Analysis of poverty shows that fuel cost is one of the major reasons for increased living expenses proportionally. Therefore most poor people spend their budget on necessary car fuel, which creates an increase in CO emission; at the same time, they fail to maintain their cars through a lack of funds. Hence I started my research to design something for green fuel to protect the environment and reduce fuel costs.

Successful On-demand Hydrogen Generator required knowledge from three major areas: First was an analysis and design skill to improve efficiency from the design aspect, which I fulfilled from knowledge of computer sciences. The hydrogen generator was designed in CAD software for pre-construction analysis. Second was to improve the surface area to get improvement in electrode performance; hence I took an MSc in nanomaterial and nanotechnology to get these skills. Third was the hydrogen control system that allows controlled production of hydrogen, a skill I obtained from my MSc course in system on a chip. Thus I started my PhD with the best possible skills required for a successful project.

Acknowledgments

I would never have been able to finish my research without the guidance of my department members, help from friends, and support from my family and wife.

I would like to express my deepest gratitude to my supervisor, Professor Jack Silver, for his excellent guidance, caring, patience, and providing me with an excellent atmosphere for doing research. I would like to thank Dr. Peter Allan, introduced me to the area of material manufacturing and behaviour of materials. I would like to thank Drs. Paul Harris and Paul Marsh for their truly grate support in electro chemistry techniques and providing materials and material safety information and helpful advice in scientific writing. I would like to thank Mrs Nita Verma for helping me out with my SEM sessions and for teaching me SEM techniques. I would like to thank Dr Siva Surendrakumar, who as a good chemist and friend was always willing to help and give his best advice.

Many thanks to Mr. Max Evans, Mr. Steve Ferris, Mr. Abdul Ghani and other workers in the laboratory for helping me to find and arrange experimental needs. My research would not have been possible without their helps.

Last but not least, I would also like too many thank my parents, three elder sisters, and four elder brothers for their unconditional support, both financially and emotionally throughout my degree. Finally, I would like to thank my wife, Komal Raza. She was always there cheering me up and stood by me through the good times and bad.

Abstract

Global warming and the energy crisis are two of the greatest challenges on which mankind is currently focused. This has forced governments and other organisations to think how to protect the environment and how to reduce fuel costs. A variety of new and exciting technologies are being investigated to address the energy problem.

Alternative energy sources such as solar power, fuel cells, wind power and tidal waves are active areas of commercial and scientific pursuit.

A major area of current research is moving towards the hydrogen economy and hydrogen based energy systems. Hydrogen can be produced in many ways, most commonly by steam reforming of hydrocarbon (70% to 85% thermal efficiency) but the downside is that it releases carbon mono oxide (CO)), compared with commercial PEM electrolysers where performance has been reported to be 56 -73% at normal temperature pressure(NTP) with zero carbon emission. Electrochemical production of hydrogen has several advantages: (i) It gives pure hydrogen. (ii) It allows portability (e.g. Solar energy could be used to power the electrochemical cell). (iii) It can be produced on demand.

The generation of Hydrogen via electrolysis has been the subject of many studies over the last two hundred years. However, there is still room for further work to improve both the efficiency of the process and methods of storage of the gas. The cleanest method at present is to produce hydrogen by electrolysis, and the main focus of this research is to design and develop such a green energy fuel cell for on-demand application. The aim of the work presented in this thesis was to further investigate the electrolysis method for hydrogen production. .

An Electrochemical fuel cell contains a minimum of two electrodes: the positively charged electrode called the anode where oxygen bubble will form, and the second negatively charged electrode called the cathode, where hydrogen bubbles will form during a chemical reaction caused by applying electrical current between these electrode.

The project was initiated with the objective of finding a low cost solution for on-demand hydrogen generation. To establish a starting point, the first cell (cell-1) design was based on the work of Stephen Barrie Chambers (see chapter 3) to check the performance levels.

The fabrication of the cell-1 design resulted in a mixture of hydrogen and oxygen in the same chamber, which means the cell-1 design, has a possible fire and explosion hazard. The device also has the drawback of lower performance of hydrogen production; columbic efficiency is between 40% to 46% at 1 amp to 3 amp current in 30% KOH alkaline solution. However, the advantage of reproducing Stephen's innovation is that it allowed a quick and deep understanding of hydrogen generation.

This thesis presents recent work on the fabrication of low cost electrolysis cells containing continuous flow alkaline (KOH, up to 30%) electrolyte using low cost electrodes (stainless steel 316) and membranes based on ultrahigh molecular weight polyethylene (UHMW PE) to produce hydrogen without the hazard of fire and explosion.

In this research an On-Demand Hydrogen Generation cell-3 achieved a 95% hydrogen generation coulombic efficiency, which is about 49% efficiency improvement as compared to the stainless steel electrode, and was 22% better than the nano structured electrode. The typical cell voltage is 2.5 V at current flow ranging from 30

to 120 mA cm-2 in 30% KOH electrolyte. The achievement here of such high efficiencies paves the way for more research in the areas of space management, electrode surface structure and flow control (based on the application requirement). This invention can be used for aeronautic, marine and automotive application as well as in many other areas.

Table of Contents

List of figures

List of Tables

Chapter 1

HISTORY OF HYDROGEN GENERATION

1) State of the Art

'Global Warming' and the 'Energy Crisis' are both established as two of the greatest challenges that mankind has to focus on. These problems have forced government organisations and the individual, to think about how to protect the environment and reduce fuel costs. This has resulted in the investigation of the potential of many new and exciting technologies to address these problems as well as in this thesis on-demand hydrogen production can contribute to protect environment and reduces fuel cost.

Liquid petroleum gas (LPG) vehicles, compressed natural gas (CNG) vehicles, solar powered electric vehicles, electric vehicles, hydrogen powered vehicles and hybrids vehicles potentially all can contribute to reduce the problem of carbon emission and reduced fuel cost. However, every technology has its drawbacks, for instance it may not be suitable in every environment and so it is unlikely that any one technology may fulfil the total energy requirements at present. Nonetheless attractive and promising solutions have been found in the hybrid fuel systems for automotive.

There is much current research on the hydrogen economy, which has lead research towards hydrogen energy systems. This chapter will explain the comparison of the technologies along with the history of the research on hydrogen as a fuel.

1.1) Alternative fuel

An alternative fuelled vehicle is one that runs on a fuel other than petrol or diesel fuel (traditional fuel) such an example would be liquid petroleum gas (LPG) or compressed natural gas (CNG). The term also refers to any technology for powering an engine that does not involve solely petroleum (e.g. electric car, hybrid electric vehicles, solar powered). Because of a combination of factors, such as environmental concerns, high oil prices and the potential for such prices to continue rising, development of cleaner alternative fuels and advanced power systems for vehicles has become a high priority for many governments and vehicle manufacturers around the world.

1.1.1) LPG and CNG

The best established solution for addressing the carbon emission and fuel cost problem is found and reported as alternative fuel vehicles, where liquid petroleum gas (LPG) or compressed natural gas (CNG) is introduced to the internal combustion engine rather than using petrol or diesel as a fuel. Due to the combustion properties of such gases carbon emission is reduced and these fuels are currently cheaper compared to petrol and diesel, resulting in both reduced cost of miles per gallon (MPG) and a lesser environmental pollution [1] [2] [3]. LPG and CNG technology is currently a kit technology as displayed in figure 1.1 [4] [5]. Due to the format of kit technology it can be back installed in any conventional vehicle, hence people don't need to buy a

new car to reduce their fuel cost and reduce carbon emission. This is the best advantage of this technology compared to present hybrid technology.

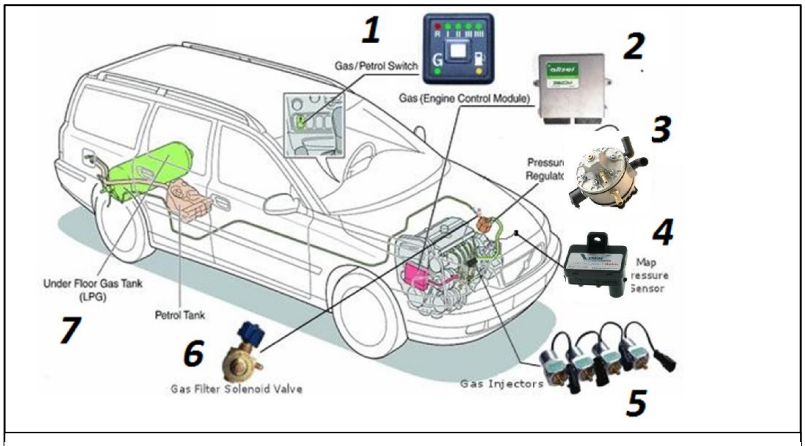

Figure 1.1: Main parts of LPG and CNG kit. 1-Gas/Petrol switch, 2-Electronic Control Module, 3-Gas pressure regulator with filter unit, 4-Map-sensor, 5-Injectors, 6-Filter solenoid valve, 7-GAS storage tank.

Figure 1.1 illustrates the LPG and CNG kit installation location and parts and figure 1.2 illustrate the connection schematic of the different parts. To supply petrol to the system (pressure in such a system is about 30-60psi) a tank is necessary (figure 1.2) to store it. For LPG/CNG an additional tank is needed to store the gas as an alternative fuel. The LPG and CNG pressure is significantly higher than that of petrol. The LPG pressure is more than 300psi and the CNG pressure is around 100 to 150psi that is beyond the limit of injectors in conventional internal combustion engine [6]. Therefore a pressure regulator is required to limit the gas based on each individual system requirement. A control module is programed to control and maintain the system requirements. A gas/petrol switch is provided for optional use for manual selection between petrol and gas. Although, when the engine starts the switching between fuel types can be automated by the control module and based on its instruction the solenoid valve can disconnect the petrol supply

(represented by the red line in figure 1.2) and open the gas supply (represent by the green line in figure 1.2) to the injectors. The injectors spray the fuel into the internal combustion chamber which converts the resulting released energy into the mechanical power that drives the vehicle. [7] [8]

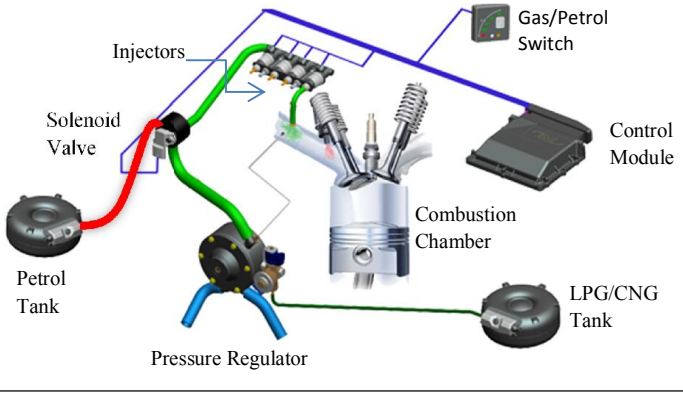

Figure 1.2: Connection schematic of LPG and CNG kit tank.

LPG and CNG gases are environment friendly and well established alternative fuels, however, their drawback is that they may not be commonly available compared to petrol. In addition to their limited global reservoir they also require an additional fuel tank that may cause a space problem in the vehicle. The need to understand the LPG/CNG system in the car in this thesis is to aid the design of a system that reduces the need for an additional fuel tank.

1.1.2) Electric vehicles

An electric vehicle is one that is propelled by one or more electric motors, using electrical energy stored in batteries or another energy storage device, charged by a charging station or a charging bay at home or office. Electric motors give electric cars instant torque, creating strong and smooth acceleration. Electric vehicles are noiseless compared to traditional petrol and

do not pollute the air with carbon dioxide. However they require filling stations (not commonly available) and a huge on board battery bank (figure 1.3). They are thus heavy and the batteries require a large space in the car. In addition they are also expensive to run and are currently more expensive cars for the majority of people. [9] [10]

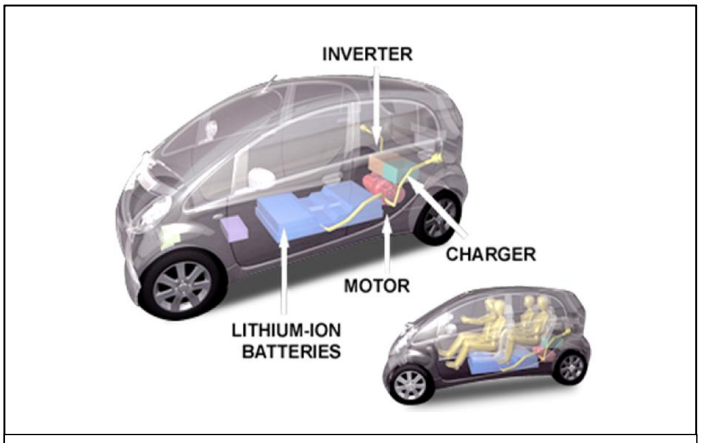

Figure 1.3: Electric car technology structure.

Electric powered vehicle technologies are currently making a major contribution to vehicle research and development. Present research on vehicles designed for the future is aimed at electric vehicles due to their use of green fuel and noise-less drive. However to overcome the problem related to the need for a battery bank, design of future vehicles is aimed at hybrid vehicles. These use hydrogen introduced as an alternative fuel, in combination with a proton exchange membrane (PEM) fuel cell to produce electricity to drive the electric cars (see details in section 1.6). The work reported in this thesis is in keeping with similar world research trends for vehicles to reduces pollution and fuel cost. Design of an on-demand hydrogen generator may contribute in reducing pollution and fuel cost (explained in detail later in this chapter). [11] [12]

1.2) History of Hydrogen

Hydrogen is a combination of two Greek words, hydro and genes. Hydro means water and genes mean forming [13]. Hydrogen gas has attributes that make it attractive and special as a sustainable energy source. It is a highly flammable diatomic gas that burns with air. Pure hydrogen burning with pure oxygen emits ultraviolet light, hardly visible to the naked eye. A hydrogen-oxygen mixture can be ignited by heat, spark, and sunlight. Pradyot Patnaik reported, that the temperature of auto-ignition is 500°C (932°F) [13].

The first time that hydrogen was artificially produced was between 1493–1541 by Theophrastus Von Hohenheim (also known as Paracelsus, Figure 1.4), he mixed strong acids and metals [14], although he was not certain about what he found. The gas produced by the acid-metal reaction became famous as "flammable air". Research in 1671 by Robert Boyle (Figure 1.5) [15] [16] facilitated more understanding. He successfully described the reaction between acid and metal. He is more famous for Boyle's law which relates gas pressure to gas temperature. [17].

Figure 1.4: Paracelsus discovered hydrogen partially.
Portrait of Paracelsus, by Quentin Massys, From *Public Domain*

Figure 1.5: Robert Boyle Founder of Boyle Law [15] [16]
Portrait of Robert Boyle, by Johann Kerseboom, c.1689. From Public Domain

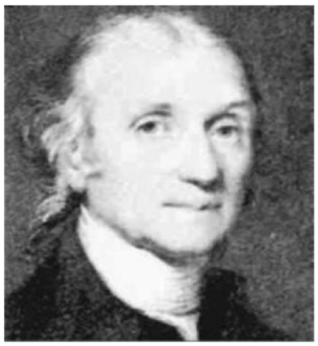

Figure 1.6: Henry Cavendish Discovered Hydrogen and noted as "inflammable air" [18]
From *Public Domain*

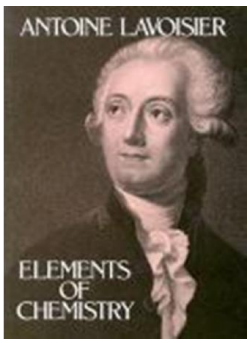

Figure 1.7: Antoine Lavoisier Introduced Hydrogen as an element. [19]
Book title

In 1766, Henry Cavendish (Figure 1.6) [16] [18], a British scientist, introduced his discovery of hydrogen as "inflammable air". Also, in 1781 his further exploration resulted in the realisation that the gas produced water after burning. In 1783 Antoine Lavoisier (Figure 1.7) [19] carefully revised Cavendish's work, and acknowledged his finding that 'gas produces water after burning', and thus he introduced hydrogen as an element [13] [19]. His experiment on combustion disproved the Phlogiston Theory that claims "materials released a substance called phlogiston when they burned" [13] [19]. Thereafter, hydrogen production started being exploited in areas such as air balloons, air ships, etc.

1.3) Hydrogen Production

Hydrogen can be produced in many ways, most commonly from hydrocarbons. Such methods give good yields and are 80% efficient, but simultaneous released carbon dioxide (CO_2) must be separated and disposed of carefully. Aluminium can also be used to produce H_2 by reaction with a base, as shown in equation 1.2.1. [20] [21]

Equation 1.2.1: $\mathbf{2\ Al + 6\ H_2O + 2\ OH^- \rightarrow 2\ Al(OH)^{4-} + 3\ H_2}$

Another method of producing hydrogen on a small scale is by electrolysis of water. This method is a clean method of producing hydrogen, by using an electrical current on water (H_2O) molecules, to generate hydrogen (H_2) and oxygen (O) gases as shown in equation 1.2.2.

Equation 1.2.2: $\mathbf{2H_2O(aq) \rightarrow 2H_2(g) + O_2(g)}$

Electrical energy can be taken from renewable resources, such as photovoltaic, hydropower, wind turbine, wave power etc. Therefore this method has potential for bulk hydrogen production. This can also be used to produce electricity for electric cars, portable chargers, devices, laptops etc.
Commercially the most popular method uses hydrocarbon for the bulk production of hydrogen. The hydrogen is produced by steam reformatting natural gas at high temperatures (around 700-1100°C), when water vapour reacts with methane to yield carbon monoxide and H_2. Equation 1.2.3 illustrates the reaction. [22]

Equation 1.2.3: $\mathbf{CH_4 + H_2O \rightarrow CO + 3H_2}$

1.4) Current uses of Hydrogen

The petroleum and the chemical industries are the biggest consumers of hydrogen. The petroleum industry uses it to modify the property (grading) of fossil fuels, and the chemical industry (for example) in the production of ammonia. A petrochemical plant also consumes large amounts of hydrogen for hydrodealkylation, hydrocracking, and hydrodesulfurization [23].

Apart from its use in chemistry as a reactant, hydrogen is also widely used in physics, engineering and design. It is employed in welding and cutting tools. These tools utilise hydrogen for welding by combining it with an oxy-fuel, the resulting high temperature can melt metals very quickly allowing the use of the cutting and welding torch. On the other hand, H_2 can also be used as a coolant in different applications because H_2 has the highest thermal conductivity of any gas. Another famous property of H_2 is its mass, which is less than air. That furthers its utilization as a lifting gas in airships, balloons and also as a tracer gas for leakage detection. [23] [24].

The unique properties of hydrogen gas facilitate its technological importance. Its multidimensional properties have led to its use in a wide range of industries, such as telecommunications, automotive, aerospace, power generation, and the chemical industry [24].

1.5) Hydrogen Vehicles

Hydrogen vehicles are currently an important research topic for environment protection organisations, and alternative energy generation organisations. In the past few years, the aerospace and automobile industries have used vehicles which carry on-board hydrogen fuel. Hydrogen powered vehicles convert energy generated from hydrogen into mechanical energy (torque). This mechanical energy can be produced by combustion, or from electrochemical conversion in a fuel cell.

In a fuel cell: hydrogen and oxygen (air) are injected into the fuel cell, which produces current from an electrochemical reaction. This current powers an electric traction motor to run the vehicles (for example, aeroplanes, buses, motorbikes, rockets, bicycles, wheel chairs, ships, trains, space shuttle launchers; all can be powered (at least in part) by fuel cells. Hydrogen provides maximum energy when combined with pure oxygen. A hydrogen powered vehicle: Buckeye Bullet 2 designed by Ohio State University, recently recorded the fastest speed yet achieved on land is 286.476 mph. Such achievements bring more confidence to the automobile manufacturers to invent hydrogen powered cars. The Ballard fuel cell is one example of the famous proton exchange membrane fuel cells (PEM). [25] [26]

1.6) PEM fuel cell

A PEM cell is made of a thin catalyst coated membrane between two gas diffusion electrodes. Hydrogen is supplied from one side of the membrane (represented by the orange bubble in figure 1.8) and oxygen (represented by the blue bubble in figure 1.8) from the other side. On the hydrogen side electrode (anode), protons defuse through the membrane and the electrons travels to the other side of the membrane through the other electrode

(cathode), and produces current. The cathode side of the electrode combines the protons with the electrons in a reaction with oxygen. Water and heat are produced as shown in the Ballard fuel cell schematic Figure 1.8. [27] [28].

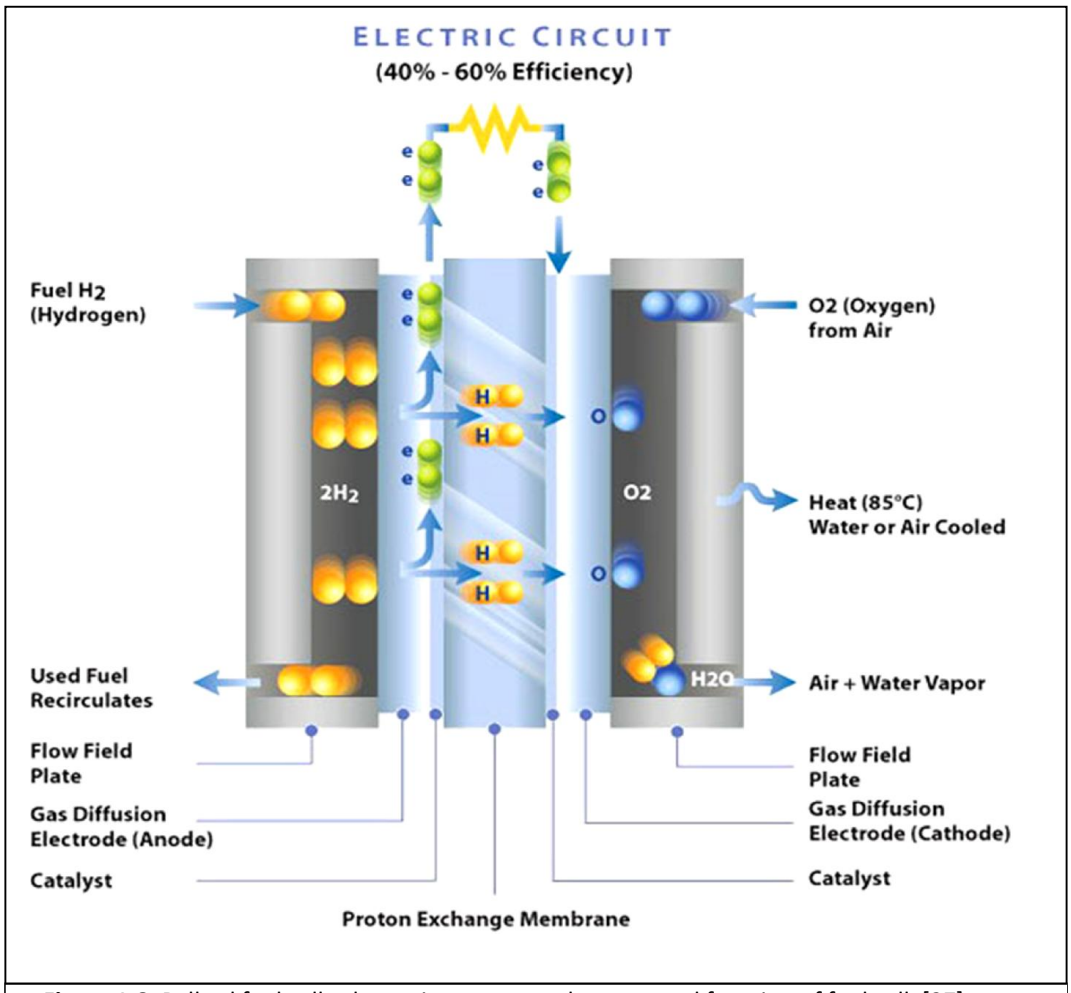

Figure 1.8: Ballard fuel cell-schematic, represent the parts and function of fuel cell. [27]

1.7) Commercial Implementation

Many automobile manufacturers are currently struggling to make it feasible to establish hydrogen powered vehicle manufacturing as a viable alternative to petroleum powered cars, Some of the potential manufacturers have already demonstrated their prototypes at the 2012 'World Hydrogen Energy Conference': Daimler AG, KIA, Honda, Nissan, and General Motors etc. [29]

Figure 1.9:
Sequel, a fuel cell-powered vehicle from General Motors
From Google image *Public Domain*

General Motors (Figure 1.9) introduced their Opel technology fuel-cell powered car in the 2005 North American Auto Show. Ford motor company (Figure 1.10) demonstrated some hydrogen cars in the past few years but then dropped their plans in this area. The company stated "The next major step in Ford's plan is to increase over time the volume of electrified vehicles" [30]. Similarly in 2009, another pull out was announced by French Renault-Nissan [31].

Figure 1.10:
Edge hydrogen-electric plug-in hybrid concept from Ford
From Google image *Public Domain*

Some of the biggest challenges for hydrogen fuel cell vehicles are the fuelling station and their storage facilities. A complete change of old framework to new technology, a cheap form of hydrogen production, and using an environment friendly method is required. Hydrogen cost is calculated as per

the application because it involves several cost rising stages as shown in the Figure 1.11. flow diagram.

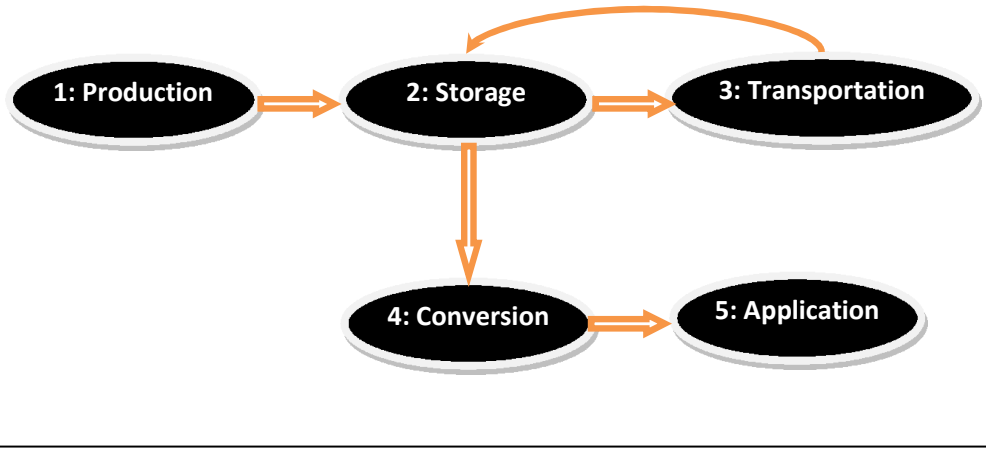

Figure 1.11: Flow diagram: Infrastructure distribution for analysis of hydrogen cost.

Commercially, the hydrogen cost increases on storage, especially storage in compressed hydrogen form. Another boost in cost is delivery and storage to the fuel station, and redistribution to the appliances.

The cost of hydrogen is higher in the form of electrical energy (for fuel cell products such as hydrogen fuel cell cars), because it requires conversion of hydrogen energy into electric energy. F. Gutie´rrez-Martı´n et. al. reported analysis of the industrial cost of "Petrol-Diesel as a reference (with oil at $40 bbl), the equivalent hydrogen prices are $0.35/Lge (in term of heating values) or approx $1.8/kg (well-to-wheel)" [32]

There are two main methods to run a car using renewable energy as shown in Figure 1.12 flow diagram. [33] The first is to run the car from a battery; this

is then known as an electric vehicle. This requires battery charging which then drives the electric motor. The grid to motor efficiency is about 86%, which is a truly high performance, and the biggest advantage is zero carbon emission, however it does have the drawback of battery life; long term energy storage and moreover, is an expensive solution which makes it not feasible for our world at present.

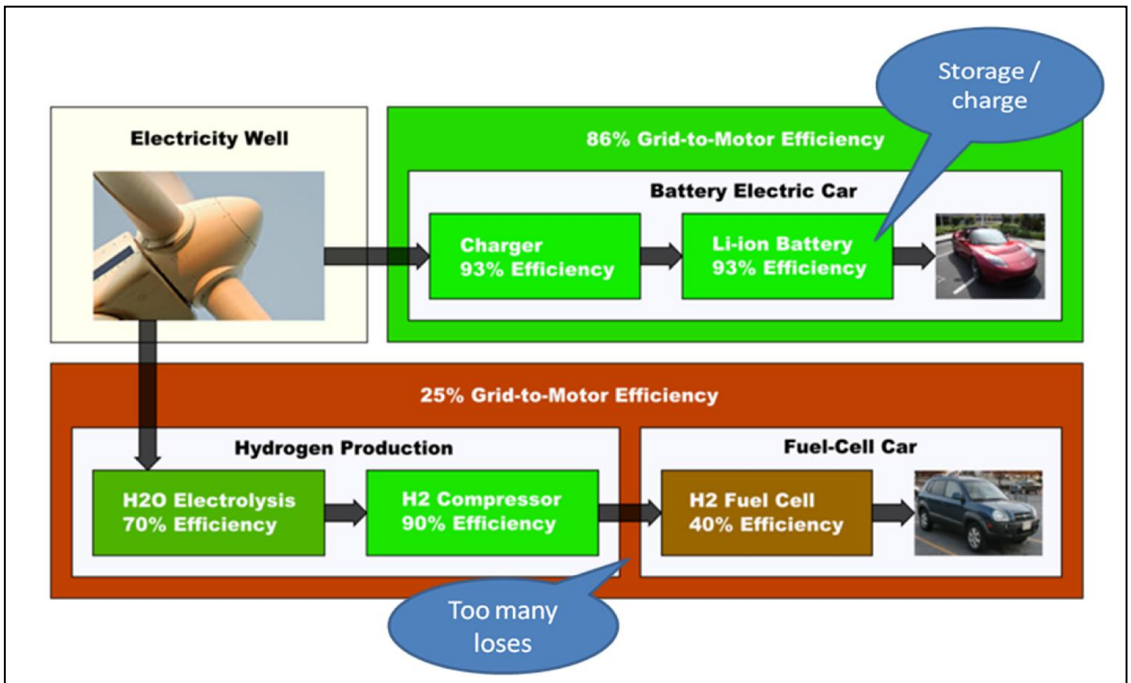

Figure 1.12: Flow diagram : [33] Two alternative method for green energy performances

The second is to run a car using hydrogen. Here, the infrastructure of the hydrogen car is influenced by the electric vehicle, however the difference is the energy for the electric motor is provided by a PEM fuel cell. The major advantage of this approach eliminates the problems of battery charging and long term energy storage. However, other problems are faced such as:-

a) Grid to motor efficiency is very low, only 25%;

b) It requires extra space for the gas storage cylinder in the vehicle; and
c) It requires expensive infrastructure,

These combined will cause slow technology implementation. Currently the drawbacks of both technologies outweigh their advantages.

The question that this thesis seeks to address is:- Why is the fuel economy is important? To begin to answer this I have developed the fuel dependency cycle as shown in Figure 1.13 flow diagram [34].

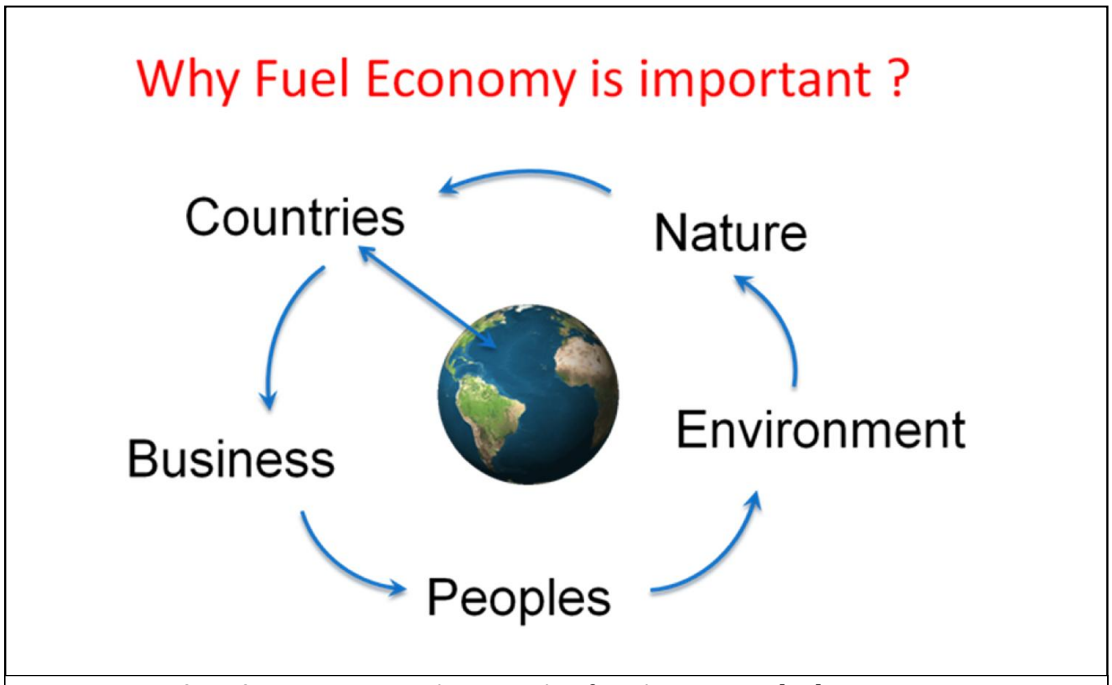

Figure 1.13: Flow diagram: Dependency Cycle of Fuel Economy. [34]

The Dependency cycle illustrates how the entire world depends on the fuel polices of countries, and future polices are needed to arrange good business structures to provide a reasonable life for the population, by being responsible for generating a better environment to restore a natural balance

with nature. Green energy would seem to be the best solution for us and hydrogen has wide applications in developing a green energy based economy. The electrolysis process, though an efficient method to produce hydrogen [32], requires a source of electricity. However, leading the concept of 'Green Energy' electricity resource can be achieved from hydro power, solar power, and wind turbine power, which, once their infrastructure is paid for, can reduce the cost of hydrogen generation.

The focus of this thesis is to design and develop on demand electrochemical production of hydrogen for present environment and energy barriers. As explained above the alternative vehicle, kit technology concept influenced one of the design objectives in this thesis which is aimed at producing a hydrogen generator for conventional vehicles (internal combustion engine) to facilitate their use by the majority people currently using conventional vehicles (detailed explanation is in chapter 3 innovation). This of course is because of the drive arising from electric vehicles influencing both the clean environment and use of an alternative source of energy. In the next chapter the state of the art of the electrochemical generation of hydrogen is explained and the necessary calculations needed to obtain hydrogen production efficiency are presented.

Chapter 2

ELECTROCHEMICAL GENERATION OF HYDROGEN

2) Introduction

Hydrogen is the chosen clean fuel of the future based on its non-polluting nature and recyclability. The "hydrogen production to consumption" cycle is the biggest advantage of hydrogen; water splitting produces hydrogen and oxygen and combustion of H_2 in air produces water again. Furthermore the source of hydrogen is water, which is abundant and cheap and the hydrogen cycle regenerates the water. Moreover H_2 is the smallest gas among all gases and possesses a very high energy storage capacity (119000 $J.g^{-1}$ H_2 per gram), whereas the energy storage capacity of oil (40000 $J.g^{-1}$) is three times lower [35] [36] [37].

Hydrogen can be produced or extracted from different sources as illustrated in figure 2.1, these include fossil fuel which is about 60% to 85% efficient but not an environment friendly process, whereas the biomass efficiency is about 35% to 50% and electrolysis efficiency is about 56% to 73% [38] [39]. The cleanest method with the highest efficiency for hydrogen production is electrolysis. Hence the focus of the research in this thesis is to improve the efficiency of hydrogen production.

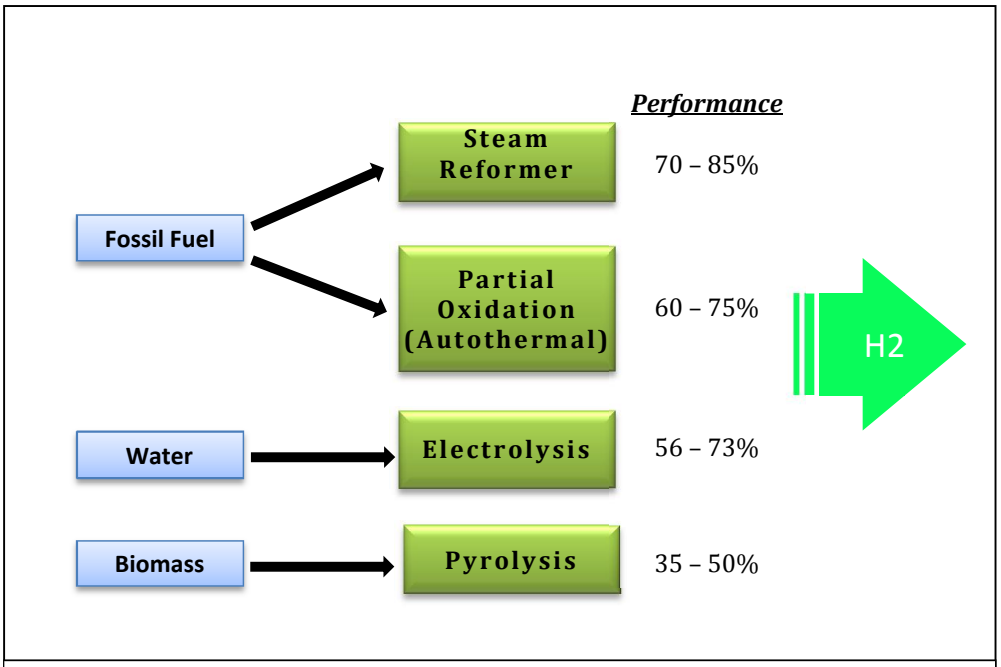

Figure 2.1: Hydrogen generation performance compression from different source.

2.1) Electrolysis

Electrochemistry can be defined as that branch of chemistry that studies chemical processes that occur in a solution at the interface between an electron conductor, (which can be a metal or a semiconductor electrode) and an ionic conductor (referred to as an electrolyte) as illustrated in Figure 2.2. Such chemical processes involve electron transfer between the electrolyte or other species in the electrolyte and the electrode.

Electrical conductors can be solids, liquids or gases (under certain circumstances. High-conductivity metals are used in the construction of cables, in transformer windings, and in electrodes. They have potential

application in semiconductor devices for high power oscillation and in hydrogen fuel cells (electrochemical cells) [40] [41].

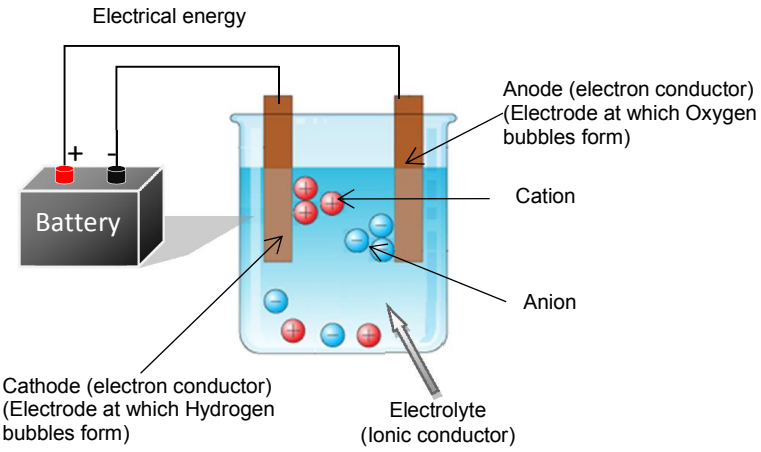

Figure 2.2: Electrochemistry Process for electrolysis.

Liquid conductors can be ionic conductor or electrolytes. As a rule, with the exception of caesium, gallium, and mercury metals they have a high melting point. Caesium, gallium, and mercury are the only metal liquid conductors at Standard temperature and pressure. [42]

The mechanism of current flow in solid or liquid metals is by the motion of free electrons. Such a conductors' property of conductivity capacity is known as its 'electrical conductivity' and materials can be grouped by their electronic conducing properties. Aqueous solutions of acid, alkalis and salts are called electrolytes. Transportation of ions in such conductors gives rise to conduction. When such conducting solutions are activated by an external electric circuit, the composition of the electrolyte slowly but surely changes. [43] [44]

The passage of electrons through a solution has the capacity to reduce species present in the solution. An electrochemical equivalent of an ion is the mass liberated by the passage of unit quantity of electricity. Equation 2.0 explains electrolysis, where **t** represents the time taken for current **i** to flow and deposits a metal, whose electrochemical equivalent is **e**. The mass **M** deposited is,

Equation 2.0 [18] **M = e i t**

The value of **e** is usually given for mass in grams, current **i** in amperes and time **t** in seconds.

Electrolytic dissociation or ionization theory – this describes the dissolving of an acid, a base, or a salt, in water or another dissociating solvent, such that its molecules become broken down either fully or partly into ions with either a positive charge called cations; and an equal number of negative charge called anions.

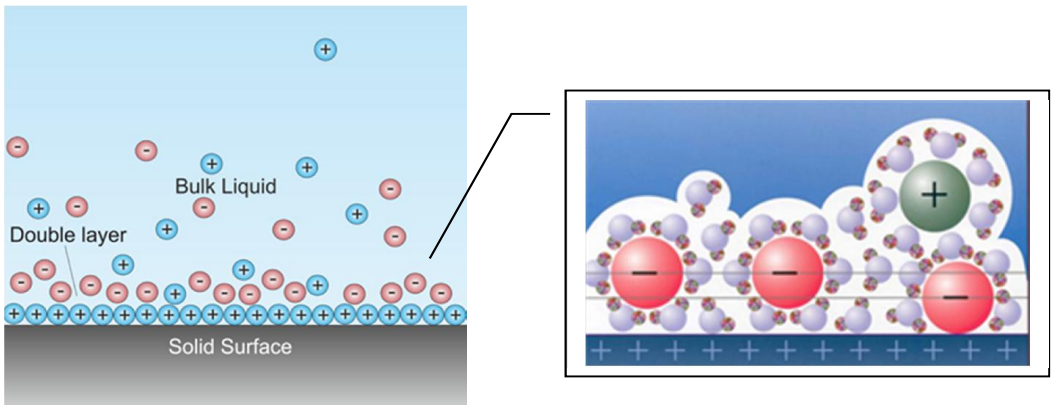

Figure 2.3: Schematic of double layer in a liquid at contact with a negatively-charged solid. The right side of the picture is the enlargement of double layer. [18]

Electrolytic solution tension theory (or the Helmholtz double layer theory) as illustrated in Figure 2.3. This describes the effect produced when any substance which is able to exist in solution as ions, such as metal, is placed in a dissociating solvent such as water; and there is a transfer of ions from the metal into the solution, leaving an equivalent amount of oppositely charged ions on the metal. This then produces a difference in potential between the metal and the solvent.

Electrolysis can be used to separate hydrogen and oxygen from water molecules. Hydrogen **H** is produced at the negatively e^- charged electrode, via a reduction reaction (reduction involves the addition of electrons) according to the reaction in equation 2.1 [28].

Equation 2.1 **(Cathode)** $2\,H^+ + 2e^- \rightarrow H_2$

The oxidation reaction (oxidation involves the subtraction of electrons taking place on the positively charged electrode (Anode), thus oxygen **O** gas is generated and electrons pass to the cathode to complete the circuit and reaction, as in equation 2.2 [28].

Equation 2.2 **(Anode)** $H_2O \rightarrow 2\,H^+ + 2e^- + \frac{1}{2}\,O_2$

Thus, from the electrolysis of water twice the volume of hydrogen molecules are expected as oxygen molecules.

2.2) Thermodynamics of the electrolysis process

Thermodynamics is a very important area in science. Thermodynamic is a Greek word: thermo (heat) and dynamic (power), which literally means power from heat. This was the early concept but we now understand that every area of nature can be understood by its thermodynamic properties such as surface tension, pressure, temperature, volume, concentration, and viscosity.

In 1849 the term thermodynamics was used in publication by Lord Kelvin for the first time, and in 1859 the first thermodynamics textbook was written by Glasgow University professor William Rankine. The first law of thermodynamics is the conservation of energy. Energy cannot be destroyed nor created, it can only change form and the total amount of energy remains the same. Therefore understanding thermodynamics is very important for hydrogen production by electrolysis, as it will help to improve the performance of the cell. [45] [46]

First law of thermodynamics basically represents the expression of conservation of energy. In physics it is stated as the total change in internal energy of a system **ΔU** is equal to the heat added to the system **Q** minus work done by the system **W** (see equation 2.3). [9-11]

Equation 2.3 $\Delta U = Q - W$

Equation 2.4 $\Delta U = Q + W$

Equation 2.4 is another form of the first law equation as normally represented in chemistry. The difference between equation 2.3 and 2.4 is that equation 2.3 is used by physics and tells us about work done *by* the system, whereas

equation 2.4 is chemistry and tells us about work done *on* the system. Typically heat is represented as $\Delta\mathbf{Q}$ (change in heat) and work is represented as $\Delta\mathbf{W}$ (change in work) but it makes more sense to represent both without Δ because heat added or work is done by or to the system, so change will happen in the system referred to as internal energy $\Delta\mathbf{U}$. Therefore Δ is not required with **Q** (heat add to system) and **W** (work done by system).

The Second law of thermodynamic explains the equilibrium of energy with the environment. For example a cup of hot water on a table cools down to the atmospheric temperature, but a cup of cold water cannot get hot by itself (above atmospheric temperature). This proves energy only travels from a higher to lower energy region. The second law not only considers the quantity of energy it also considers the quality (purity, limpidness) of the energy. [47] The electrolysis of water to form the diatomic molecules of hydrogen (H_2) and oxygen (O_2), is a good example to use in order to understand the application of the four thermodynamic potentials. The concept of thermodynamic potential was introduced by Pierre Duhem in 1886. The four common thermodynamic potentials are shown in table 2.1.

Table 2.1: Thermodynamic potentials

Name	Symbol	Formula	Description
Internal energy	U		Energy need to create system
Helmholtz free energy	A	U – TS	TS is energy you get from system
Enthalpy	H	U + PV	PV is the work required to produce gas
Gibbs free energy	G	U+PV-TS	Total energy needed

Internal energy **U** is a thermodynamic potential and is derived from the first law of thermodynamics, it helps to identify the total energy in the system.

Helmholtz free energy denoted by **A** (sometime represented by **F** in physics) is the thermodynamic potential, it provides work information obtained from a closed system. **T** is the absolute temperature and **S** is final entropy, therefore **TS** is an energy you get from the system as illustrated in Figure 2.4 [48].

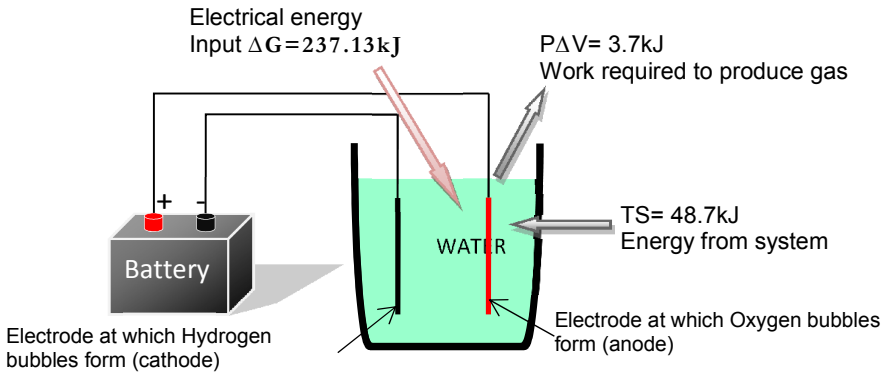

Figure 2.4: Electrolysis process illustrates energy requirement at different stages.

Enthalpy **H** is also a valid state variable because it is the combination of other state variables as shown in equation 2.5, where **U** is internal energy, **P** is the pressure change and **V** is the change in volume in equation 2.5. The red dot in Figure 2.5 indicates an initial state of internal energy, pressure and volume. Green lines show the net work done by system and the loop shows the complete reverse process of system, which explains no matter which path you chose or get it will come back to the initial state. Therefore **U, P** and **V** are valid state variables and because **H** is a sum of valid state variables then that makes it also a valid state variable and it is known as the enthalpy [49] [50].

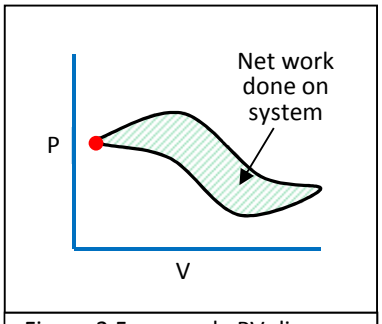

Figure 2.5: example PV diagram

Note: Energy the exchange process for one mole of water is 285.13kJ [50].

Equation 2.5 $\Delta H = U + PV$

Gibbs free energy is another thermodynamic potential, which is denoted by **G.** Its use enables the total energy required for a system to be found as illustrated in equation 2.6. For the electrolysis of water, 237.13kJ [50] of electrical power is required.

Equation 2.6 $\Delta G = U + PV - TS$

The above mentioned thermodynamic **G** potential allows us to know the behaviour of a system and identify the key area for its control, therefore using this approach; low cost hydrogen production can be achieved.

2.3) Electrochemical hydrogen generation cell

There are two kinds of electrochemical cell used to generate hydrogen. One is a conventional cell that does not contain a membrane to separate the gases and the other contains a membrane.

2.3.1) Non-membrane cell

A conventional electrochemical cell for the generation of hydrogen is presented in figure 2.6. The distance between the electrodes means that ion exchange takes place over a longer distance then in a PEM electrolyser

(polymer electrolyte membrane electrolyser) cell hence the efficiency of the hydrogen production is less. In attempts to increase the efficiency of this kind of cell research focussed to minimize the space between the electrodes.

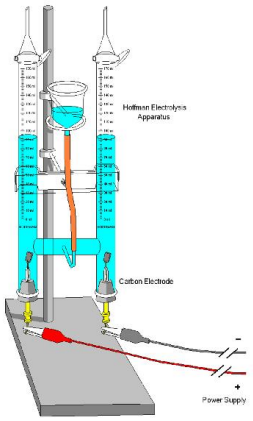

Figure 2.6: Conventional electrolysis of water to produce hydrogen.

Figure 2.7 illustrates two different hydrogen generators patented by Stephen Barrie Chambers (figure 2.7-B) and Stanley A. Meyer (figure 2.7-A) both of these approaches were left with the problem of mixed gas (H_2 and O_2) production [51] [52]. Other new designs are similar to the Mark cell (figure 2.7 C,D and E) which is a non-membrane cell [53]. The major problem common to all these cells is that due to mixed gas production explosions and flashback can occur. Therefore present research is focussed on obtaining pure hydrogen for secure storage and consumption.

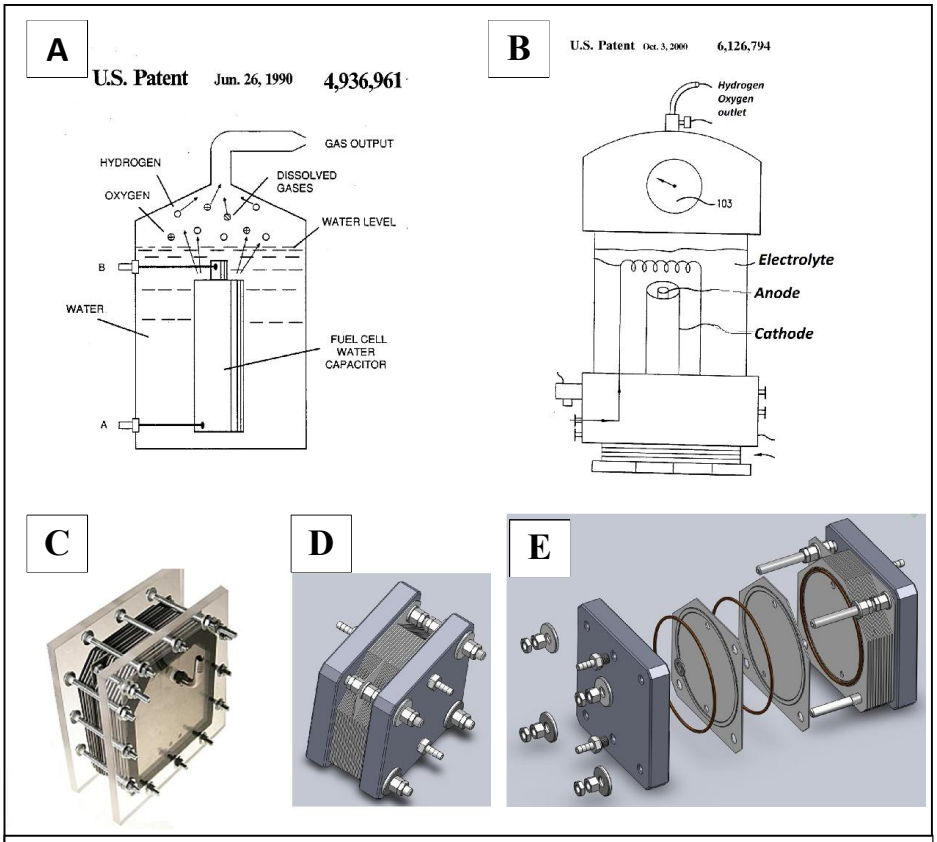

Figure 2.7: new method of hydrogen generation in principal of non-membrane cell. A- Stanley A. Meyer cell, B-Stephen Barrie Chambers cell, C-Mark cell physical picture, D- CAD assembly and E-Exploded view of Mark cell.

2.3.2) Membrane Cell (PEM electrolyser)

Membranes containing electrochemical cells are conventionally called PEM (Polymer electrolyte membrane) electrolyser cells and are currently the safest way to produce hydrogen [54] [55]. However bubble trapping inside the porous electrode causes the efficiency to decrease due to diminishing contact between water and the electrode surface [56] [57] [58] [59]. A PEM electrolyser has four major parts:- a proton exchange membrane (to keep hydrogen and oxygen apart and provide proton exchange:) a catalyst layer to

speed-up the reaction; two porous electrodes (gas diffusion layer (GDL) to generate hydrogen and oxygen) as illustrated in figure 2.8 grayscale picture [60]. All three layers are constructed separately and then assembled with high temperature and pressure to form a combined layer. The resulting cell is called the polymer electrolyte membrane fuel cell (PEMFC). A PEMFC is then placed between end plates and is used to generate hydrogen and oxygen which when released to storage chambers allow feed electrolyte to enter the cell.

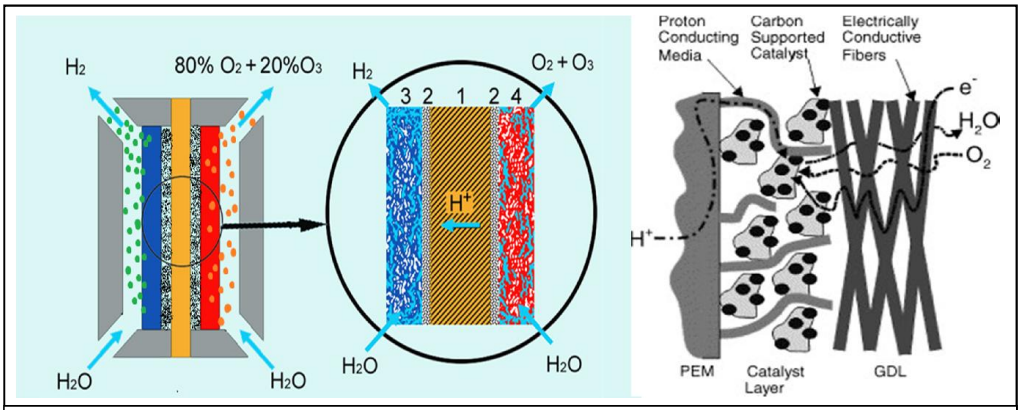

Figure 2.8: PEM electrolyser cell structure. 1-Membrane, 2-Catalyst, 3-Porous cathode and 4-Porous anode. Grayscale picture illustrate PEMFC enhanced view.

Catalyst layer (CL)

The catalyst layer is placed and bonded between the membrane and the electrode to enhance the electrochemical reaction as illustrated in figure 2.8. The first generation of PEMFC catalyst was PTFE bonded platinum black this cell though exhibiting long term performance was compromised by high cost [61]. The loading of platinum on these conventional catalysts is 4 mg/cm^2. Research has been directed at reduced platinum loading to less than 0.4 mg/cm^2 [62] [63].

Gas diffusion layer (porous electrode)

The gas diffusion layer (GDL) in PEM fuel cells ensures that reagent commendably diffuses to the catalyst layer. In addition, it allows electrons to commute to and from the catalyst layer (due to the GDL electrical properties). The most common materials used in construction of gas diffusion layers are 100-300µm porous carbon paper, or carbon cloth (Donghao Ye et al. have provided a comprehensive comparison between carbon cloth and carbon paper, see Appendex-2) [64]. The gas diffusion layer is typically made from Teflon (PTFE) to achieve best resistance from water adhesion during the chemical reaction. It provides balanced flow of water by having hydrophilic and hydrophobic properties, in addition minimizing the bubble trapping in the GDL [65] [66].

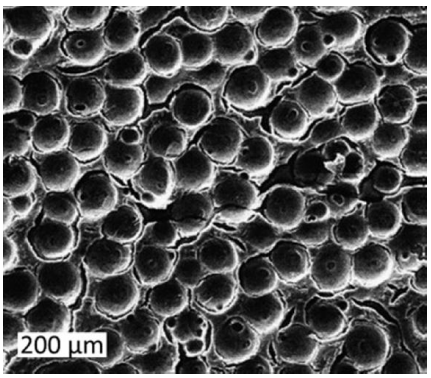

Figure 2.9: SEM micrograph showing the top view of a porous electrode.

There are two types of well-established and proven electrode designs. PTFE-bound and thin-film electrodes, both of these are porous (an example in figure 2.9 is an SEM micrograph showing the top view of a porous electrode) [67].

The catalyst layer structure and the fabrication method distinguish the type of electrode gas diffusion layer. However, conventional carbon cloth or paper, are mostly used in commercial PEM fuel cells. There has been a significant amount of research aimed at the optimisation of the homogenous porosity in the gas diffusion layers, wet-proofing and optimisation of PTFE and carbon loading in the gas diffusion layer [58] [68].

Membrane used in the cell

The membrane in the cell is bounded by the catalyst and electrode (GDL). Therefore selection of the type of membrane is based on the method of PEMFC construction. A thin film design is the most commonly reported for the electrode design. Such thin-film designs which contain sulfonated tetrafluoroethylene based fluoropolymer-copolymer and combine this with carbon supported catalyst particles, are known as thin Nafion film. The carbon supported catalyst is necessary to transport the protons and is categorised as a significant improvement. However, the problems with the Nafion thin-film are:-

1) it is an expensive film due to complicated method of its' production and;
2) the proton conductivity is reduced at high temperature and to overcome this requires more expensive material to construct it. [61] [69] [70] [71] [72]

The design of a PEM electrolyser is a very delicate procedure, which requires careful construction to provide balanced conduction and transportation of gas to and from the electrochemical reaction [60]. In conventional PEM water

electrolysis technology, the common material for the hydrogen evolution reaction (HER) is metallic platinum, which is used for the cathode catalyst and metallic iridium (or iridium oxide) is used for as the anode catalyst material for the oxygen evolution reaction (OER). The use of such noble metals is necessary to resist the highly acidic environment encountered in the solid polymer electrolyte (SPE), which would initiate corrosion in less noble metal. [73] [58]

As the material costs are high in the PEMFC to make this technology more commercial it is necessary to significantly reduce the use of the noble metals for both the anode and the cathode. To reduce the cost of electrode material P. Millet presented carbon-supported platinum at the cathode for the hydrogen evolution reaction (HER) and iridium at the anode for the oxygen evolution reaction (OER). The research presented [67] high (80%) efficiency with reduction in noble metal material content to about 0.3-0.5 mg cm^{-2} and it can produce up to 5 Nm^3H_2/h in a single stack cell, however 1000 N litre H_2/h was reported with stack of 12 plates cell (250 cm^2 active area each) [67]. In comparison to the Millet cell (GenHy®1000) the work reported in this thesis achieved 95% efficiency and used relative low cost material (both the anode and cathode where stainless steel 316). Moreover production of hydrogen was greater (438 milliliter H_2/h) and the active area of the electrode was 48 cm^2 which is a lot smaller compared to the GenHy®1000 cell (see chapter 3 for design and chapter 4 for results). [74] [75]

One of the important factors that have to be considered is the pressure uniformity in the system, due to the fact that the volume production of hydrogen is twice as great as that of oxygen. Hence every electrolyser cell required time to reach a uniform production stage (displayed in figure 2.10 is a graph presented by P. Millet [67]. A similar problem was faced in the "on-

demand hydrogen generation cell design 2" that was overcome successfully in cell design 3 in this work (see chapter 3 & 4 and to measure the pressure and efficiency calculation section 2.4 explains the steps to be fallowed). The technological change presented in this thesis is based on a hybrid of both non-membrane cell and PEM cell technologies. Where the best attributes of both are amalgamated:- the non-membrane design cell which provides the better environment for reducing bubble trapping can be combined with the presence of having a membrane in the cell to give pure hydrogen (see chapter 3 & 4). [73] [76] [77]

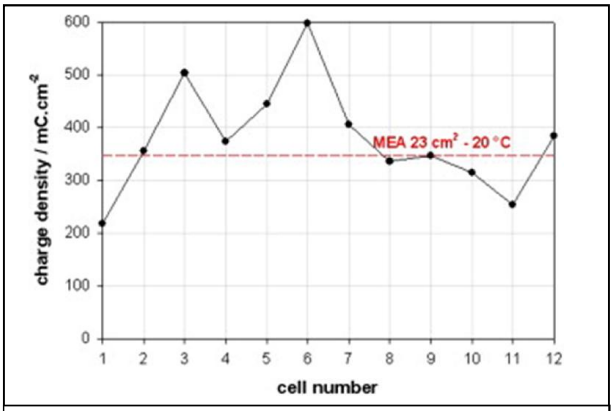

Figure 2.10: P.Millet's PEM electrolyser cell pressure analysis, charge densities measured at 18.5°C on each cell of the GenHy®1000 PEM water electrolyser.

2.4) Experimental steps

The electrolysis of water produces hydrogen and oxygen gas molecules. This occurs by OH bonds of water breaking during the electrochemical processes. Although energy is invested in the electrolytic production of hydrogen gas, H_2, the latter can be considered as an energy carrier. Therefore H_2 becomes a fuel because energy stored in the form of H_2, can be released later by recombining hydrogen with abundant oxygen from the atmosphere or pure

oxygen. Pure oxygen can provide better combustion then air alone, therefore the by-products of water electrolysis, hydrogen and oxygen, are both useful to store. Hydrogen fuel cells are one of the practical applications that can be used to produces electricity from the intake of hydrogen and oxygen (as illustrated in Chapter 1 Figure 1.5: Ballard fuel cell-Schematic). Such kinds of application can use pure hydrogen and oxygen from an "on demand hydrogen generator". To facilitate such application and for perfect hydrogen generation the following set of calculations helps to identify factors involved in electrochemical hydrogen production. These calculations are further explained in chapter-3 in 'Innovation' and in chapter-4 in 'Result and Discussion'.

Step.1: The theoretical calculation

A theoretical calculation allows us to determine the production of gas based on the premise of 100% coulombic efficiency taking a place. This is also known as the Faraday efficiency.

Equation 2.7 [78] $$\mathbf{V = R\ I\ T\ t\ /\ F\ p\ z}$$

Faraday's first law in equation 2.7 above has three variables, **I** is current in Amperes (A), **T** is temperature in degrees Kelvin (K) and **t** is time in seconds (s). Where the universal gas constant is **R** = 8.314 J mol^{-1} K^{-1}, the Faraday constant is **F**=96845 C mol^{-1}, hydrogen density is **p** = 101325 Pa and **z** is number of electrons required to discharge one molecule. In the case of hydrogen generation two electrons are required to release one hydrogen molecule therefore **z**(H_2) = n2. The result of using the above variables and

constants is the volume of theoretical production of hydrogen which is denoted by **V** in m^3.

Using equation 2.7 we can answer the following question:-

What will be the volume of hydrogen at current **I** = 1A, temperature **T** =26°C and time **t** = 20sec?

Converting temperature C to K

T = 273.15+26 = 299.15K

Putting values into equation 2.7

$$\mathbf{V = R\ I\ T\ t\ /\ F\ p\ z}$$

$$= \frac{R\ (8.314\ J\ mol^{-1}\ K^{-1})\ \mathbf{*}\ I\ (1\ A)\ \mathbf{*}\ T\ (299.15K)\ \mathbf{*}\ t\ (20s)}{F\ (96845\ C\ mol^{-1})\ \mathbf{*}\ p\ (101325\ Pa)\ \mathbf{*}\ z(2)}$$

$$\mathbf{V =}\ 49742.662/\ 19625639250\ \mathbf{= 2.5E^{-6}\ m^3}$$

Converting into mL.

V = 2.5E-6 ***** 1E+6

V = 2.5 mL

Therefore 2.5mL of hydrogen can be produced at 1A, 26°C in 20sec.

Step.2: The experimental calculation

The second and major phase of the calculation is to find out the accurate actual amount of hydrogen produced by a hydrogen generator. Therefore an understanding of the behaviour of hydrogen gas is important to get accurate results. The Kinetic-Molecular Theory of gases explains the forces between the molecules and the energy they possess. Thus the Kinetic-molecular theory gives us an understanding of gas molecular motion.

Important outcomes from Kinetic theory and gas laws are the developments of variables and constants, which aid the understanding of gas quantities and behaviour. Thereafter, continuous motion in a gas creates pressure and temperature. Pressure is defined as force per unit area and is denoted by **P** and temperature is denoted by **T.** A real life example to support the above statement is in a balloon:- blowing air into a balloon will expand the balloon and keep the shape at a certain pressure and temperature. If you keep blowing air into balloon it will eventually explode. This of course varies with the surface strength of the balloon.

The Combined Gas Law was formulated by combining Boyle's Law and Charles' Law with various different combinations. To get an accurate measurement of hydrogen generation, equation 2.8 illustrates the appropriate relationship with the simultaneous change of pressure and temperature.

Equation 2.8 [79]

$$\frac{P_1 \cdot V_1}{T_1} = \frac{P_2 \cdot V_2}{T_2}$$

The above equation 2.8 illustrates two different conditions in the relationship of PVT, where the left hand side can be considered as the initial values, and the right hand side can be consider as final values.

Equation 2.9

$$\mathbf{V_{STP}} = \frac{P_{EXP} \cdot V_{EXP} \cdot T_{STP}}{T_{EXP} \cdot P_{STP}}$$

Where two variables are constant, temperature STP (T_{STP}) is equal to 273.15 K and pressure STP (P_{STP}) in the case of hydrogen is equal to 101325 Pa, where the experimental temperature (T_{EXP}), volume (V_{EXP}) and pressure (P_{EXP}) values comes from the hydrogen generator.

In this thesis T_{EXP} is measured with an infrared thermometer and V_{EXP} is calculated using equation 2.11, which is based on pressure readings. To get the value of P_{EXP} requires a manometer or a barometer. In our case manometers were utilised and designed to obtain perfect measurements (see chapter 3 'INNOVATION' for more detail about the experimental implementation of the above formula).

French mathematician Blaise Pascal introduced a law, which states that pressure applied to a static fluid increases the pressure throughout the fluid.

[47]. Therefore applied pressure on one end of a manometer will displace all fluid towards other end with the same force, which is represent in equation 2.10.

Equation 2.10 $\mathbf{P = \rho\ g\ h}$

In equation 2.10 **P** is the pressure in Pascal 'Pa', $\boldsymbol{\rho}$ is a fluidic density in Kg/cm^3, the gravitational force on the fluid is **g** and **h** is the height of the water displacement from the calibration point. This equation (2.14) is used to explain how to calculate pressure below:-

Example using equation 2.10

What will be the added pressure on the manometer? Where the displacement height is **h = 1.8**cm, the gravity constant is **g = 9.81**m/s2 and the density of water $\boldsymbol{\rho}$ = **1000**kg/m3.

Feeding values into equation 2.10

$\mathbf{P = \rho}\ kg/m^3 * \mathbf{g}\ m/s^2 * \mathbf{h}\ m$

$\mathbf{P} = 1000kg/m^3 * 9.81m/s^2 * (1.8cm/100)$

Converting **cm** to **m** by dividing 100

$P = 1000kg/m^3 * 9.81m/s^2 * 0.016m$

P= 170 Pa

Equation 2.11 $\mathbf{V_{EXP} = \Omega\ r^2\ h\ /\ z}$

Where Ω is a constant = 3.14, r^2 is the radius of the tube and h is displacement of water in cm. Equation 2.11 then provides the value of V_{EXP} to equation 2.9.

Feeding values in equation 2.11, where Ω = 3.14, the tube radius $r^2 = 0.8^2$ cm, the displacement height h = 1.8cm and one molecule of hydrogen $z(H)$ = 2.

$$V_{EXP} = \Omega * r^2 * h/z$$

$$V_{EXP} = 3.14 * (0.95)^2 * 1.8 / 2$$

$$\boxed{V_{EXP} = 2.550 \text{ cm}^3}$$

Using the above values we can now return to equation 2.9

Example for Equation 2.9

$$V_{STP} = \frac{P_{EXP} \cdot V_{EXP} \cdot T_{STP}}{T_{EXP} \cdot P_{STP}}$$

$$V_{STP} = \frac{P_{EXP}(170+101325 \text{ Pa}) * V_{EXP}(2.550 \text{ cm}^3) * T_{STP}(273.15\text{K})}{T_{EXP} \ (26+273.15)\text{K} *. P_{STP}\,(101325 \text{ Pa})}$$

$$V_{STP} = \frac{70587996.615}{30311373.75}$$

$$\boxed{V_{STP} = 2.3 \text{ ml}}$$

So to evaluate the performance of the Hydrogen generation, the value obtained from equation 2.9 above is divided by the value obtain from the example equation 2.7.

The performance of hydrogen production = 2.3 / 2.5 = 92%. So this is the kind of value that needs to be achieved for best performance of the cell. In the next chapter the practical implementation of the above formulae is reported.

Chapter 3

Innovation

3) Introduction

The generation of Hydrogen via electrolysis has been the subject of many studies over the last two hundred years [80]. However, there is still room for further work to improve both the efficiency of the process and methods of storage of the gas. The cleanest method at present is to produce hydrogen by electrolysis, and the main focus of this research is to design and develop a green energy fuel cell for on-demand application. The aim of the work presented in this chapter was to further investigate the electrolysis method for hydrogen production. .

An Electrochemical fuel cell contains a minimum of two electrodes: the positively charged electrode called the anode which forms oxygen bubbles, and the second negatively charged electrode called the cathode, which forms hydrogen bubbles during a chemical reaction caused by applying electrical current into the system.

The project was initiated with consideration of finding a low cost solution for on-demand hydrogen generation. To establish a starting point, the first cell design was based on the work of Stephen Barrie Chambers [81] to check the performance levels.

3.1) Introduction of first electrochemical Cell (cell-1)

Stephen's cell (invention) as shown in Figure 3.1 was to produce hydrogen in the manner of orthohydrogen and/or parahydrogen [81]. The most important property of orthohydrogen is the parallel spins of two nuclei, this makes the molecule unstable and highly combustible and easy to make. Although parahydrogen is less flammable, it is more difficult and expensive to generate, and has antiparallel movement between two nuclei [82] [83]. Thus parahydrogen is more stable and is the ground state of the hydrogen molecule. Orthohydrogen is more preferable in this research because of its relative stability as illustrated in Figure 3.2.

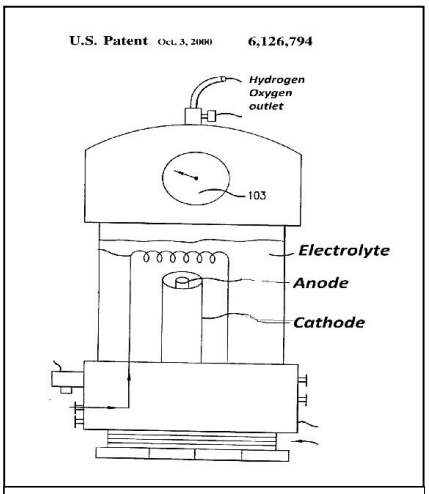

Figure 3.1: [81] Stephen's Invention diagram of hydrogen generator.

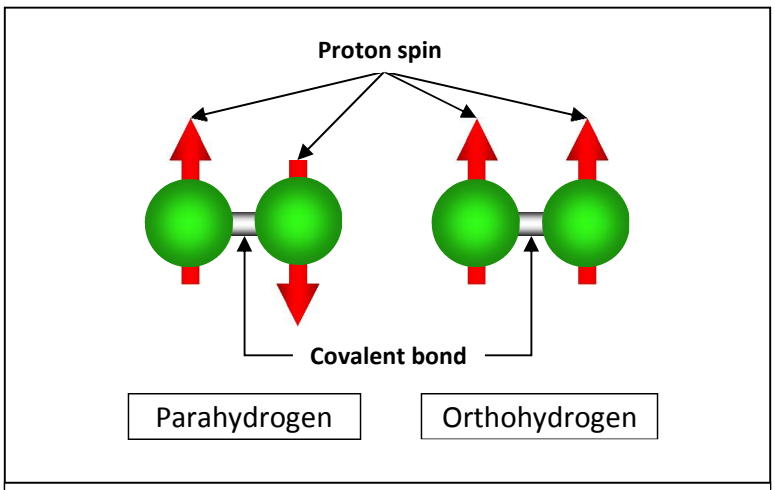

Figure 3.2: Parahydrogen and Orthohydrogen proton spin schematic.

Stephen sets the objectives for his invention as follows [81].

1. Cheap and controlled production of orthohydrogen and/or parahydrogen.
2. Production of a large quantity of hydrogen in the shortest time by electrolysis from tap water without using any chemical catalyst.
3. Production of hydrogen without generating heat, with modest amount of input power.
4. The bubbles of hydrogen and oxygen produced will not bunch around the electrodes.
5. Cell will be self-pressurized without any pump aid.
6. At-least one pair of electrodes in a cell with close spacing.

Figure 3.3: First electrochemical hydrogen generator cell digital camera picture. (cell-1)

As per Stephen's description in his patent, orthohydrogen can be produced by simply disconnecting the coil from the system [81].

In regards to this objective of producing orthohydrogen, the first electrochemical cell design used in the work presented in this thesis(cell-1) as shown in Figure 3.3 does not contain a coil, but the rest of the design was considered to be a close repeat of Stephen's experiment.

A hydrogen generator was carefully constructed in the Wolfson Centre, Brunel University Laboratories, with the help of one of the technicians. His expertise on lathe machines and other fabrication machines, enabled fabrication of this device design. Details of the design stages are explained (see section 3.1.1) below.

3.1.1) Brief description of First electrochemical cell design.

A more complete appreciation of the cell-1 design and its physical implementation stages, to deepen understanding of its advantages, drawbacks and development stages are explained as follows:

Figure 3.4. Part-A is a picture of a top lid made from a 20mm acrylic sheet, which has a 250mm diameter circle etched, as shown by the arrow, 10mm in depth and 10mm wide. This groove is made to protect/deter any leakage at the top.

Figure 3.4. Part-B isa picture of the base of the cell. This has three etched circles: one as Part-A, and the other two are etched for electrode placement. Perfect electrode placement stops electrolyte flow beneath the electrodes and provides for a controlled flow and space between electrodes.

Parts of cell-1,

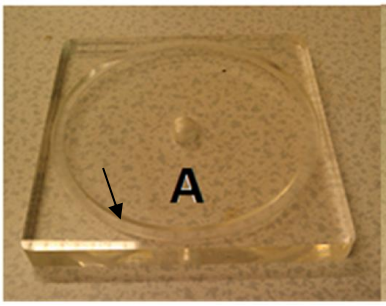

Part-A is a top lid,

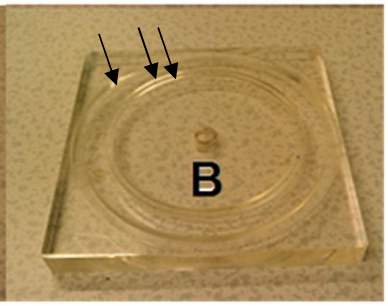

Part-B is a base

Figure 3.4. displays the parts required in cell-1 design. A is top lid and B is base of the cell hold electrode.

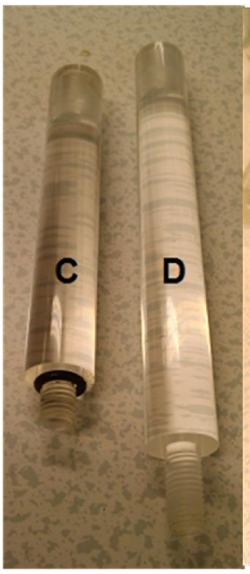

Part-C & D is centre rod

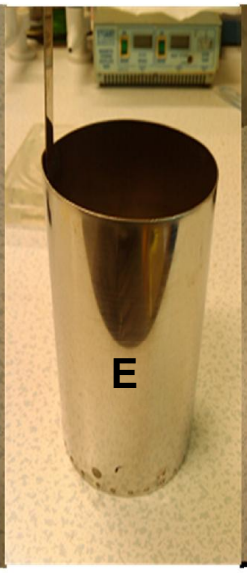

Part-E electrode

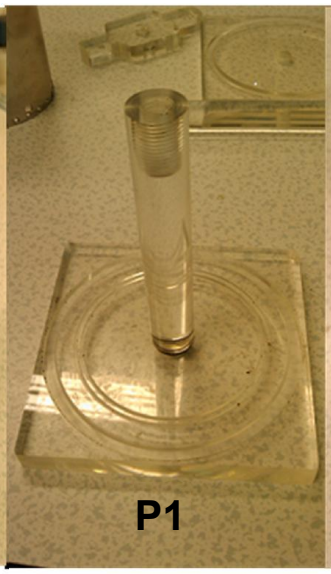

P1: Part-C positioning on Part-A

P2: Part-E positioning on Part-A

Figure 3.5. Cell-1 parts. Part-C & D is a cetre rod to connect top plate and base plate to close thecell and E is electrode. P1 represent first stage of asembly and P2 represent secon stage of positioning.

Figure 3.5: Part-C is a centre rod which connects with the base as shown in P1.

Figure 3.5: Part-E is an electrode that sits on the inside circles of the base as shown in P2. The second electrode is similarly placed.

Figure 3.6: Part-F is an electrode holder used to hold both electrodes from the top by joining with part-D with screws, as can be seen in figure 3.6 position P3.

Figure 3.6: Part-G are spacers which maintain the circular gap between electrodes during the system stress, as illustrated in position P4 and P5 of Figure 3.6.

The next step was to solder the 2.5mm single core wire to each electrode, a heat shrink tube was applied to shield the wire and solding area.

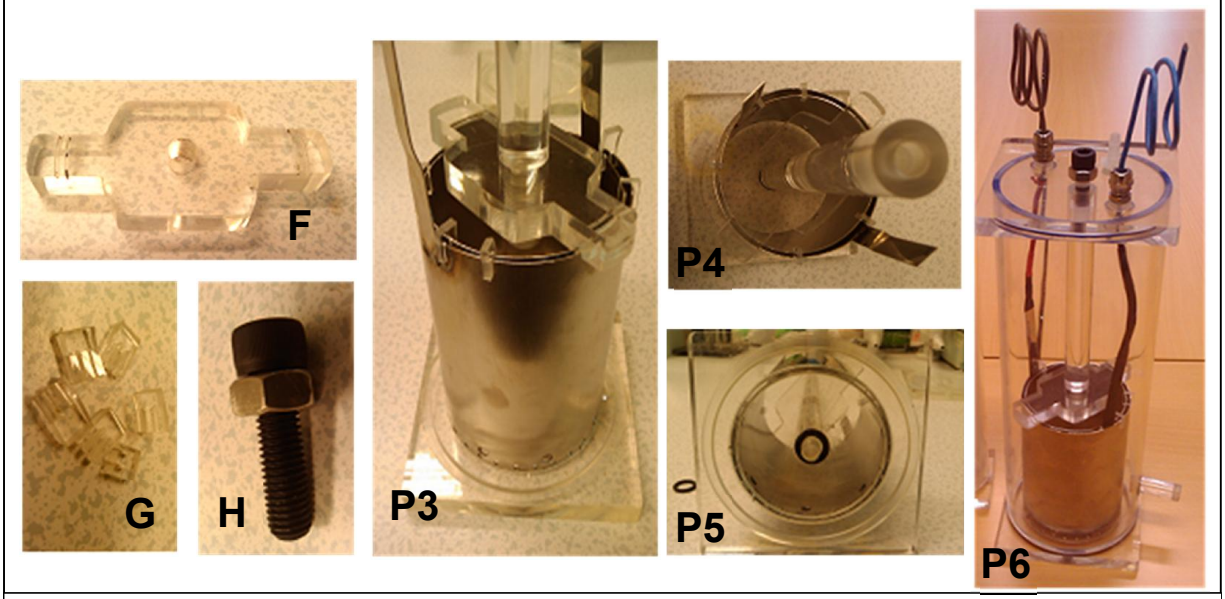

Figure 3.6: Part-F Electrode holder, G is spacer, and H is lid holder. P3, P4, P5 and P6 are parts placement stages.

The final step was to tighten the lid with bolts (part-H) on part-D. This seals the electrochemical cell, and it is thus ready for testing as shown in position P6 in Figure 3.6.

3.1.2) Measurements

Cell-1 was run at room temperature (26^{O}C) with 30% KOH alkaline solution for 280 seconds measured at intervals of 20 seconds for three different currents (1, 2, 3 amps). The results are discoursed (in 3.1.3) below.

3.1.3) Results and discussion of cell-1

The fabrication of the cell-1 design lead to the formation of a mixture of hydrogen and oxygen in the same chamber, which means that the cell-1 design has the possibility of fire and explosion hazard. The device also has the drawback of lower performance of hydrogen production. However, the advantage of reproducing Stephen's innovation is that it allows us to gain a quick and deep understanding of hydrogen generation.

Figure 3.7: (A) Gas filter and Pressure balancer
(B) First design of gas measuring device
(C) First Design of Hydrogen Generator

In Figure 3.7(A) pressure balancing arrestors are presented, these are used to clean the gas and control the pressure. The In-let of the arrestor receives the generated gas from the Hydrogen generator; and the outlet feeds to the measuring device Figure 3.7(B) for measurement. Figure 3.7(B) presents the device designed to measure the low pressure gas volume.

Cell design one; measurement Figure 3.8 explains the behaviour of the cell in terms of efficiency, which was found to be a maximum of 46% at 3Amp. The most interesting outcome of this experiment was an understanding of the natural behaviour of bubble formation and evacuation.

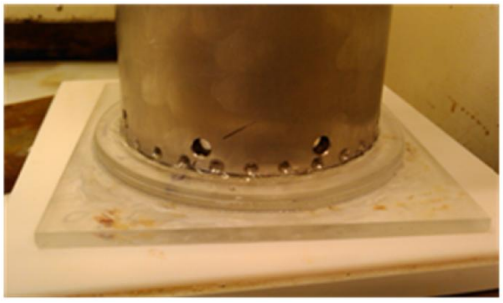

Figure 3.8: lower part of cell 1

The most important 'performance barrier' in the production of hydrogen is bubble formation at the electrode. This is because if bubbles are attached to the electrode surface, the process will stop producing gas on the area where bubbles are formed and stuck [84] [85]. This is one of the reasons for the low performance of the cell in the production of gas. In this experiment, attempts to evacuate bubbles were made using a simple technique to encourage natural flow to lift the bubbles. As such, the water inlet between two the plates was through the lower part of the cell as shown in Figure 3.8. Thus, when

hydrogen was produced between electrodes by electrochemical splitting of the water molecules, the level of water was reduced. Then the gravitational force and the equilibrium behaviour and nature of the fluid, allowed the (surrounding) outside solution to flow through the holes shown in Figure 3.8 between the electrodes, and that flow in turn pushed the bubbles out from the surface.

In the performance of cell-1, about 1% boost can be seen in Figure 3.9 at the point of 280; 40% to 41% and 45 to 46%. Figure 3.10 illustrates the comparison of theoretical and experimental production of hydrogen. The Line graph represents theoretical data at 1Amp, 2Amp and 3Amp; and the Bar presentation shows experimental data, where Red (3A), Yellow (2A) and Green (1A) represent the change in performance after fluidic flow.

3.1.3) Conclusions on Cell 1

Development of the first electrochemical cell design opened the doors for exploration in hydrogen generation. Analysis of the system behaviour revealed two major problem areas:

1) The bubble evacuation system
2) Hydrogen- oxygen separation.

Initially, the performance of hydrogen production kept falling due to bubbles attaching to the surface of the electrode. Hence, the area occupied by the bubbles resulted in reduced bubble formation and coulombic efficiency, which was maximum 45% under without flow and 3 amp current flow as shown in figure 3.9 with read line. After introducing a natural flow in the system, which facilitated evacuation of the bubbles from the surface, a result

of 46% was achieved as illustrated with green line in figure 3.9; this gave a 1% boost in performance. Similarly in figure 3.9 brown line represent 1 amp and pink line represent 2 amp without flow hydrogen generation results and natural flow results illustrate with black line under 1 amp and blue line under 2 amp current flow, also gave 1% boost in efficiency. Therefore flow in a cell is one of the key factors to improve performance. The second barrier was to separate hydrogen and oxygen which was impossible in the design of cell 1. Therefore, further research lead to the design of a new cell 2, which allowed separation of hydrogen-oxygen bubbles; and the bubble evacuation system in one device.

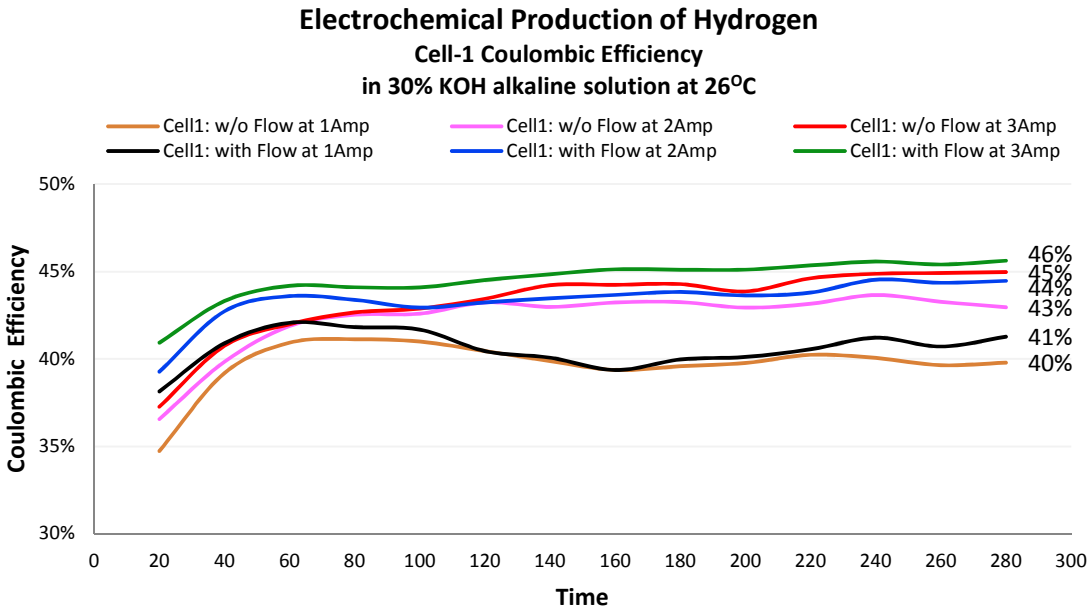

Figure 3.9: Change in electrochemical production of hydrogen performance because of natural fluidic flow behaviour conducted in 30% KOH alkaline solution at 26^{O}C temperature.

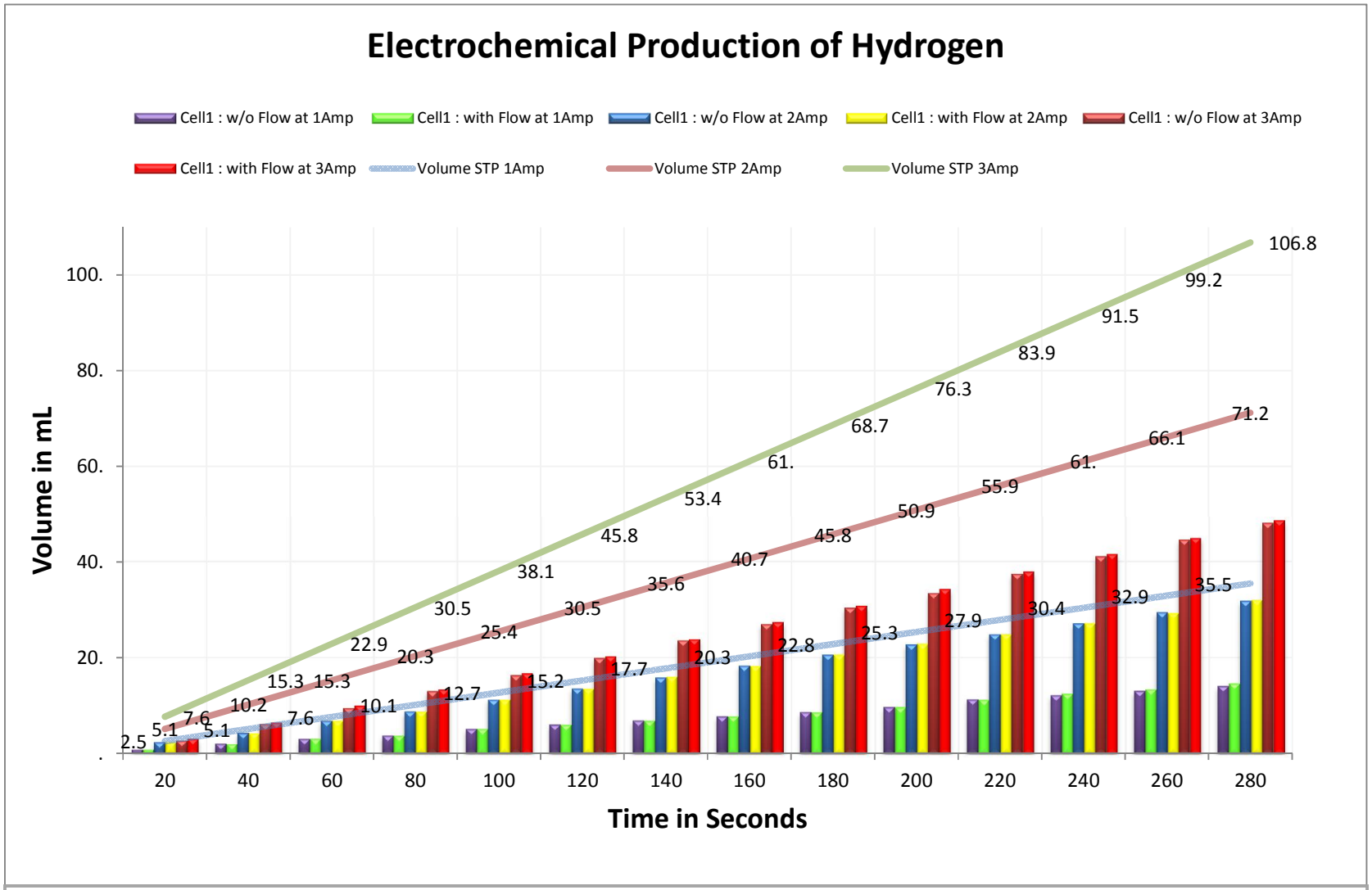

Figure 3.10: Comparison between theoretical represent with line graphs and experimental represent with bar graphs data of hydrogen production produced in 30% KOH alkaline solution at 26^{O}C temperature.

3.2) Introduction to the second electrochemical Cell (cell-2)

The Cell-1 study leads to the cell-2 design as shown in Figure 3.11. However, from the very first test the following design drawbacks were discovered:

1. Difficulty in controlling leakage because grip holes are far as displayed in Figure 3.11 A and B.
2. Inability to control electrolyte flow caused by same point for electrolyte inlet and gas outlet.

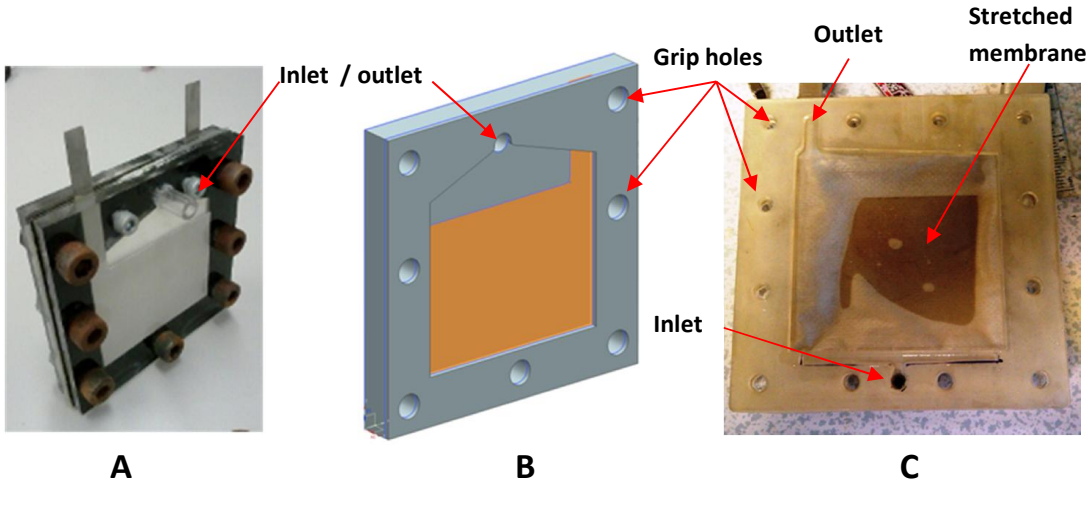

Figure 3.11: Cell-2 design, 'A' is digital picture of the cell, 'B' cad design and 'C' is pressure effect on membrane

3. Bubble evacuation was not stable due to a combined inlet and outlet system design as displayed in Figure 3.11.A and B.

4. Attempts to keep the gas diffusion membrane in place were impossible during the experiment, due to the pressure generated in the system which stretched the membrane towards the lower pressure chamber.

Analysis of these drawbacks led to the third electrochemical cell design (cell-3). (see detailed explanation of cell-3 in section 3.3).

3.3) Introduction to the third electrochemical Cell (cell-3)

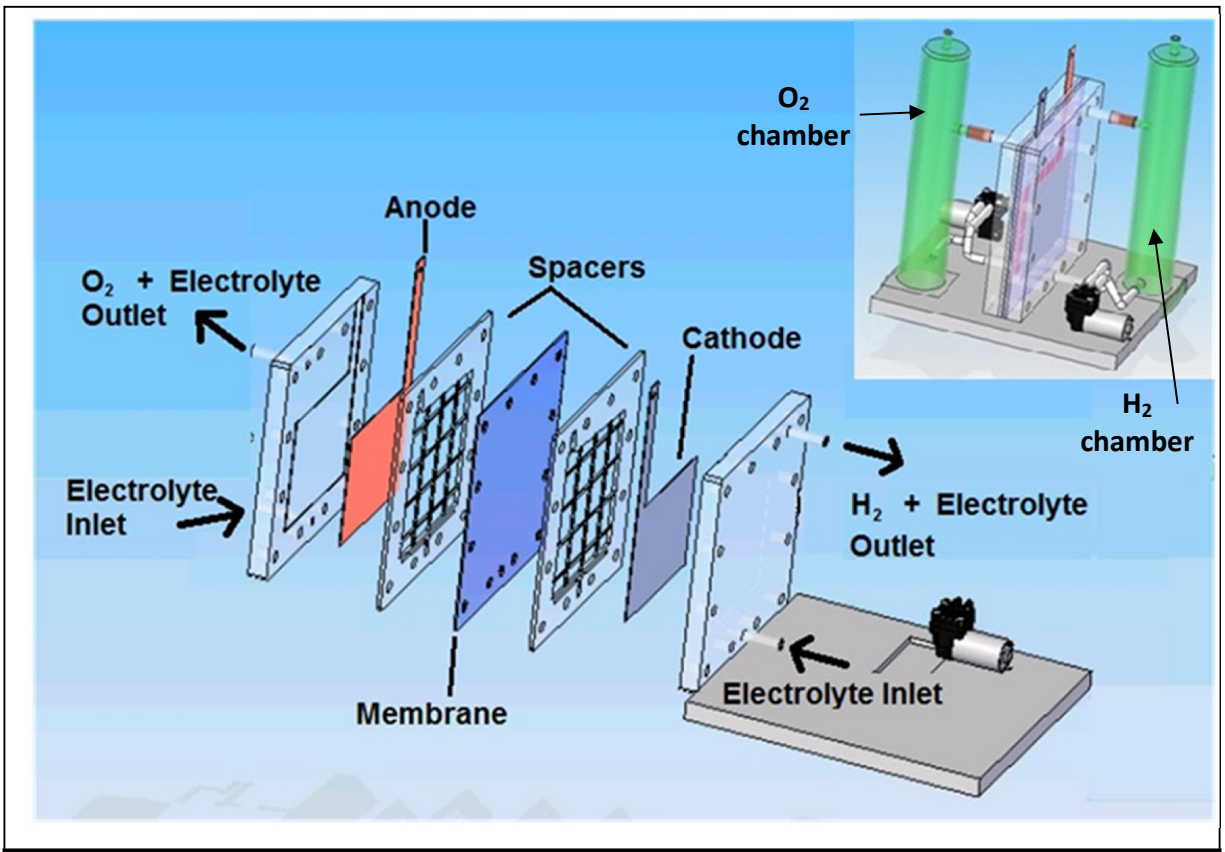

Figure 3.12: cell-3 design expanded 3D view to illustrate parts of cell-3.

The third electrochemical cell design for hydrogen generation, presented in figure 3.12 was designed in Siemens NX CAD software [86]. This software enabled

perfect drawing and visualisation of the cell. Following analysis of the cell-3 design in NX software, design drawings were implemented into the physical form with the help of the CNC laser cutting machine. The CNC machine ensured an error free cut to measure parts of the cell-3. See section 3.3.1 for detailed explanation of cell-3 design.

3.3.1) Brief description of the third electrochemical cell design (cell-3).

The third electrochemical cell design proved to be successful and was the foundation of the rest of the work presented in this thesis. Consequently, this section of the thesis is the most interesting and innovative for the present work and paves the way for future prospects. The cell parts are explained and illustrated in figure 3.12.

Figure 3.12 shows an assembled cell in the top right corner, and the rest of the figure shows an expanded view of the cell-3. Cell-3 contains seven major parts connecting together in a sequence of:

1) cathode placed on
2) the cathode-endplate, which connects with
3) a hydrogen-spacer; then
4) a gas diffusion membrane is placed between the hydrogen-spacer
5) and the oxygen-spacer.
6) Thereafter the anode connects with the
7) anode-endplate which is placed on the oxygen-spacer and

Finally all the parts are bolted together with stainless steel bolts.

Part-1- Anode and Cathode endplates: these were designed with the same drawing specifications which are illustrated in figure 3.12. The Cell-3 dimensions in terms of height and width are standard set to 120mm square. Therefore the endplate was cut out from a 10mm [1] thick acrylic sheet, where the height and width were set to 120mm [2]. All four edges were bevelled at 2mm [3] radius to protect other components from its sharp edge.

The endplate contains 14 holes of 6mm [4] diameter: 12 locating holes for the bolts to grip and keep all parts parallel to each other in the right place. These 12 holes were set at equal distances of 33.3mm [5] between them to keep equal clutch pressure over the cell.

The Electrolyte inlet as shown in figure 3.12 was used to inject electrolyte inside the cell. Figure 3.13 2D view illustrates the distance of 16.7mm [6] between electrolyte hole and bolt hole. Similarly, the oxygen and hydrogen outlet distance from the bolt hole was 16.7mm as illustrated at position [13] in figure 3.13.

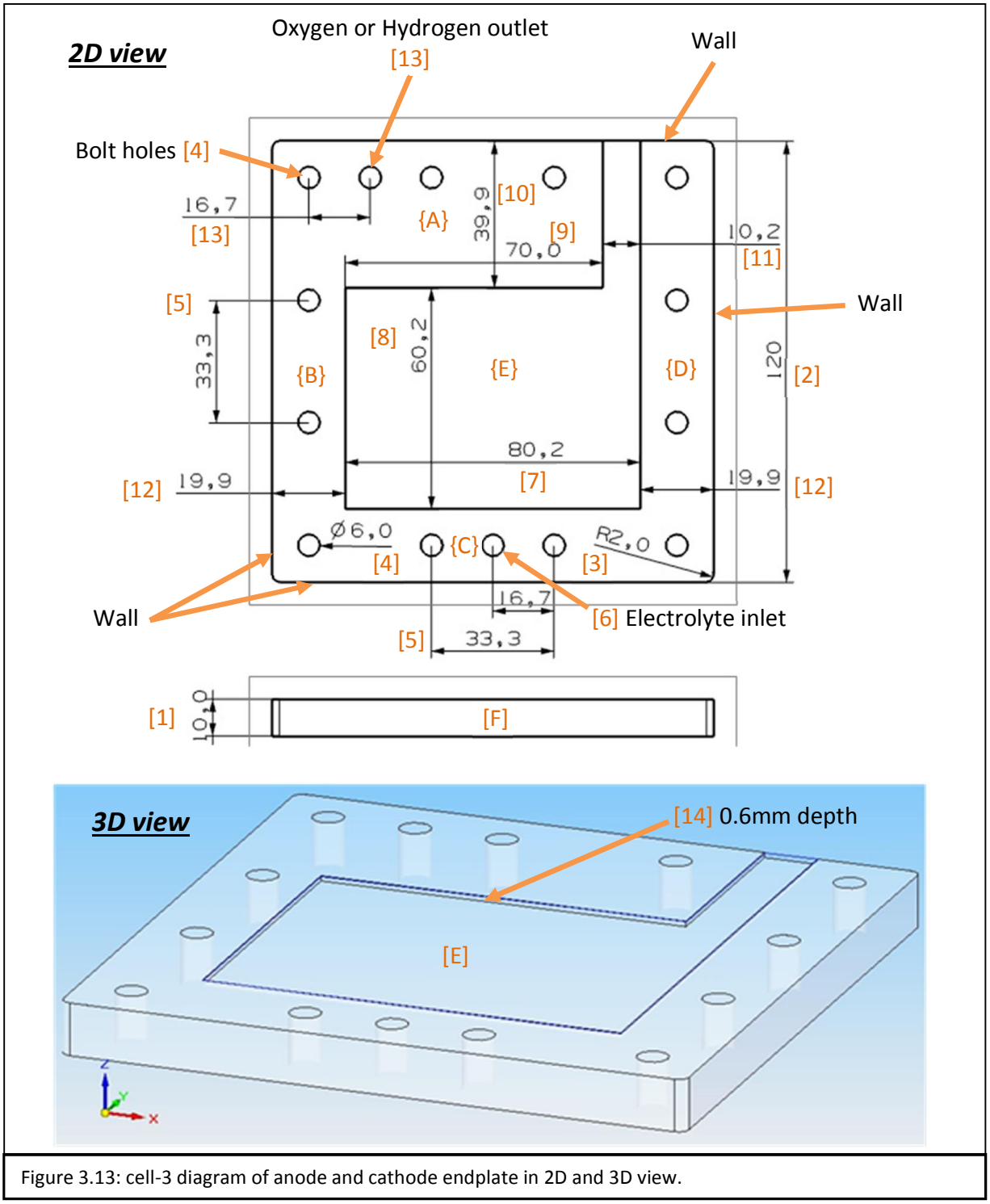

Figure 3.13: cell-3 diagram of anode and cathode endplate in 2D and 3D view.

The size of area {E} as shown in figure 3.13 was based on the electrode dimensions, and each side of dimension of the space E was increased by 0.1mm for electrode clearance. The depth of the engraved area {E} was set by adding + 0.1mm to the electrode thickness, (where the electrode thickness is 0.5mm) giving 0.6mm as shown in position [14] figure 3.13 3D view. Therefore an 0.6mm engraving was carried out by the laser etching method. The figure 3.14 displays the final result of the assembly of part-1 the anode and the endplate, the cathode and cathode endplate are the mirror image of this. Both were the assembled after laser fabrication.

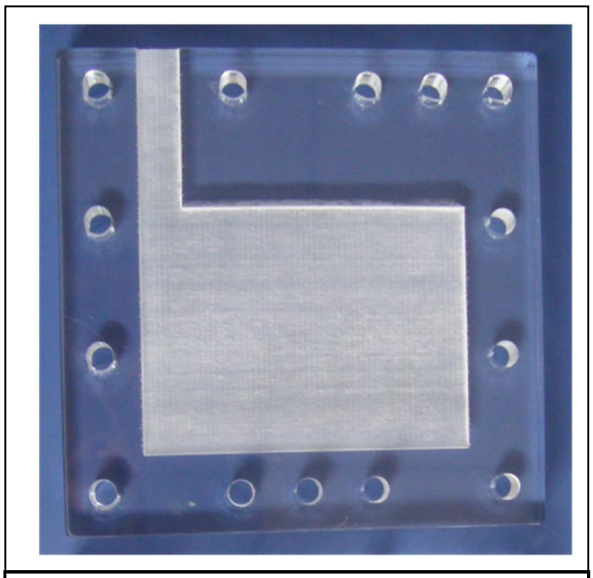

Figure 3.14: anode and cathode endplate picture
After laser fabrication

Part-2- Anode and Cathode Electrode: the bubble formation area width was 80mm and height was 60mm. The connection arm width was 10mm and height 70mm as illustrated in figure 3.15. Therefore, adding 0.1mm to each side of electrode dimension increased the engraving dimension as illustrated at position [7], [8] and [11] in figure 3.12. Walls {B}, {C} and {D} are reference walls for

electrode placement area {E} on the endplate and the offset distance is set to 19.9mm.

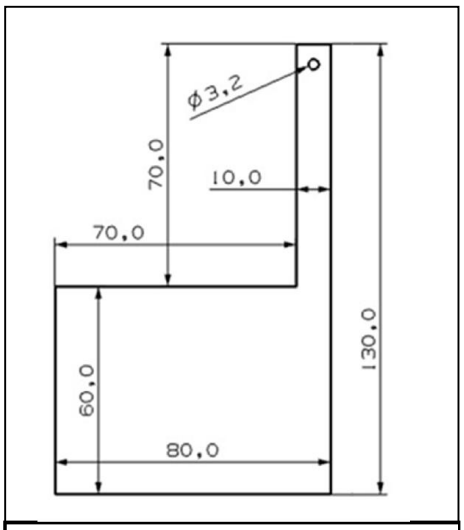

Figure 3.15: Electrode diagram

Part-3- Spacer: figure 3.16 displays an actual picture of the spacer which was designed with the same drawing standards which are illustrated in figure 3.13. Similarly the spacer dimensions in height and width were set to 120mm square as illustrated in figure 3.17 at position [1].This was cut out from a 1.9mm thick acrylic sheet as illustrated at position [2] in figure 3.17 3D view. All four edges were bevelled at 2mm [3] radius for safety reasons. [4] The bolt holes placement profile was the same as the electrode endplate profile. Therefore the assembling of the cell was perfect with a balanced lock pressure.

[5] An Electrolyte dispenser injected the electrolyte into the chamber as illustrated in figure 3.17. This area of the spacer plate played a very important role in boosting cell performance. Control of bubble formation is crucial in hydrogen generation, because the area where the bubbles form on the electrode cannot generate more bubbles until the already formed bubbles are cleared. Therefore the

electrolyte dispenser was designed in such a way that it wiped the already formed bubbles from the surface as soon as they were produced. This contributed greatly in accelerating the performance of the cell, and also was a low cost solution for hydrogen production. The electrolyte was injected from a 6mm [6] diameter hole, and fed into a 2mm [8] dispenser chamber through a 2.9mm [7] pass-through area.

The grid was designed to keep the membrane in place. All the boxes within the grid were cut out and separated by a rectangular wall 1.3mm by 1.0mm in width and height respectively. The grid started from a 2mm offset distance from the dispenser chamber as illustrated in figure 3.17 at position [9], and 21mm offset from the side wall. The width of all boxes in the grid was 18.7mm and the height of the first lane boxes of grid was 9mm. The three lanes of boxes above were 17.69mm in height, and the height of the top lane (gas directional lane) was variable from 9.0mm to 5.6mm creating an angular edge which redirected the gas to the outlet. The gas outlet tunnel was 6mm in width. The spacers played a very important role in the performance and stability of the device environment.

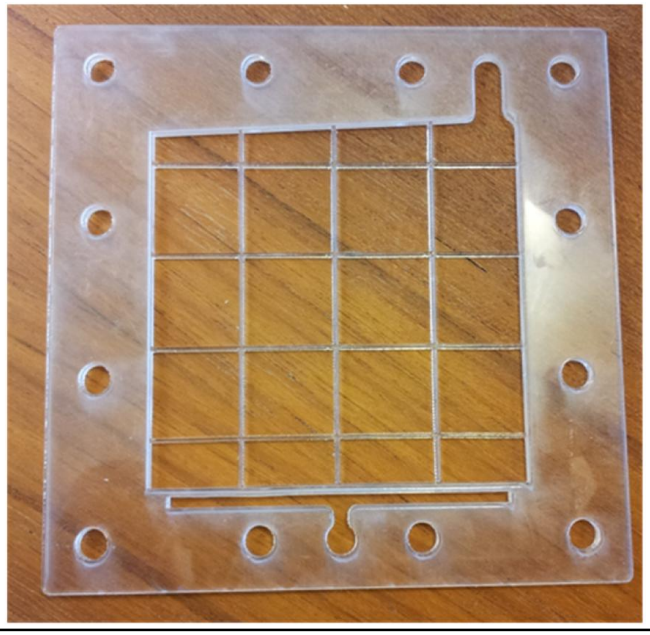

Figure 3.16: Spacer picture keep the membrane in place.

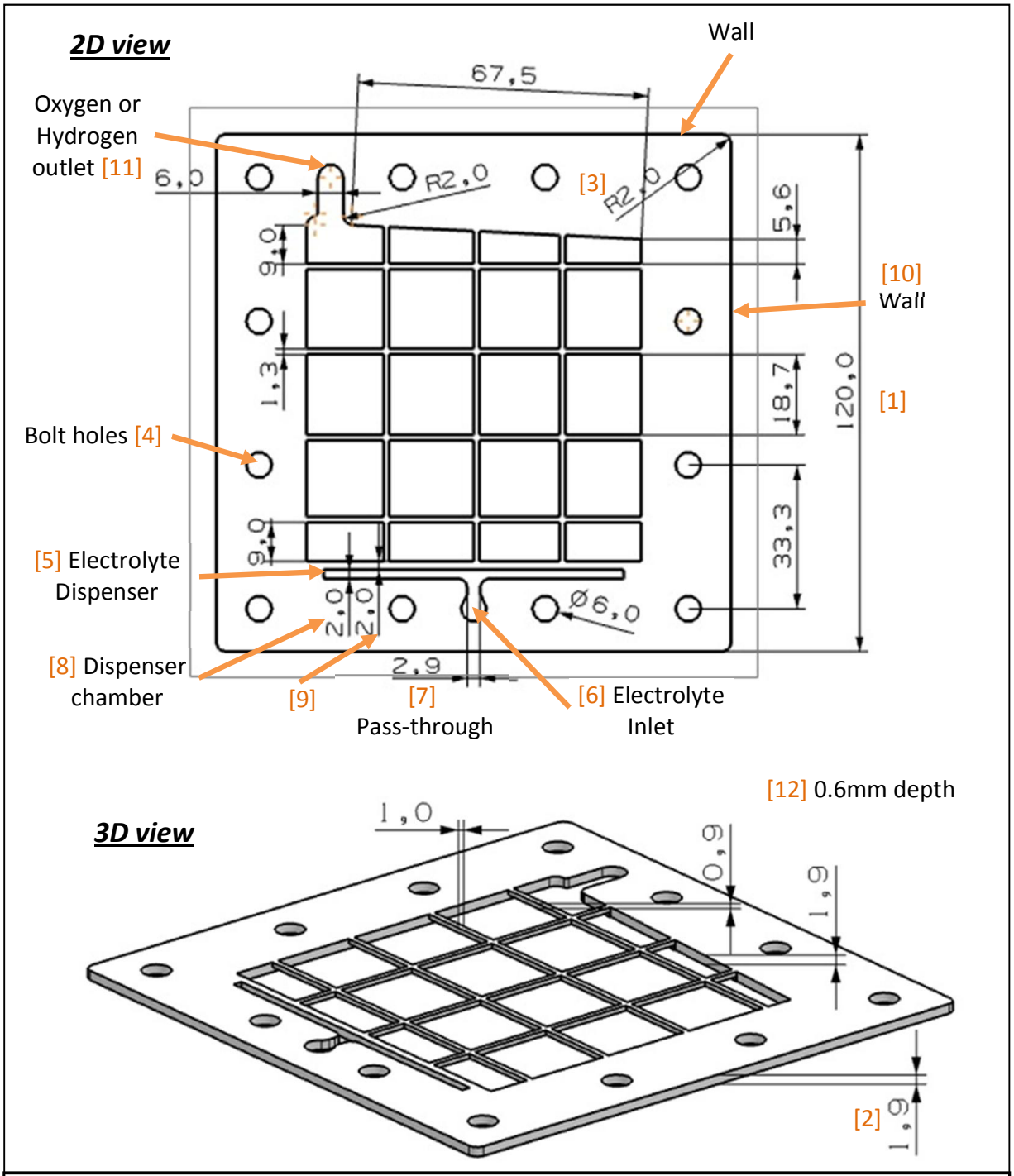

Figure 3.17: cell-3 diagram of spacer in 2D and 3D view.

Part-4- Membrane: This was used to keep hydrogen and oxygen separate which ensured collection of pure gas and also protected against the combustion hazard; because hydrogen cannot burn without oxygen. Each cell contained one membrane, which was cut-out with the same profile as the end-plate by the laser cutting machine, where the height and width were set to 120mm square as illustrated in figure 3.18, and the holes were 6mm.

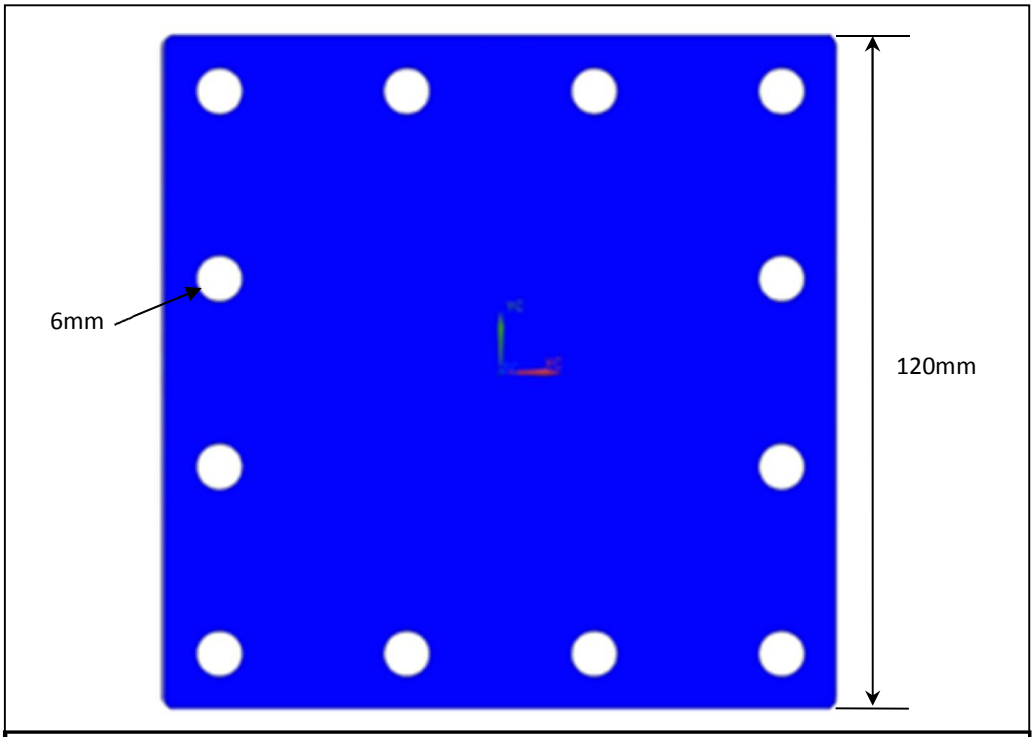

Figure 3.18: Membrane keeps hydrogen and oxygen a part.

Part-5- Gasket: This was used to protect the device from leakage. The gasket was also cut-out with the laser cutting machine with the same drawing standard as shown in picture of figure 3.19 (any gasket material can be used i.e. PTFE).

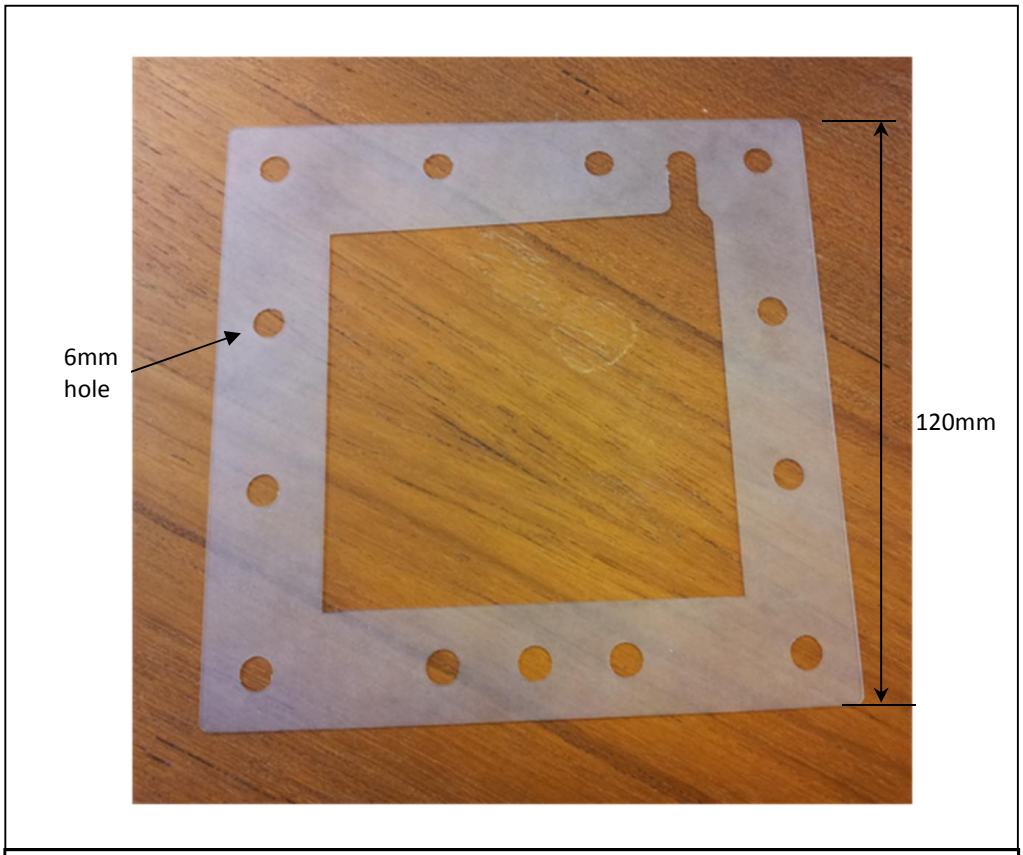

Figure 3.19: Gasket prevent the leakage in the system.

Part-6- micro-pump: figure 3.20.A is a part 3D diagram and figure 3.20.B is a picture of an actual micro-pump, which is easily available in the market and played another very important role in this project. It allowed continuous flow in the system which in turn helped to boost performance of hydrogen generation (for more details of result see chapter 4).

A

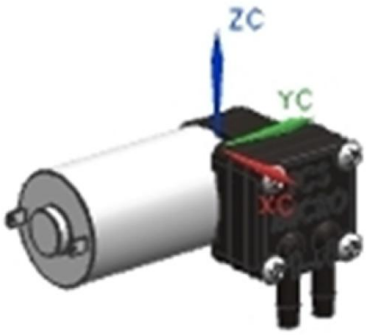

B

Figure 3.20: Electrolyte and Gas feeder pump.

Part-7- Electrolyte and Gas feeder: The cylinder height was 150mm and width 50mm diameter as illustrated in figure 3.21. The lower side of the cylinder had a 6mm electrolyte outlet which fed electrolyte to the electrochemical cell. The upper and lower side had a 6mm inlet which collected electrolyte and gas from the electrochemical cell. The gas collected in the cylinder was evacuated through a 6mm gas outlet, and the collected electrolyte was pumped out to the cell-3 module through the electrolyte outlet.

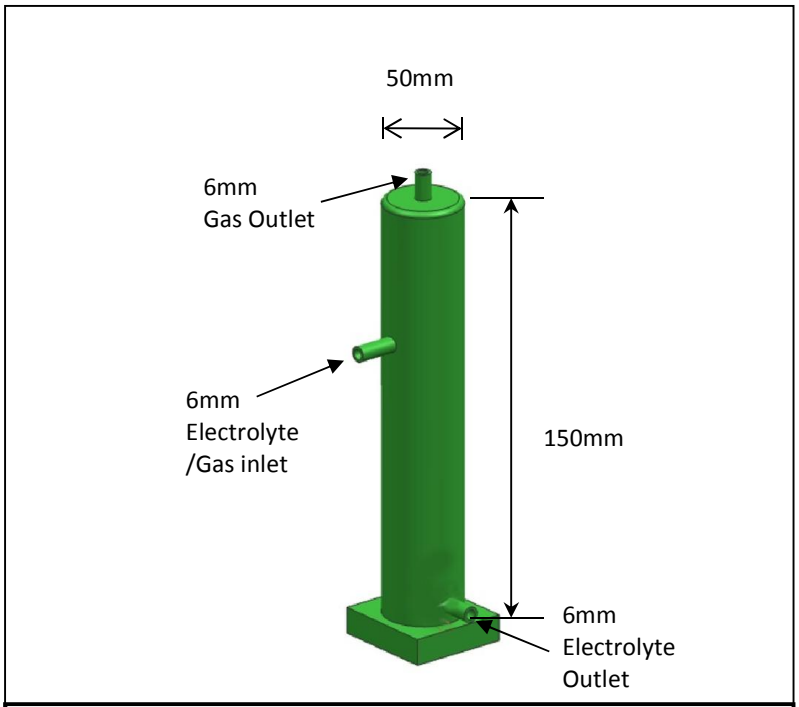

Figure 3.21: Electrolyte and Gas feeder

3.3.2) Assembling of the third electrochemical cell design (cell-3).

In the Third electrochemical cell, all the parts were carefully assembled in the following steps.

Step-1. 50mm long M6 standard stainless steel bolt used and slid into anode endplate, then placed on working desk.

Step-2. Cathode electrode set into the endplate electrode grove.

Step-3. Gasket placed in position.

Step-4. Hydrogen spacer placed on top of the gasket.

Step-5. Next the next gasket and then the membrane and then final gasket were placed in position.

Step-6. The oxygen side spacer is then placed in position.

Step-7. The anode electrode is set in the grove of the anode endplate and placed onto the spacer.

Step-8. The nuts are tightened with balanced pressure.

Step-9. The electrode and gas feeder are connected with electrochemical cell via the pump.

3.3.3) Measurements on cell-3.

Cell-3 was also run at room temperature (between 24^{O}C to 28^{O}C) with various percentage of KOH in alkaline solution (5%, 10%, 15% and 30% KOH) for 280 seconds measured at intervals of 20 seconds for three different currents (1, 2, 3 amps). The results are discussed in chapter 4..

Thereafter the power source was connected and the cell filled with electrolyte to generate the results, which are presented in chapter 4.

3.4) Introduction of gas measuring device.

Many instruments have been invented with different advantages and disadvantages to measure the gas, some of these are limited to the type of gas. Nevertheless the theme of measurement is common amongst them all, which is to measure the pressure and to calculate the volume of gas produced. This was explained in chapter-2-experimental calculation.

This project required hydrogen measurement. Therefore a customised device was constructed to get a near perfect measurement of the generated hydrogen. The device measurement concept was inspired from an old instrument called the 'manometer', which was invented by Evangelista Torricelli in 1643. The U-Tube was invented by Christian Huygens in 1661. Figure 3.22 shows the first gas

measuring device constructed in our laboratory to solve equation 2.10 in chapter 2 (P=*ρ*gh). The device contained two different sized tubes, one of 50mm in diameter which was glued on top of a 60mm square gas inlet base, the second tube was of 45mm in diameter, and was closed from one end and placed inside a 50mm tube by keeping the closed end on top. The device was filled with water and the gas was injected through the gas inlet, which lifted the cylinder based on pressure. This device was monitored closely and a gas measurement error was (±10%) found due to the 45mm tube weight, and wall resistance applying compression on the gas which caused an inaccurate result. The error in the result leads to second design of gas measuring device.

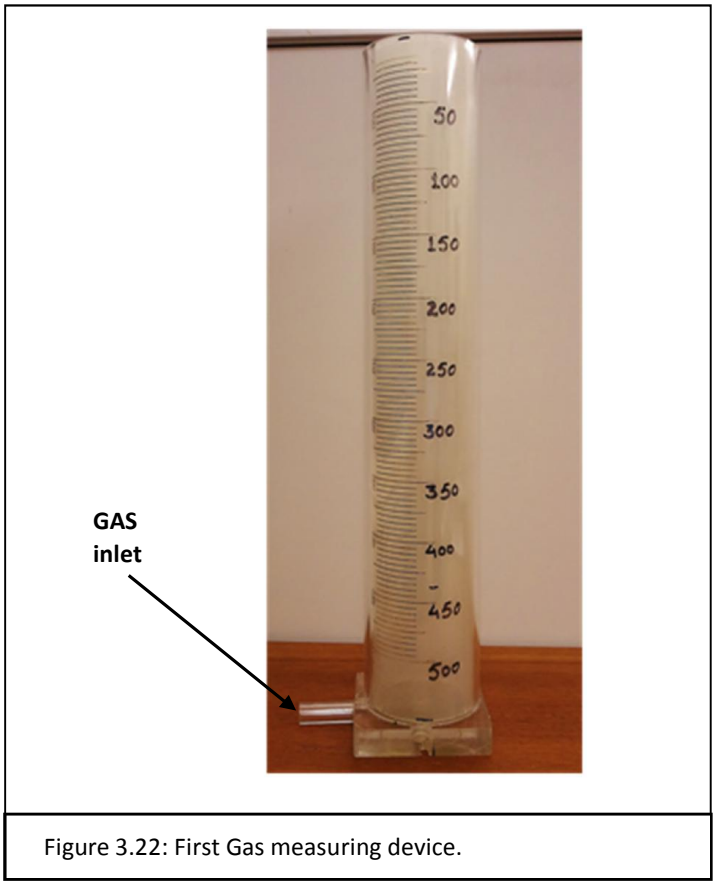

Figure 3.22: First Gas measuring device.

Figure 3.23 shows the second device design, which worked similar to the first device. The differences in this device were lighter tube materials which contained the oxygen and hydrogen measuring system. However after experiencing measurements with this device, it was found that the error reduction was (±2%) not quite satisfactory, therefore the designs presented in figure 3.24 based on atmospheric pressure were tried. Here the injected gas pushed the water through the u-tube system.

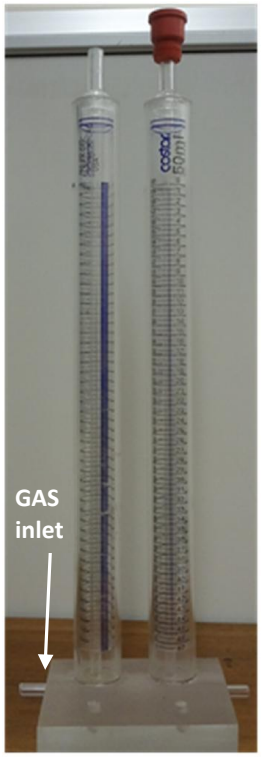

Figure 3.23: Second Gas measuring device.

Figure 3.24: Third Gas measuring device.

The third gas measuring device was constructed, where the tubes were half filled with water. This device gave rise to another issue which caused imperfection in the results (error is ±4%), which was empty space above the water. The fact that all empty space contains air unless it is under vacuum conditions, meant that this device design was also imperfect. Therefore the fourth gas measuring device design was constructed as shown in figure 3.25.

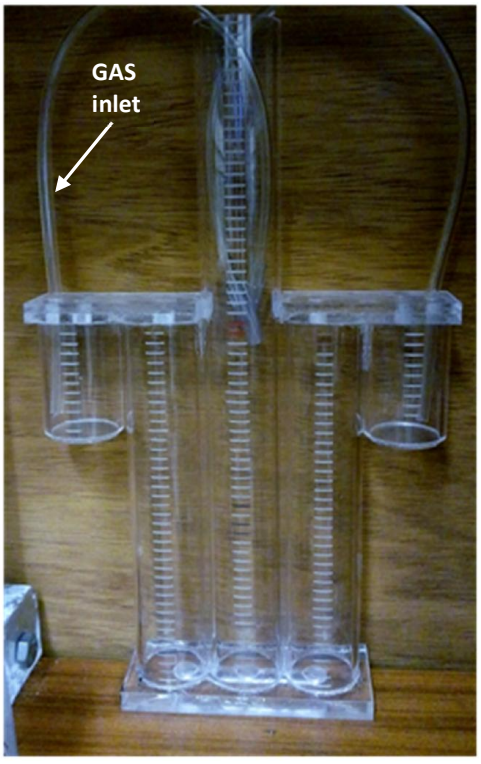

Figure 3.25: Fourth Gas measuring device.

Figure 3.26: Fifth Gas measuring device.

The fourth gas measuring device was designed to eliminate the issue of empty space, which was successfully dealt with in this design, but after the test experiment, it was realised that it was difficult to reset (released the gas from the measuring chamber) the measuring device for the next test, because the oxygen and hydrogen gases pushed the water into the centre of the tube, leaving no place to release the stored gas. Therefore the fifth gas measuring device design had a gas release valve, which released the collected gas after taking readings as shown in figure 3.26.

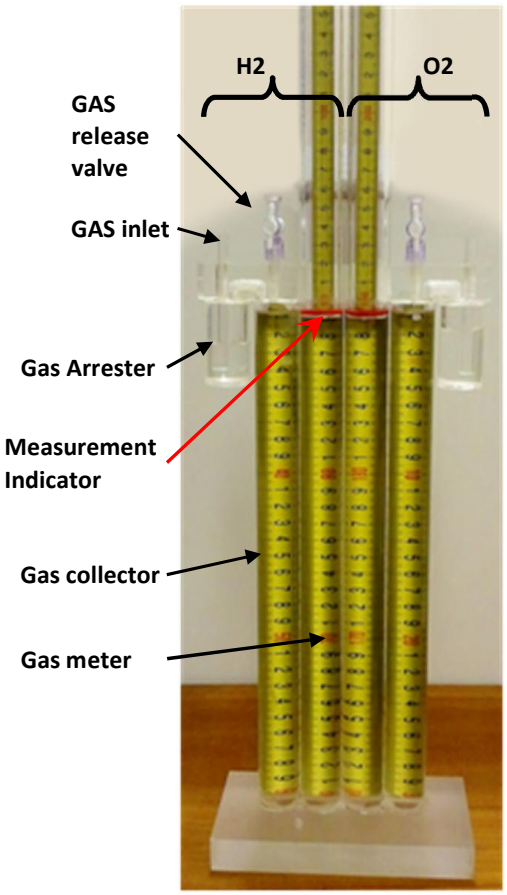

Figure 3.27: Sixth Gas measuring device.

The fifth gas measuring device results were very promising. After the good progress that resulted from the fifth measurement device, it was felt that further improvement could be afforded to achieve near perfect measurements. Therefore the sixth gas measurement device was designed and constructed as shown in figure 3.27.

The sixth gas measuring device design was the best design to measure the generated gas. It contained two gas arresters, two gas collectors, two gas meters and two gas release valves. The gas arresters passed the injected gas from the inlets to the gas collectors. The gas collector pushed the water into the gas meter tube to measure the pressure of gas. After completing the measurement, the gas release valve released the gas to reset the device for next measurement.

3.5) Conclusions

This chapter explained both the basis of the cell device design for hydrogen generation and explained the design of the measuring device which helped to verify the performance of hydrogen generation. The data collected from the measuring device was entered into the formulas explained in chapter-2 to compute the performance of the hydrogen generating cell. This is explained and discussed in the next chapter: Chapter-4 Results.

Chapter 4

RESULTS AND DISCUSSION

4) Introduction

This chapter explains the results of experiments conducted in this research. To aid in the understanding of some of the results studies were made on the structures of some of the membranes using various kinds of microscopy. These microscopic techniques are explained in appendix 1.

The objective associated with this research was to design low cost and high performance (in terms of hydrogen production rate) on-demand electrochemical hydrogen generation. The following four areas were considered in this research in order to improve the performance of the process.

4.1) Membrane : To find the best possible membrane to keep the generated hydrogen and oxygen separate.

4.2) Electrolyte : To make the best possible composition of electrolyte material to get a higher ion exchange[1].

4.3) Electrode : To find the best electrode material to generate hydrogen.

[1] *Ion exchange is a known process entailing exchange of ions between two electrolytes or between an electrolyte solution and a complex.*

4.4) Device Design : To optimise the equipment design to facilitate facile breakup of water molecules in to hydrogen and oxygen.

4.1) Membrane

The universal use of a membrane is to filter solid particles from a liquid or a gas. Alternatively a filter may be used to separate a liquid from a gas. The membrane selection to filter materials from each other is based on classifications such as their morphology (symmetrical distribution of pores, size of pores (or area that is non-porous, and strength of material of the membrane) and method of molecular movement (electrical potential difference, concentration difference, pressure difference) to achieve filtration. The hydrogen generation required safe production of the gas (free from the risk of fire); therefore the membrane is an important part of the cell, and is used to separate the hydrogen and oxygen. There are two categories of membranes used in electrolysis; one is a mono-polar ion exchange membrane and the other is a bi-polar ion exchange membrane. Mono-polar membranes are available in the market for fuel cell technology such as 'Nafion membranes'[2] [1-3] which bear a higher economical cost compared to microporous bi directional membranes which are cheaper. The monopolor membranes only allow one directional ion exchange and prevent electron flow. The bipolar types however, allow movement of molecules in both directions while allowing electron flow. The unique design associated with the apparatus applied in this project, enabled use of the cheaper type of membranes, as the design undertaken in this work allowed exchange of electrons and protons in any direction. Hence, to evaluate the efficiency of this design (which was aimed at low cost hydrogen

[2] *Nafion membranes are the membranes that only exchange protons, therefore these membranes are widely used for proton exchange membrane (PEM) fuel cells to generate electricity.*

production), several micro pores gas separator membranes were evaluated, these membranes and their specifics are highlighted in table 4.1.1 [87] and were obtained from Freudenberg Nonwovens L.P.

Table 4.1.1: *Specific properties of various bi-polar microporous membranes*.

Membrane	Thickness (um)	Ion Exchange Capacity (mmol/g)	Porous	Strength	Residue	Description
1001	180	0.5	Fully Blocked	Fragile	Yes	Not suitable
1007	171	0.68	Porous	Strong	Less	Gas mixing on high pressure
1008	140	0.5	Fibre structure	strong	No	Gas mixing on high pressure
1009	125	0.69	Woven Fibre	strong	No	Gas mixing on high pressure
1010	32.51	1.11	Porous but does not allow gas to pass	very strong	No	suitable for high pressure and chemical

The membrane 1001 thickness is 180 microns that is the largest membrane in terms of thickness among all the membranes that were tested. Its ion exchange capacity was 0.5 millimoles per gram which had one of the lowest ion exchange capacity values among the membranes tested in this work. Suitable properties of membrane for the objectives of this research were structural stability of the

membrane, symmetric distribution of pores, size of pores in relation to pressure resistance, strength of membrane against the electrochemical reaction occurring during the electrolysis process in potassium hydroxide; and the higher ion exchange capacity which causes a higher rate of hydrogen production.

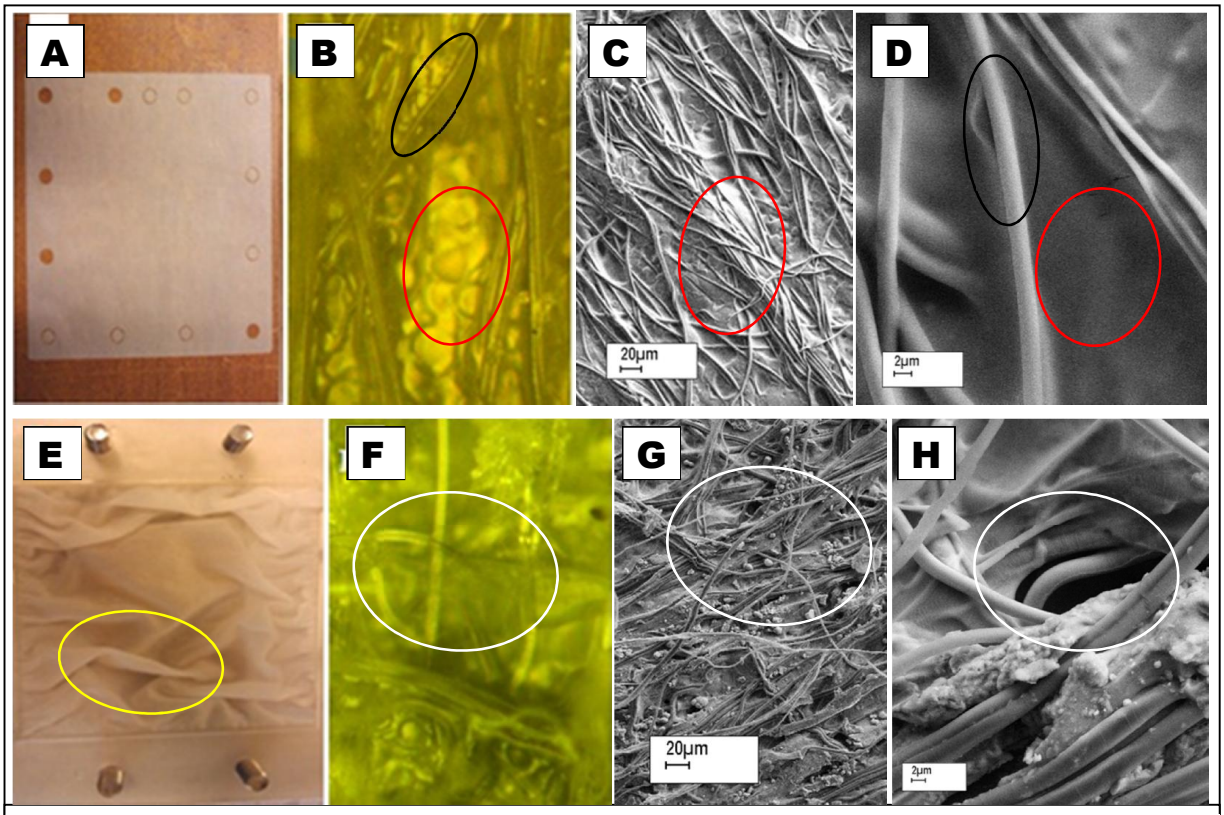

Figure 4.1: Various images of membrane 1001. (A)- Digital camera image, (B)- Optical microscope images under 100 times magnification before the electrochemical reaction, (C), (D)- SEM images before any process, (E)- Digital camera image showing the expansion due to the electrochemical reaction and (F)- Optical microscope images under 100 times magnification after the electrochemical reaction the changes are due to the electrolysis process in 30% KOH alkaline solution at 1amp and 26°C for 10min [34]. *(G, H)- SEM image after process.*

In the various images of membrane 1001 shown in figure 4.1. Figure 4.1(A) is the actual appearance of the membrane taken by digital camera before any process was applied. The membrane 1001 is a fragile membrane to an extent that it cannot resist even slight pressure induced by touching, thus it was difficult to hold the

membrane in a hydrogen generation cell. Apart from this, it has fully blocked pores as pointed to in the red circle in figure 4.1(B), 4.1.1(C) and 4.1.1(D), this limited the ion exchange process (see figures 4.1.1(B) taken by Carl Zeiss Axioskop 2 MAT optical microscope fitted with a camera Axiocam MR-5 under 100 time magnification and 4.1.1(C) and 4.1.1(D) which show the scanning electron microscope (SEM) image taken using the SE detector at 10KV, working distance (WD) 8mm, and x500).

Whereas the effects of the electrochemical reaction caused by electrolysis in the potassium hydroxide (KOH) alkaline solution, in the presence of the membrane shows the latter has expanded as illustrated in figure 4.1(E), (picture taken by digital camera). Similarly figure 4.1(F) is an optical microscope image (100 times magnification), here a disordered/disrupted membrane structure is apparent, and open pores are highlighted with the white circle. Figures 4.1.1(G) and (H) are (SEM) images of the disordered/disrupted membrane structure. In addition figure 4.1(H) also shows an open pore caused by the electrochemical process. The black circle demonstrates how a stable membrane structure should appear (see figure 4.1(B) and (D). This is very different to the area shown in the white circle in figure 4.1(F).

Therefore the membrane 1001 is not a suitable membrane for hydrogen generation. Several other membranes were tested with a view to finding a suitable membrane for hydrogen generation. The physical structures (morphology) of membranes 1007, 1008 and 1009 as summarized in Table 4.1.1, were all good with regards to symmetric distribution of pores and membrane strength when working in the system; however, the thicknesses of membranes 1007, 1008 and 1009 are less than that of membrane 1001. The ion exchange capacity of membrane 1007 is 0.68 mmol/g and that of 1009 is 0.69mmol/g which are both slightly higher than that of membrane 1001.

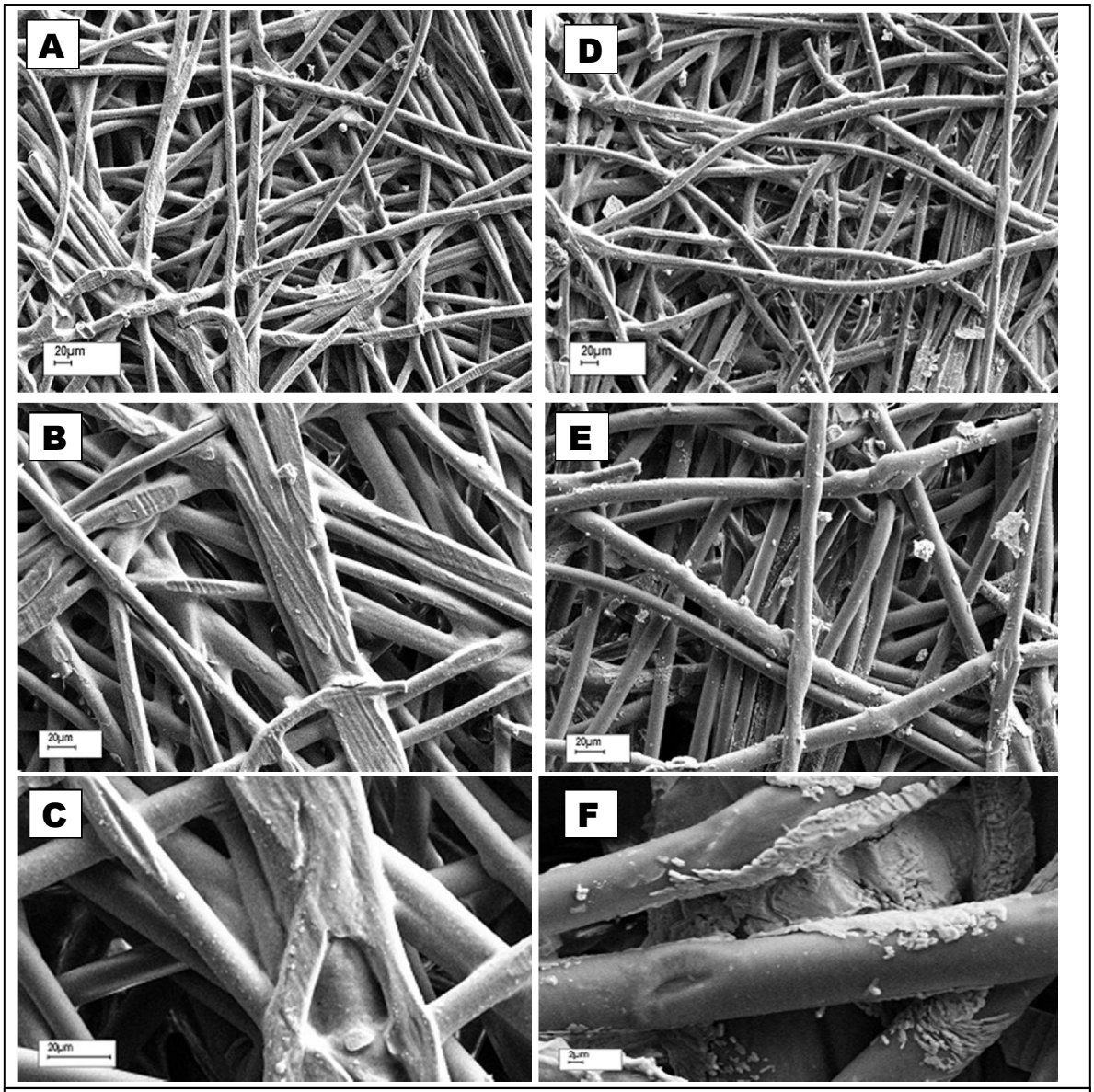

Figure 4.2: Various SEM images of membrane 1007. (A) SEM image is taken at x500 resolution, (B) is taken at x1000 resolution and (C) was captured at x2K resolution before any process was allowed to occur. Similarly (D), (E) and (F) are after the electrolysis process in 30% KOH alkaline solution at 1amp and 26^{o}C for 10min.

SEM images of membrane 1007 show the effect of electrolysis on the membrane in figure 4.2. Figure 4.2 (A), (B) and (C) are the before any process images and figure 4.2 (d), (E), (F) and (G) are after the electrolysis process in 30% KOH alkaline solution has occurred.

In figure 4.2 (A) the micrograph shows that the fibres making up the membrane are around 20 to 30 μm thick and very long. Each fibre is predominantly straight lying alongside each other or over each other. In contrast in figure 4.2 (D) after electrolysis each fibre displays a more curved appearance. This change is most probably due to pressure build up during the process as gas is evolved. There is also evidence in figures 4.1.2 (D), (E) and (F) of enlarged pores caused by the increase in pressure. Furthermore there is also evidence for some particulate residue in these micrographs particularly in figure 4.2 (E) and (F). In contrast no such particles are visible in the intact undisturbed membrane in figure 4.2 (B) and (C). There is some evidence of a coating on some of the fibres in figure 4.2 (C) (the highest magnification), this may be the binder that holds the fibres together. In figure 4.2 (F) there is also evidence of a partial coating; this appears to have been affected by the electrolysis process and may have been partially removed during the process.

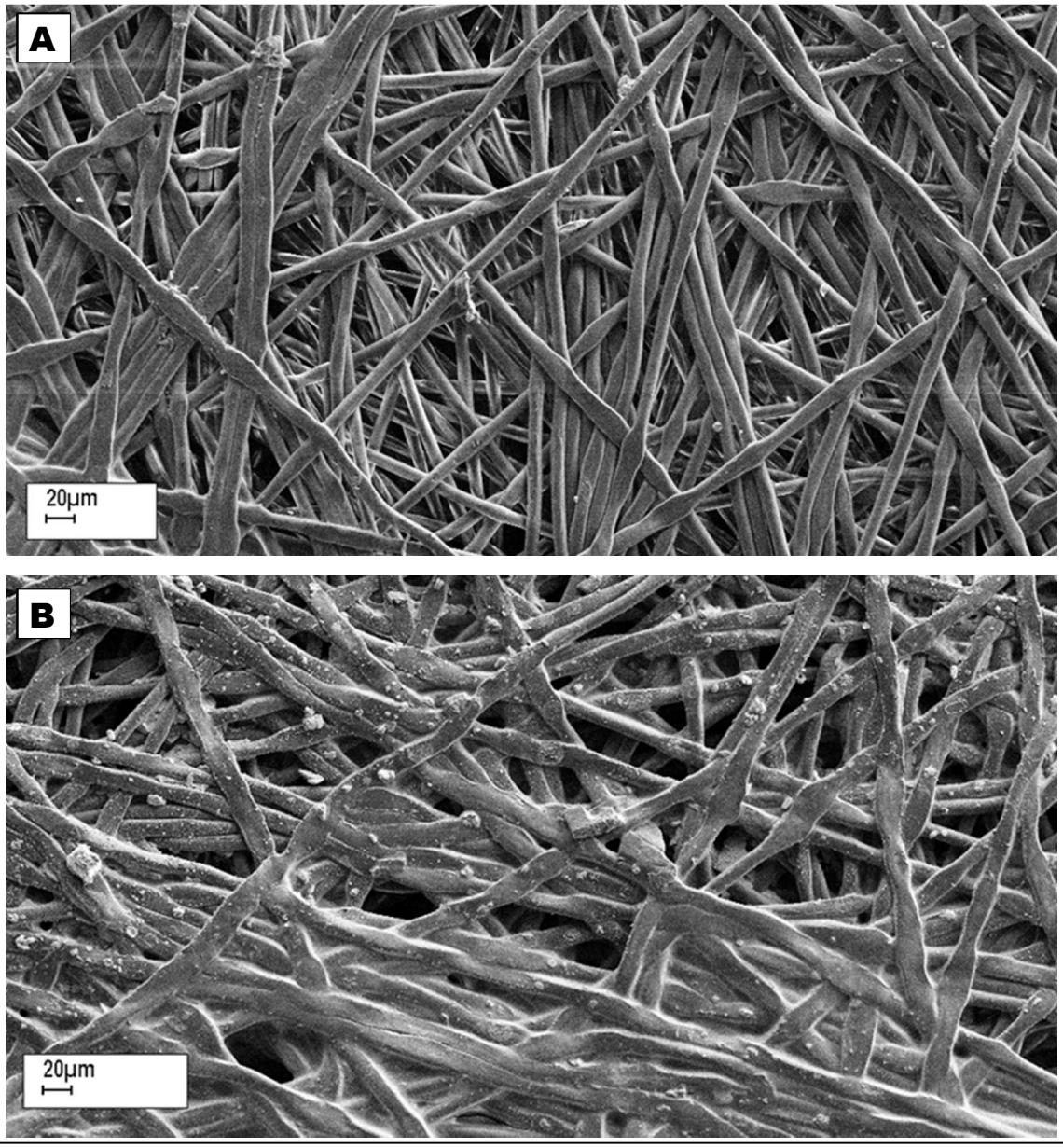

Figure 4.3: SEM images of membrane 1008 taken at x500 resolution, (A) is before any process is carried out, and (B) is after the electrolysis process in 30% KOH alkaline solution at 1amp and 26^{o}C for 10min.

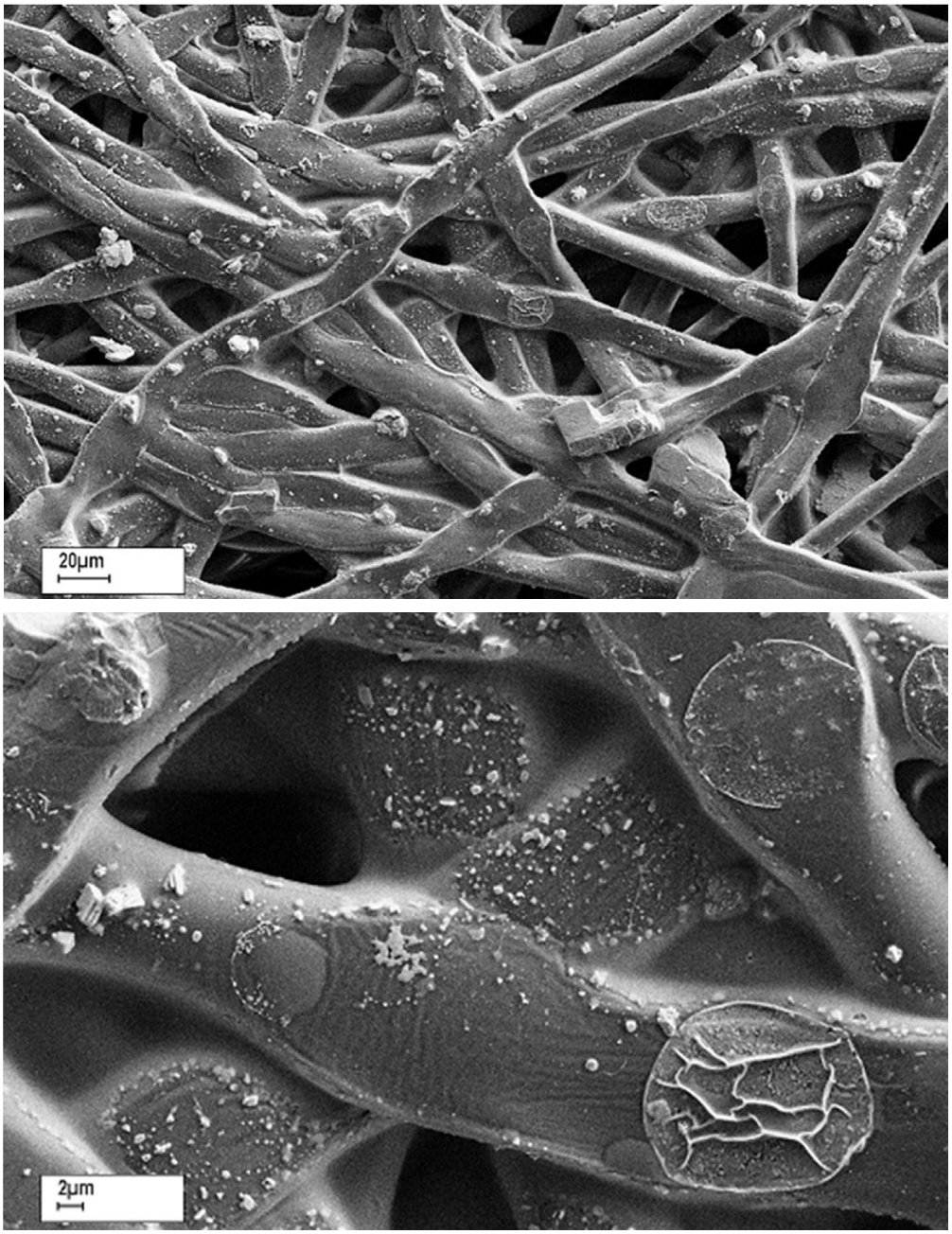

Figure 4.4: SEM images of membrane 1008, (A) is taken at x1000 resolution and (B) is taken at x5K resolution after the electrolysis process in 30% KOH alkaline solution at 1amp and 26^{o}C for 10min.

Membrane 1008 gave an ion exchange capacity that is slightly lower than membrane 1007 but it does not release obvious residue into the solution. This may be why the fibres remain intact in relation to each other as shown in the SEM micrographs in figure 4.3 and figure 4.4. Thus for membrane 1008 there is no distortion in the fibres after electrolysis. It is obvious from figures 4.1.3 and 4.1.4 that membrane 1008 is much more close packed/dense than membrane 1007. Again particulate residue is visible in figures 4.1.3(B) and 4.1.4 (A) and (B). In the latter case there is evidence that this particulate has been deposited from remaining solution droplets when the membrane dried out. The most likely candidate for this material is crystalline KOH.

Images of Membrane 1009 SEM are shown in Figure 4.5. Micrograph (A) was taken at x500 resolution and (B) at x2K resolution of a before any process take place and after electrochemical reaction micrograph shown in figure 4.5 (C) and (D). The structural properties of Membrane 1009 (close packed/dense, strong, not releasing residue) are similar to membrane 1008, however, the ion exchange capacity is slightly higher. Therefore membranes 1001 to 1009 in table 4.1.1, are not suitable for this hydrogen generation project. Consequently other membranes were considered for use and membrane 1010 had the most desirable properties (as shown in figure 4.6 to figure 4.9).

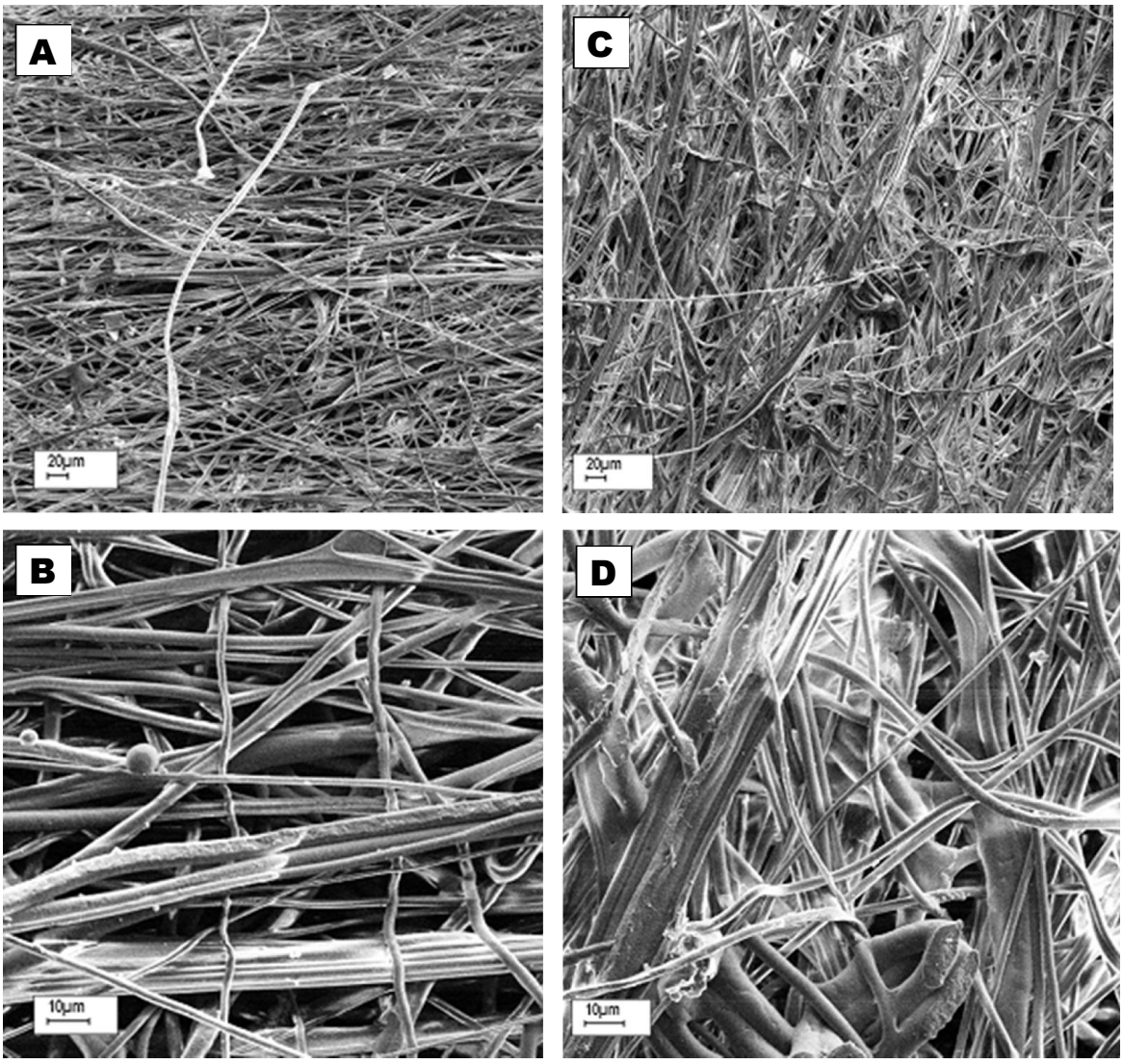

Figure 4.5: Various SEM images of membrane 1009. (A) and (B) SEM image is taken at x500 resolution, (B) and (D) is taken at x2K resolution. (A) and (B) are before any process images, (C) and (D) are after the electrolysis process in 30% KOH alkaline solution at 1amp and 26^{o}C for 10min.

In Figure 4.6 the image shown was obtained by Brussieux C et.al. [2], with a high speed camera (PCO 1200hs) mounted on a microscope (Zeiss STEMI SV-11). These images display bubble formation at the electrode surface [88]. Brussieux C et.al, discussed/explained the formation of bubbles in relation to the size of a H_2 bubble in his paper, he found the bubble size before and after release is about 5.5mm in diameter [88].

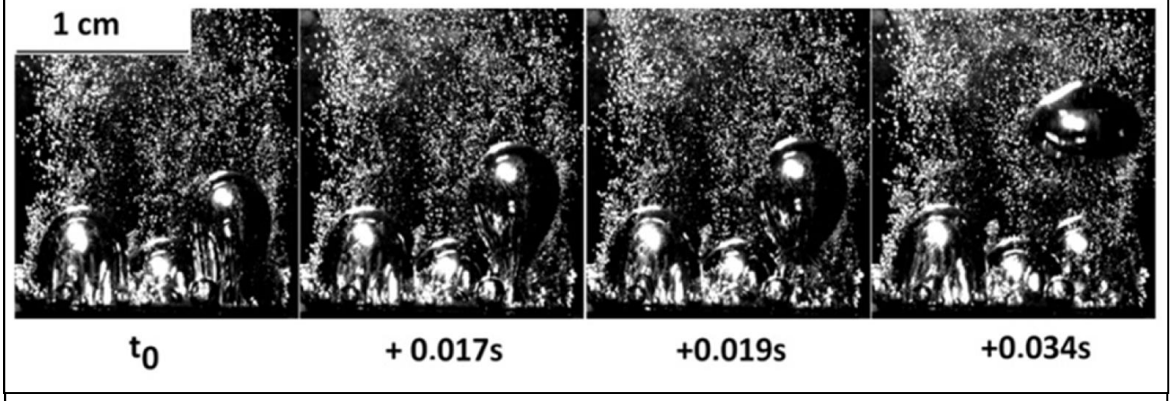

Figure 4.6 Image displays H_2 bubble size taken by high speed camera (PCO 1200hs) mounted on a microscope (Zeiss STEMI SV-11) [88]

figure 4.7 and figure 4.8 show the micrograph of membrane 1010 at different resolution as received before any process take place. Micrographs of membrane 1010 illustrate the stable structure with less than 220nm pores. These will block the gas mixing and provide more strength to membrane. Therefore membrane 1010 was tested under different conditions for its reliability and strength.

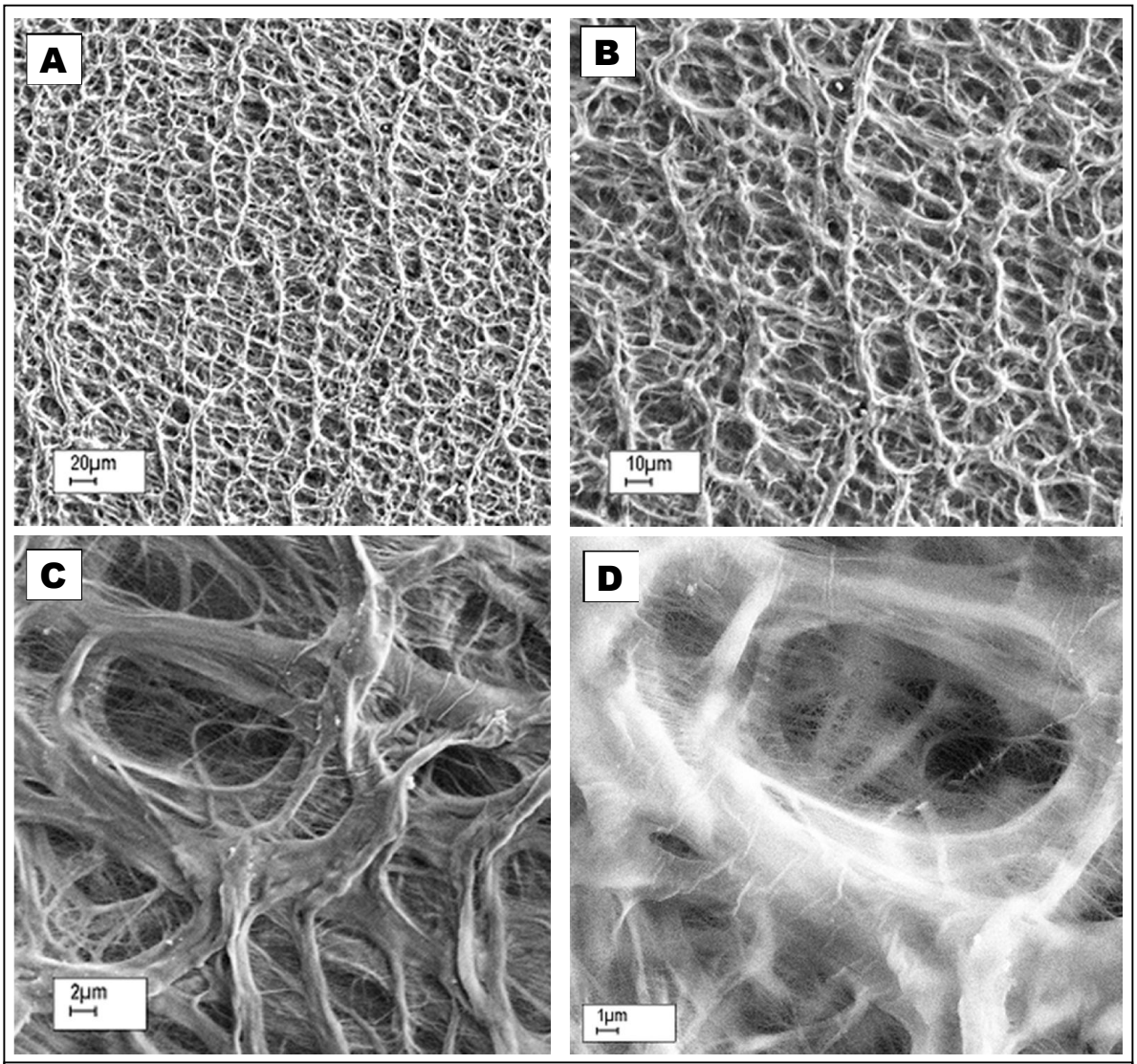

Figure 4.7: Various SEM images of membrane 1010 at different resolution in its as received condition. Micrograph (A) is taken at x500 resolution, (B) at x1K resolution, (C) at x5K resolution and (D) micrograph is at x10K.

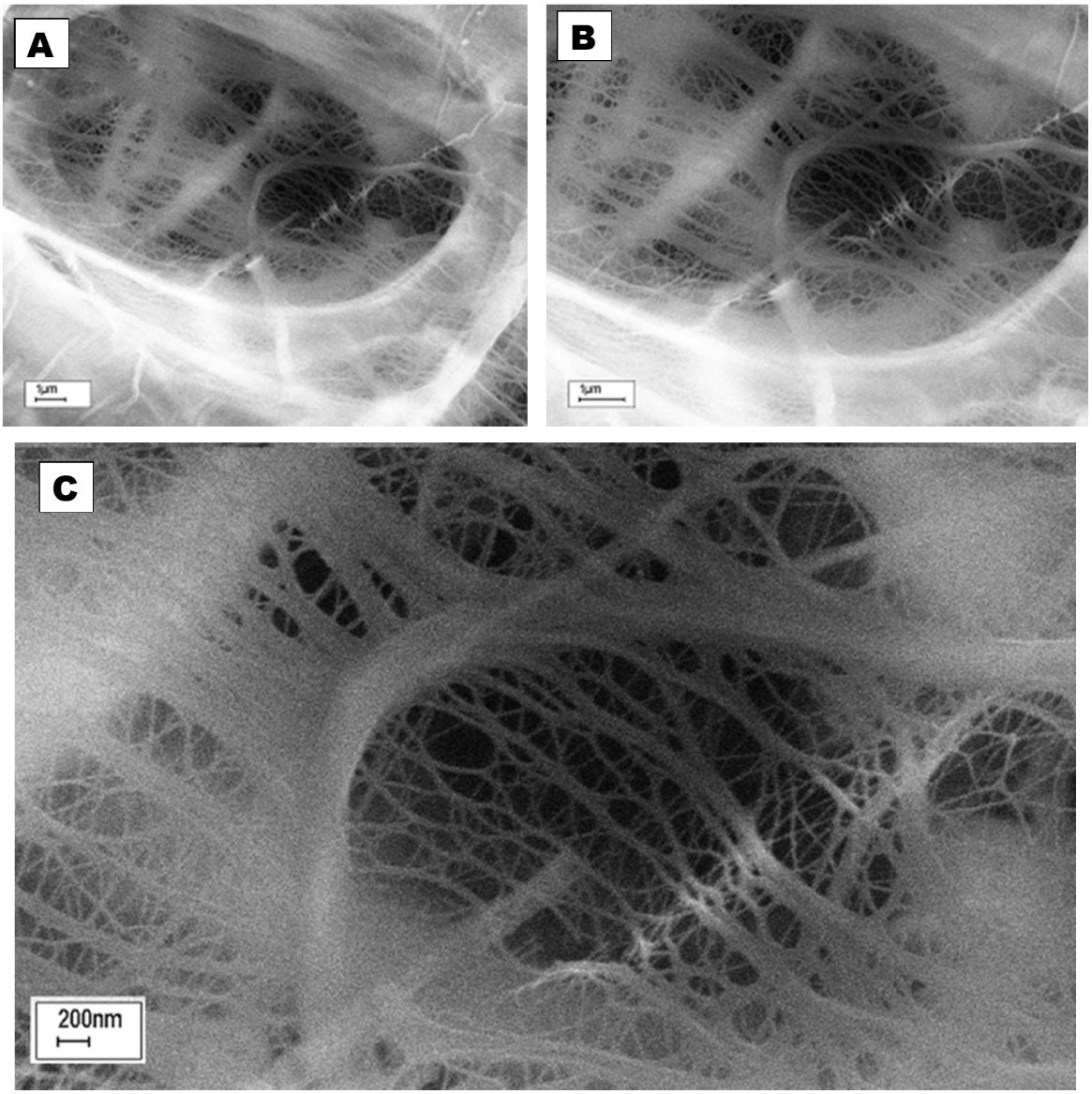

Figure 4.8: Various SEM images of membrane 1010 at different resolution again as received. Micrograph (A) is taken at x20 K resolution, (B) at x30K resolution, and (C) micrograph is at x50K.

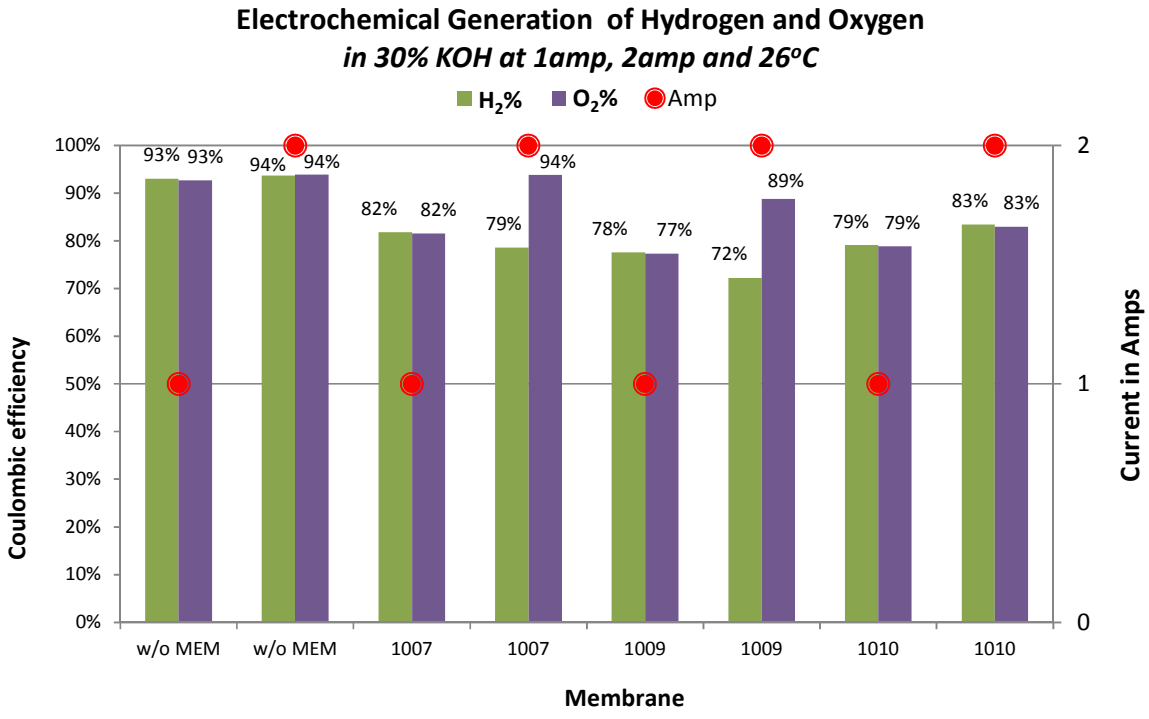

Figure 4.9: Graph of coulombic efficiency comparison for with and without membrane

Figure 4.9 illustrates the coulombic efficiency [3] comparison of hydrogen and oxygen generation from several types of membranes. The first test was conducted without a membrane and 93% hydrogen and oxygen production performance was observed, which meant the ratio of hydrogen and oxygen production was the same under 1 amp & 2 amps of current flow. Similarly at 1 amp current flow, all three membranes 1007, 1009 and 1010 had the same rate of hydrogen and oxygen production. However at a current flow of 2 amps, for membrane 1007, the oxygen production was 94%, which is higher than the apparent hydrogen production. Similarly under a current flow of 2 amps for membrane 1009, the oxygen

[3] *Faraday efficiency is also known as the coulombic efficiency, which explains the efficiency of electron transfer in the system to facilitate an electrochemical reaction.*

production was 89%, also higher than the apparent hydrogen production as illustrated in figure 4.9. This is an indication of the gases mixing under high pressure. The mixing of gas is dependent on the pressure equilibrium in the system, therefore the higher ratio of oxygen generation is due to the higher pressure in the hydrogen chamber that expands the pores of the membrane and pushes the hydrogen into the oxygen chamber. This results in a higher apparent efficiency of oxygen production. Hence the drawback of membranes 1007 & 1009 were that they mix the two gasses at high pressure which renders them unsuitable for our objective.

Using membrane 1010 resulted in a figure of 83% production of hydrogen and oxygen using a current flow of 2 amps. This represents a stable production under high pressure. The Ion exchange capacity of membrane 1010 was 1.11mmol/g (the highest among all the membranes in table-4.1.1). This membrane also had a high degree of strength and had suitable reliability to produce hydrogen better than all the membranes highlighted in table-4.1.1. In addition it did not appear to contaminate the electrolyte by releasing any residues. Most importantly it provided pure hydrogen and oxygen (displaying the same efficiency of oxygen and hydrogen generation as these observed on membranes 1007 & 1009). This is illustrated in figure 4.9. Therefore the properties of membrane 1010 are by far the best for its application in terms of being low cost, high performance, safe[4] and in a reliable morphology for hydrogen production. Therefore, membrane 1010 was the membrane of choice for the next phases of our program.

[4] *Hydrogen is highly combustible gas if it combines with oxygen. Therefore it is highly explosive if both gasses are generated and stored in one chamber.*

4.2) Electrolyte

Electrolysis is a process by which electrons are forced via electrodes through/into an electrochemical cell, thus causing a chemical reaction. The cathode is the metal surface which provides the electrons for the process, and does not dissolve in the solution because reductions take place at its surface. The anode is positively charged, it attracts negative ions (by electrical potential) these give up electrons (and become oxidised) and in this process drive the circuit. The common method of reducing the oxidation on the electrode surface is to add enough ions into the electrolyte to maintain the desired chemistry.

The electrolyte is a substance that contains atoms (in the form of ions) or small groups of atoms that carry an electric charge to conduct electricity. Deionised water is a weak electrolyte and a very poor conductor of electricity because it only has a very small quantity of H^+ and OH^- ions in the solution. Similarly plain water is also a weak conductor but better then deionised water, due to more ions being present in the plain water.

4.2.1) Electrolyte tests in a cell.

Initial experiments were conducted using plain water to see the effect of corrosion in the cell-3 design. Figure 4.10 illustrates the corrosion on the electrode and membrane surface. Similarly in figure 4.11 the micrograph displays corrosion depositions on membrane 1010

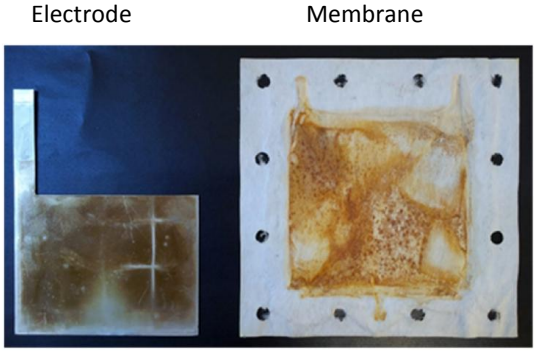

Figure 4.10: Corrosion effects of electrolysis in water at 1amp and 26°C

surface and the red circle in figure 4.12 underlines the corrosion presence by material analysis at the membrane 1010 surface, The analysis was conducted using Energy Dispersive X-Ray analysis (EDX).

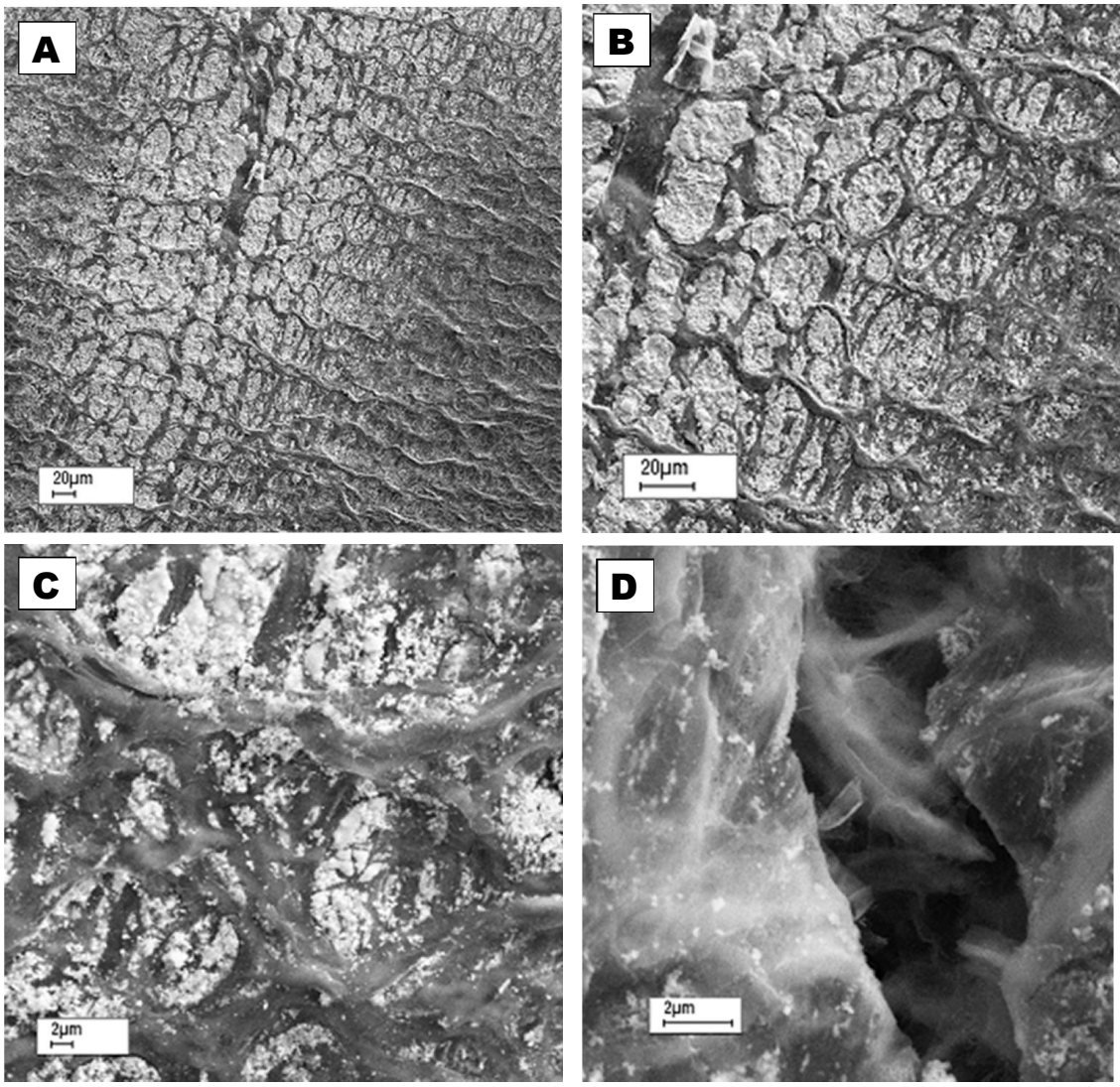

Figure 4.11: Various SEM images of membrane 1010 at different resolution taken after it has been used in the electrolysis of water at 1amp and 26^{O}C. Micrograph (A) is taken at x500 resolution, (B) at x1K resolution, (C) at x5K resolution and (D) micrograph is at x16K.

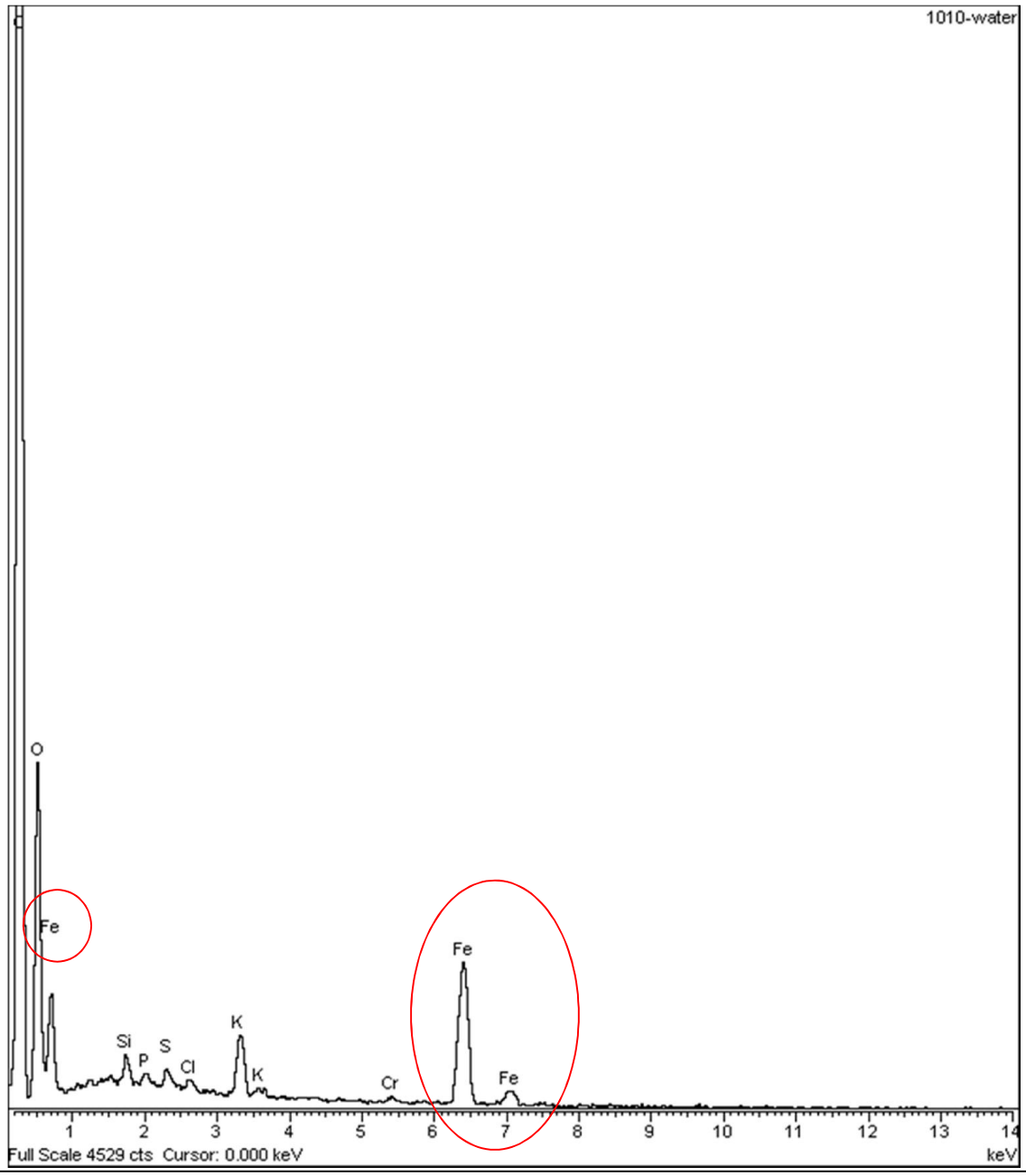

Figure 4.12: Membrane 1010 material analysis by EDX is taken after electrolysis process in tab water. Red circle underline the corrosion presence.

The cell was then run using several different KOH concentrations with numerous current flows, with and without the membrane to achieve a suitable comparative data set. The micrographs in Figure 4.13 show the membrane 1010 surface analysis after the electrolysis process in 30% KOH and indicate a smooth surface area. The bulk material on membrane surface is due to the electrolyte dried at membrane surface.

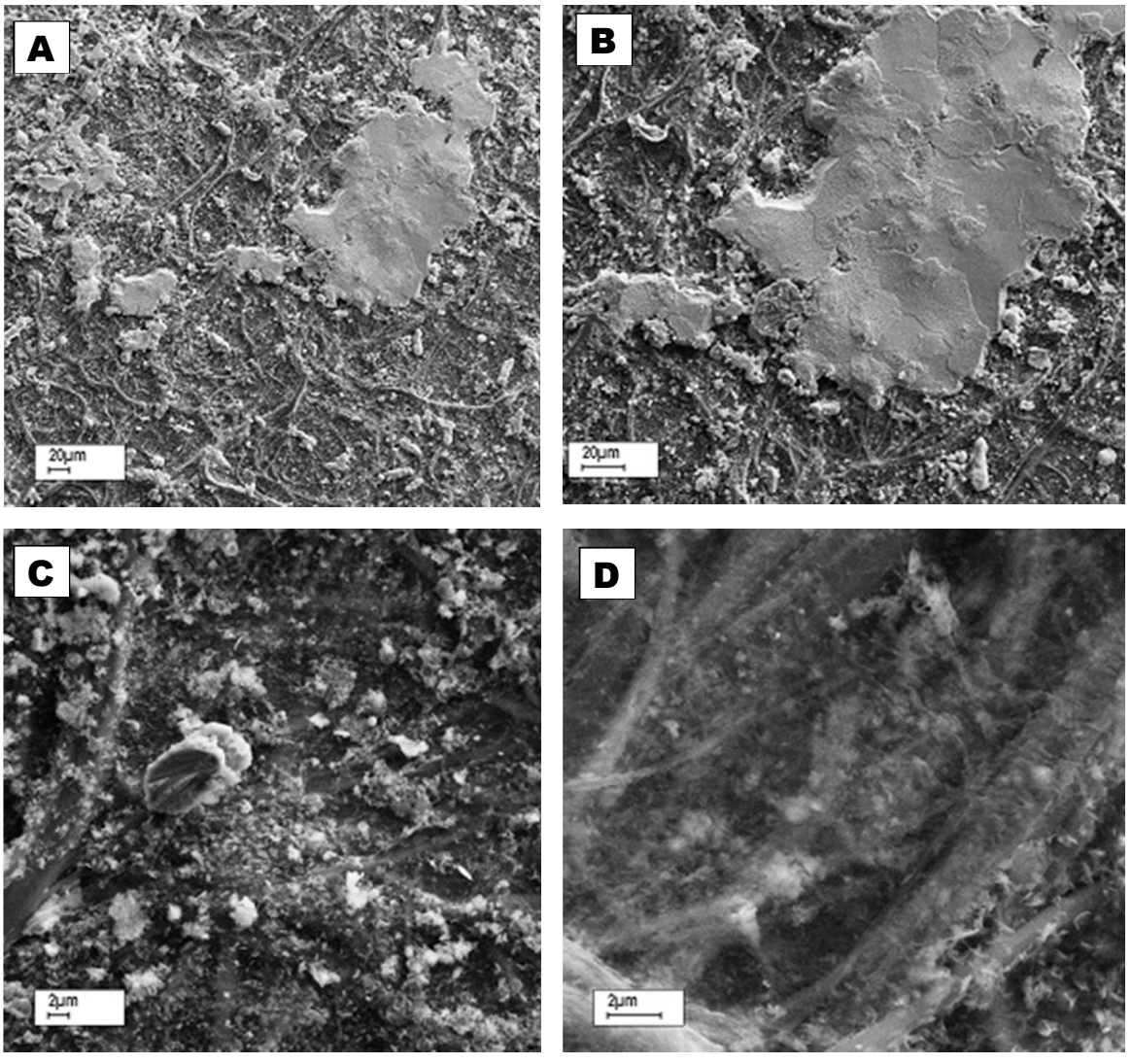

Figure 4.13: Various SEM images of membrane 1010.at different resolution. Micrograph (A) is taken at x500 resolution, (B) at x1K resolution, (C) at x5K resolution and (D) micrograph is at x12K are taken after electrolysis process in tab water at 1amp and 26^{O}C.

The EDX analysis shown in Figure 4.14 demonstrates that the material present on the membrane surface is only what is expected of the membrane and no trace of corrosion products were found in the membrane surface. Therefore the electrolyte composition is suitable for keeping the electrode surface intact and thus provides the best ionic solution for the desired performance of the cell.

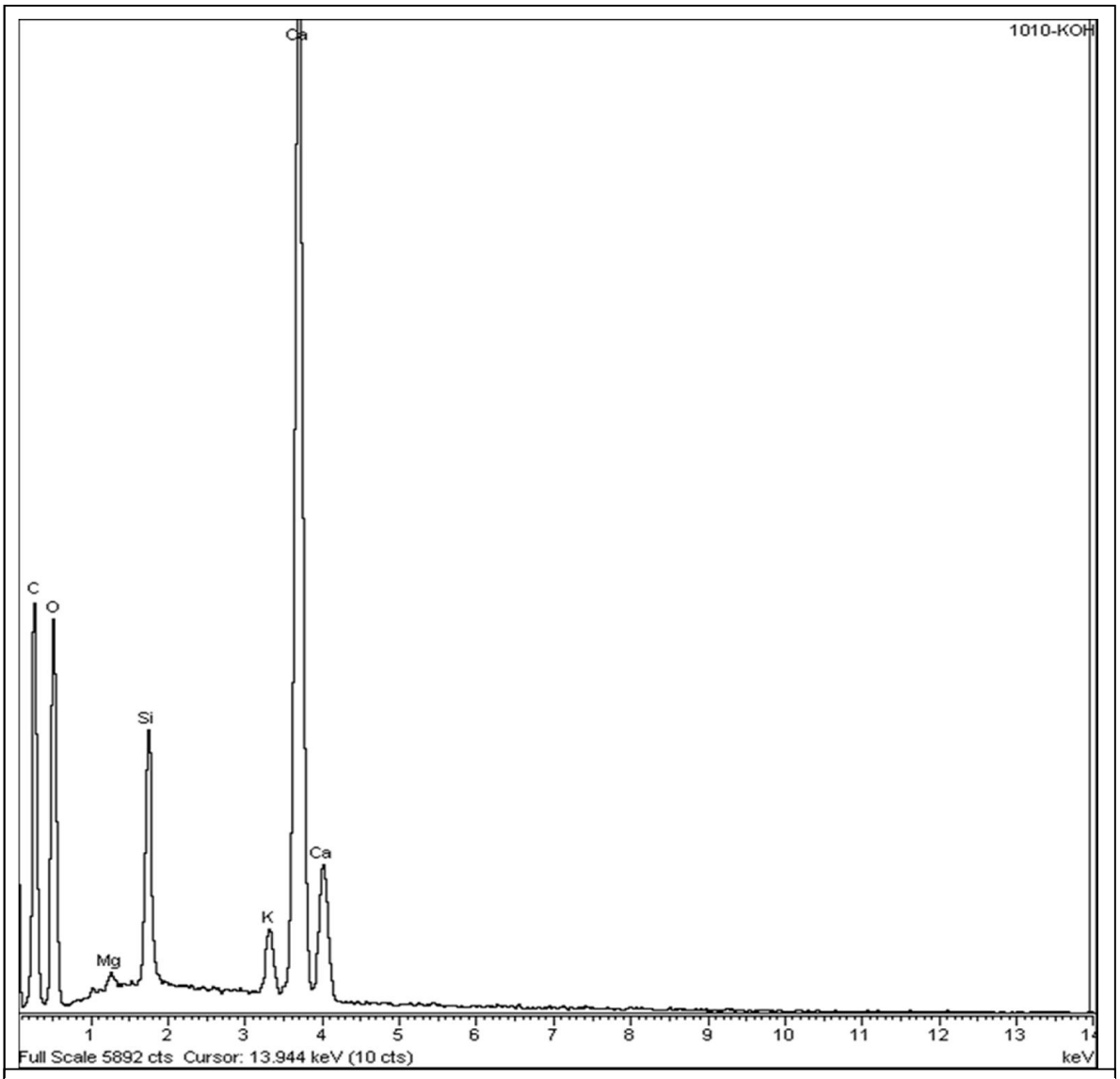

Figure 4.14: Membrane 1010 material analysis by Energy Dispersive X-Ray analysis (EDX) is taken after electrolysis process in 30% KOH at 1amp and 26^{O}C.

Figure 4.15-A shows the plain water as a black line. The result will be discussed in the next paragraph. This corrosion is a well-known phenomenon and there have been many reports in the literature that indicate to the use of potassium hydroxide (KOH), to increase the ionic strength in the electrolyte [5-8] to overcome the corrosion problems. The black line (see Figure 4.15-A) shows the results for the water test. In the first 20 seconds although gas bubbles were observed to form it was not simple to collect enough volume to evaluate. The values for coulombic efficiency would have been low (lower than 76%). This is partially due to the time taken to set up defusing layers in the cell and double layers and electrodes.

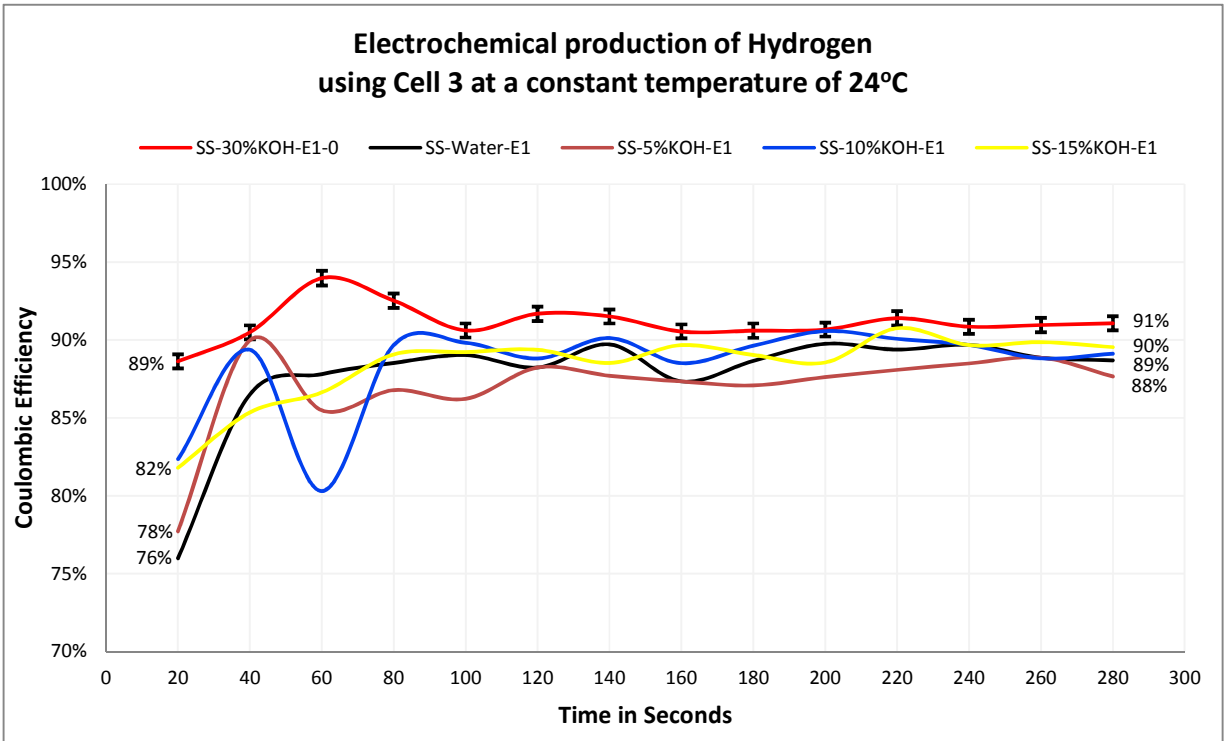

Figure 4.15-A: Electrode Coulombic efficiency comparison at different electrolyte composition without membrane cell at 1amp and 24°C.

In the second test experiment 5% KOH aqueous alkaline solution was used without a membrane, this is shown as a brown line in figure 4.15-A. Here an average performance of 88% was achieved in conditions of 1 amp and 2.5V at 24^{O}C. The hydrogen production rate was not very different compared to the plain water electrolyte, except that the ion exchange balance was a little faster under the lower voltage, compared to the plain water.

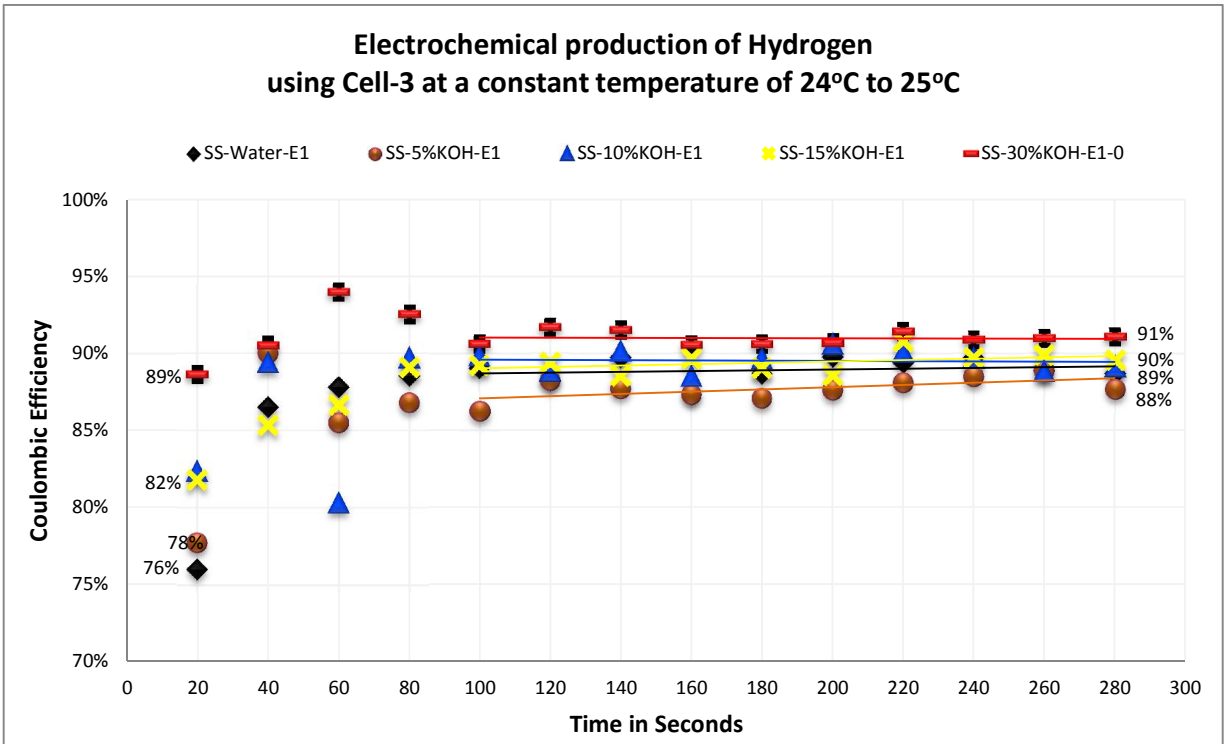

Figure 4.15-B: Electrode Coulombic efficiency linear trend comparison at different electrolyte composition without membrane cell.

In the next experiment 10% potassium hydroxide (KOH) alkaline solution was used, by the 1% performance increase (as sheen in the graph with a blue line). Similarly another 1% performance boost was achieved with 15% KOH alkaline solution at 1 amp and 2.5V (at 25^{O}C) test conditions (yellow line). The last test on

the without membrane cell was conducted with a 30% KOH alkaline solution, (red line) and a 91% average performance was achieved in conditions of 1 amp and 2.2V at 26^{O}C. The average performance difference between 5%, 10%, 15%, and 30% KOH electrolyte composition is about 1%, except for the 30% KOH concentration which required less voltage to decompose water into hydrogen and oxygen, and provided better protection to the anode electrode from corrosion. It also achieved a 7% boost at the activation point (first 20 seconds) as illustrated with the red line in figure 4.15-A. Similarly figure 4.15-B illustrates the results as linear trends from the stability point, these are almost parallel to each other once the cells had stabilised. In addition the 30% KOH solution behaved better in the initial stages of the experiment coming to equilibrium faster and over a smaller range of variation in efficiency.

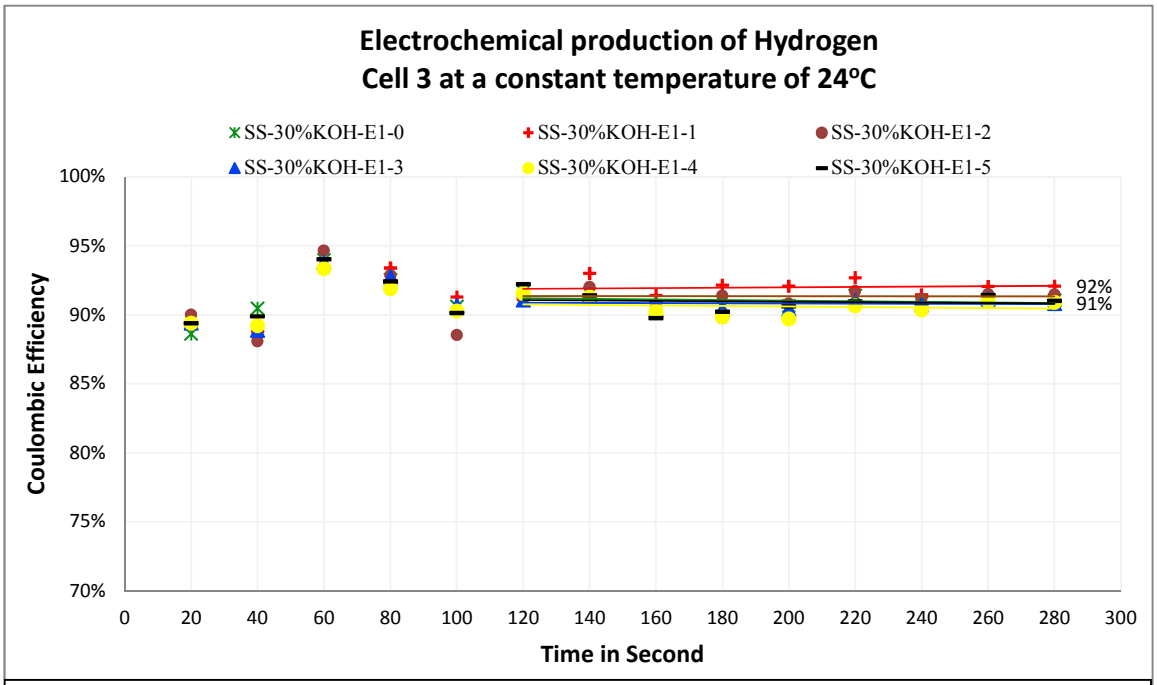

Figure 4.16-A: Performance stability test on 30% KOH electrolyte in an electrochemical cell at 1amp and 24^{O}C (without a membrane). A stable linear trend is apparent after the homogeneous point.

Based on the above results, 30% potassium hydroxide (KOH) is the best composition for electrochemical hydrogen production. Therefore the 30% KOH alkaline solution was selected for carrying out reliability tests. The experiment was repeated several times to establish the performance of hydrogen production over time without using a membrane. Figure 4.16-A illustrates the stability test of hydrogen production at 30% KOH electrolyte for six independent runs. In total twelve results were considered for the standard deviation calculation, and the reliability of the electrolyte was found with an error of ±1% (as illustrated in figure 4.16-B) and the linear trend shown in figure 4.16-C illustrates continued stability.

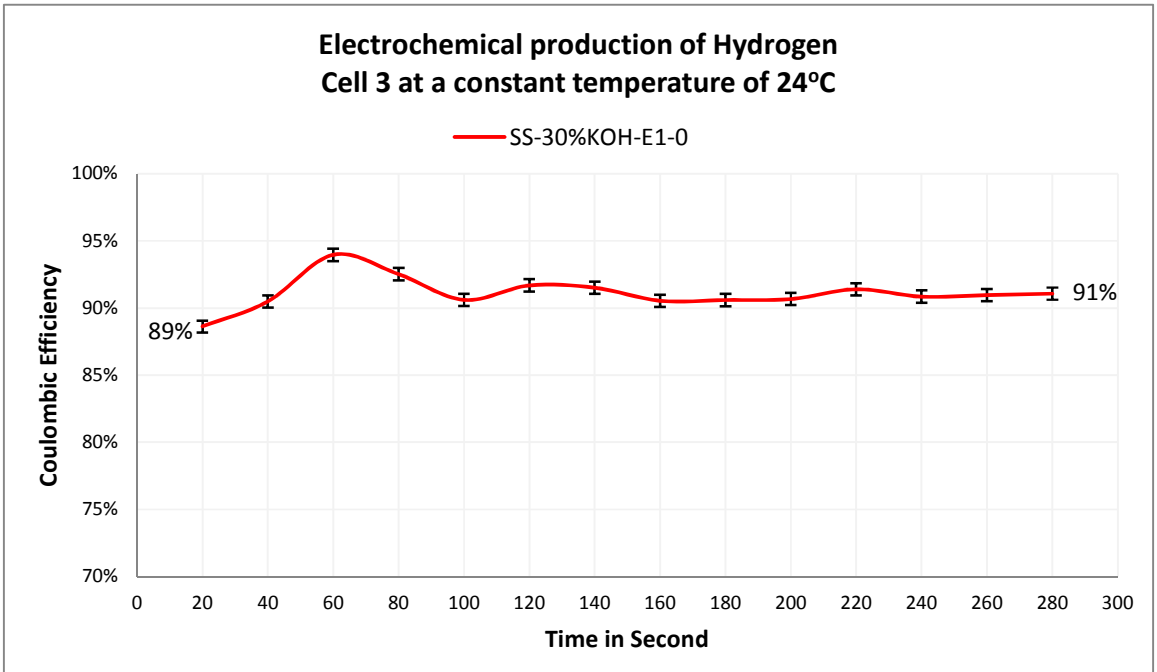

Figure 4.16-B: 1% error illustration of 30% KOH electrolyte at 1amp and 24°C.

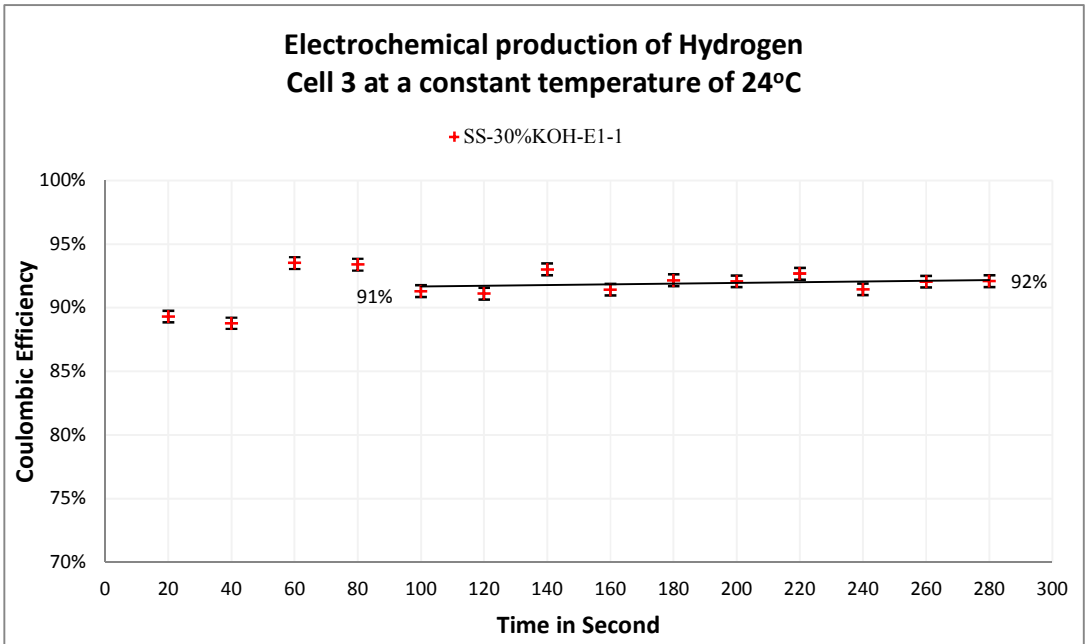

Figure 4.16-C: Linear trend illustration of 30% KOH electrolyte at 1amp and 24°C.

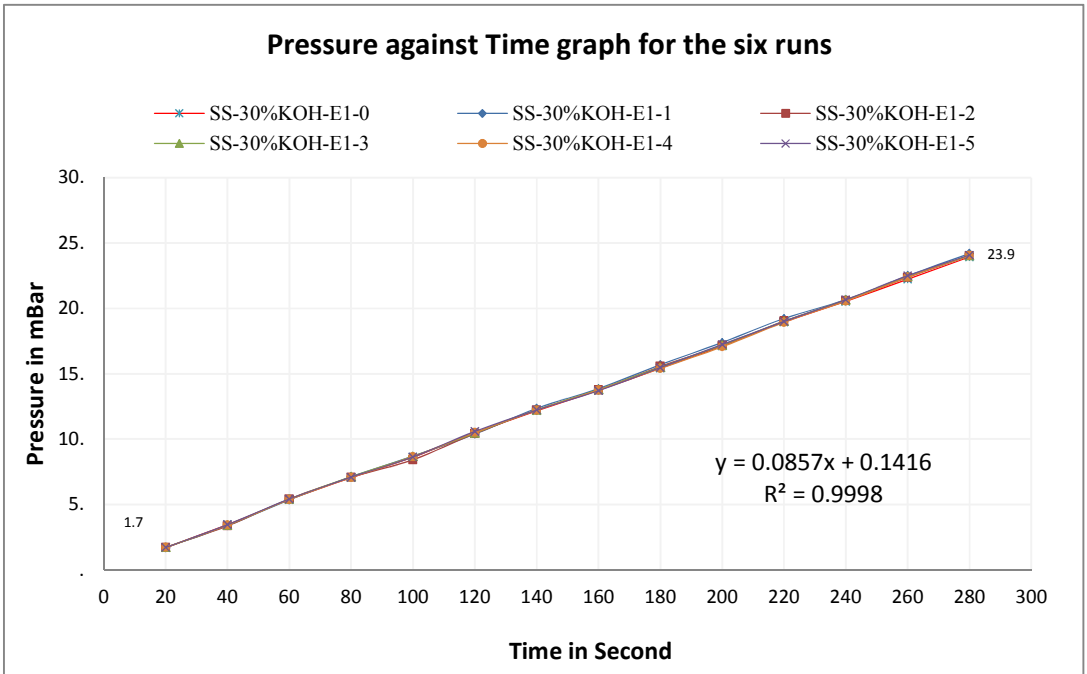

Figure 4.16-D: Pressure comparison on 30% KOH electrolyte at 1amp and 24°C.

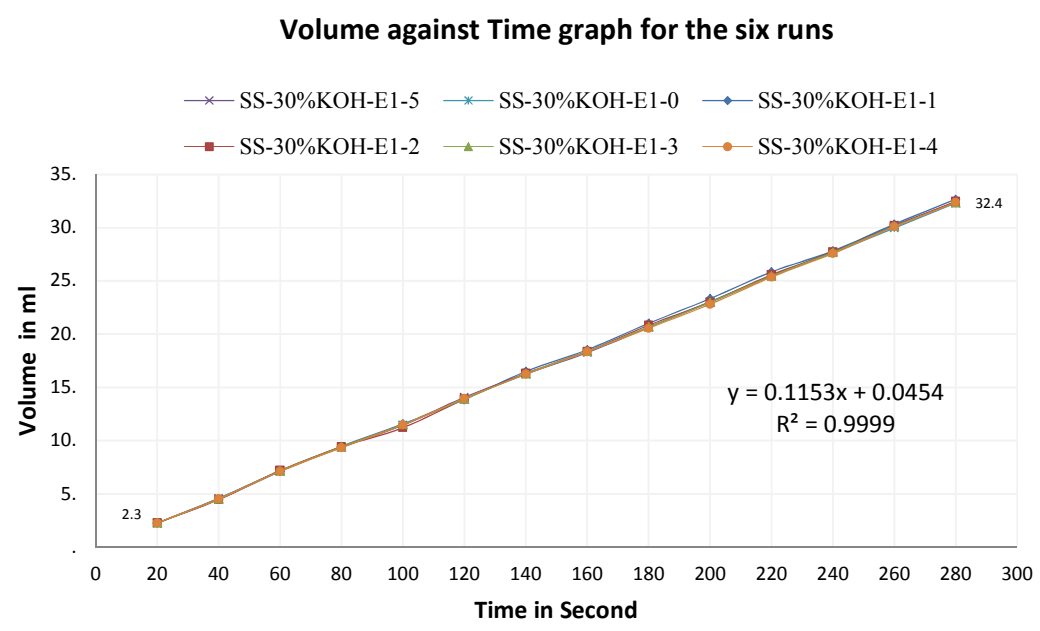

Figure 4.16-E: Volume comparision of 30% KOH electrolyte at 1amp and 24^{O}C.

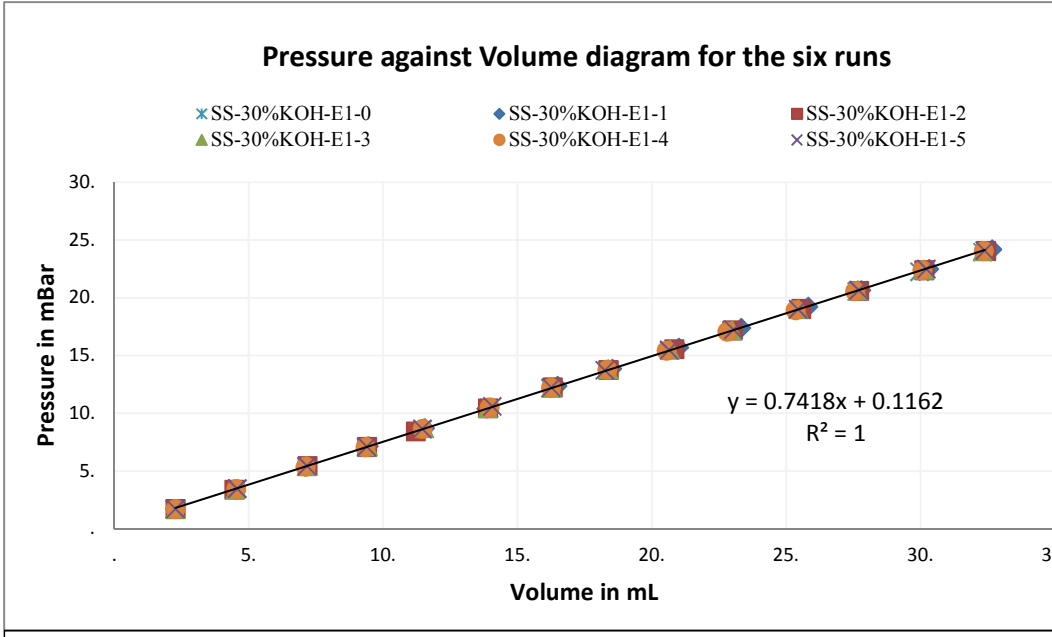

Figure 4.16-F: Pressure and volume comparison on 30% KOH electrolyte at 1amp and 24^{O}C.

Figure 4.16-D presents a pressure against time comparison that illustrates how the pressure in the cell increases almost linearly with time over the duration of the experiments presented in figure 4.16-A. In figure 4.16-E the volume compression against time for the same experiments is presented, again a linear correlation is observed, finally figure 4.16-F illustrates pressure against volume comparisons for the same experiments as expected this too manifest a linear relationship. In all these graphs the tests conducted resulted in results that show that at equilibrium the production of the total gases is constant with time. This explains the consistent values obtained for the hydrogen production. It can also be concluded that constant gas collection from the cell in a working environment would be necessary to avoid pressure build up being a problem in cell design.

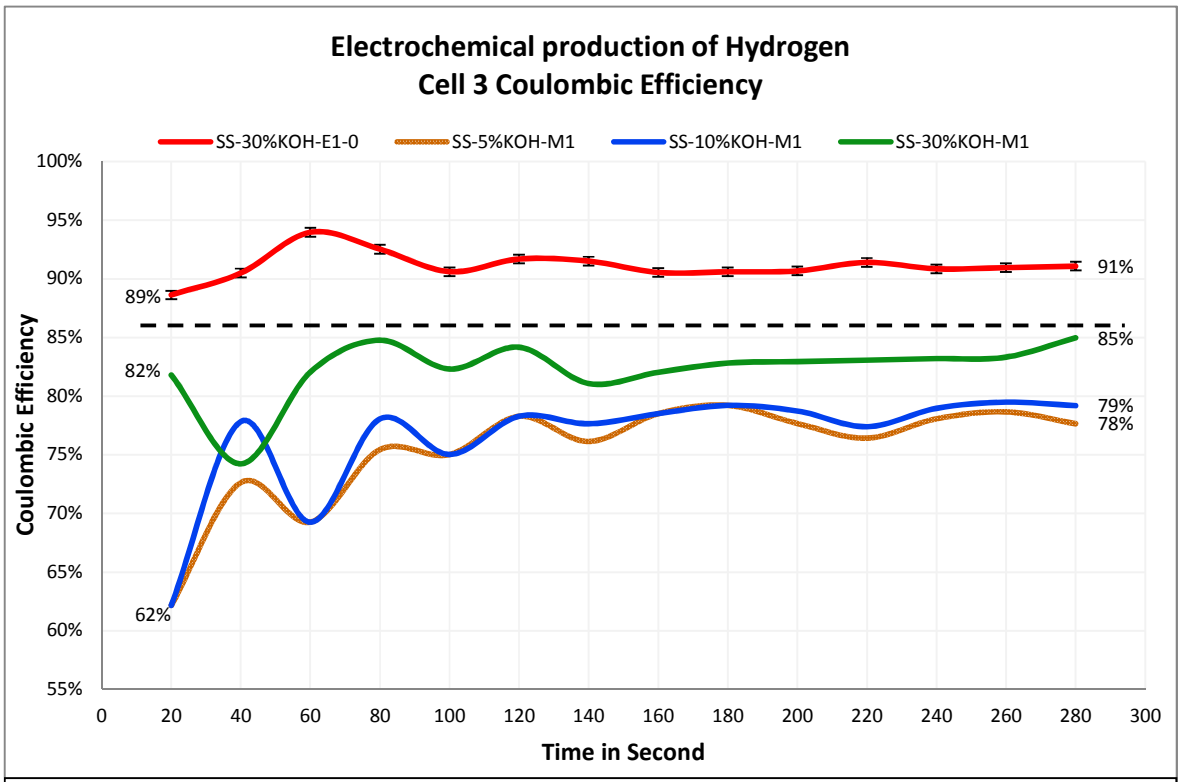

Figure 4.17-A: Coulombic efficiency comparison of different electrolyte compositions within a membrane cell at 1amp and 24^{O}C.

4.2.2) Electrolyte tests in a cell with a dividing membrane.

On-demand electrochemical production of hydrogen was designed by a process of collecting hydrogen and oxygen separately with the help of a gas separator membrane. The graph in figure 4.17-A illustrates the experiment with a membrane containing cell, where 5% KOH is represented with a light brown line (78% efficiency at 24°C), 10% represented with an orange line (79% efficiency at 24°C at 1amp), and 30% KOH alkaline solution represented with a green line (85% efficiency at 26°C at 1amp).

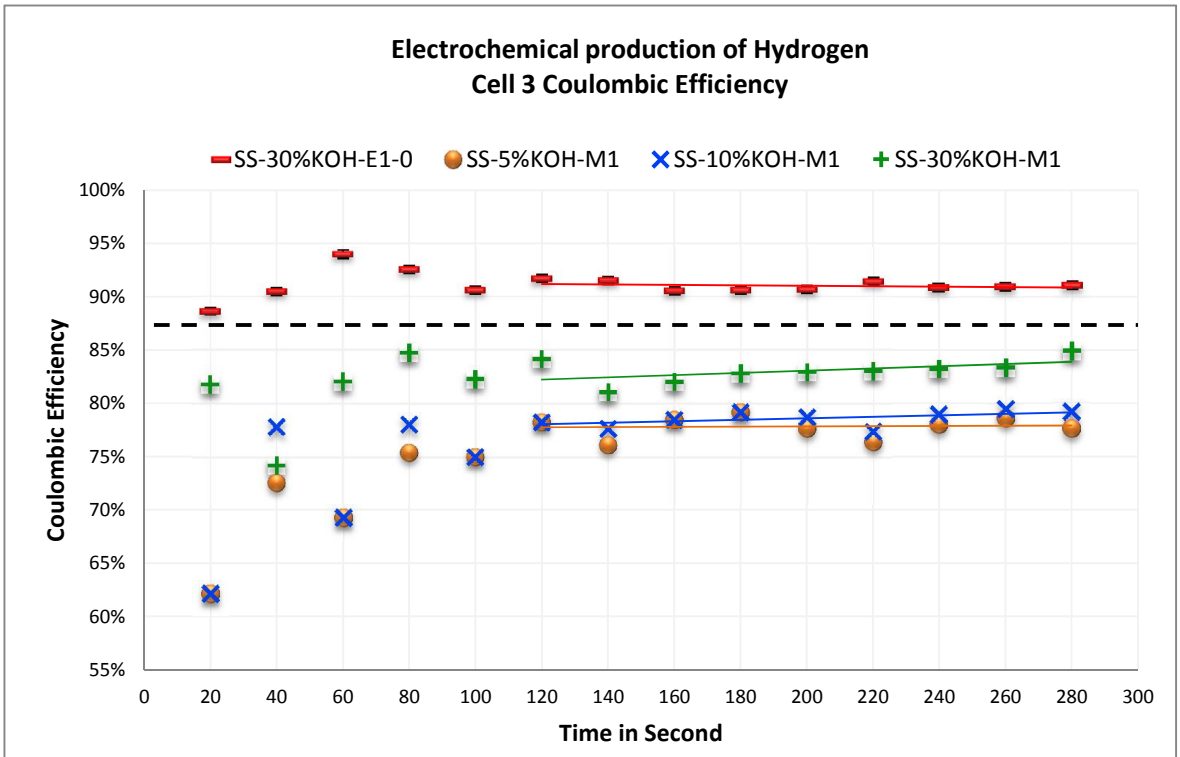

Figure 4.17-B: Coulombic efficiency showing a linear trend comparison at different electrolyte compositions within a cell with a dividing membrane at 1amp current.

The test results show the peak performance of 85% at 30% KOH alkaline solution with a membrane present. Therefore a 30% KOH alkaline solution is the best

electrolyte for on demand electrochemical hydrogen generation in cell 3. The red line represents the 91% performance of 30% KOH electrolyte without a membrane in the cell (as in figure 4.17-A), hence a 6% performance fall is because of the membrane ion exchange capacity. Therefore a 6% performance loss has to be compromised in order to protect the device from explosion in case of fire. Figure 4.17-B presents similar stable linear trends to those found in Figure 4.15-B. Again these show the region of stable performance.

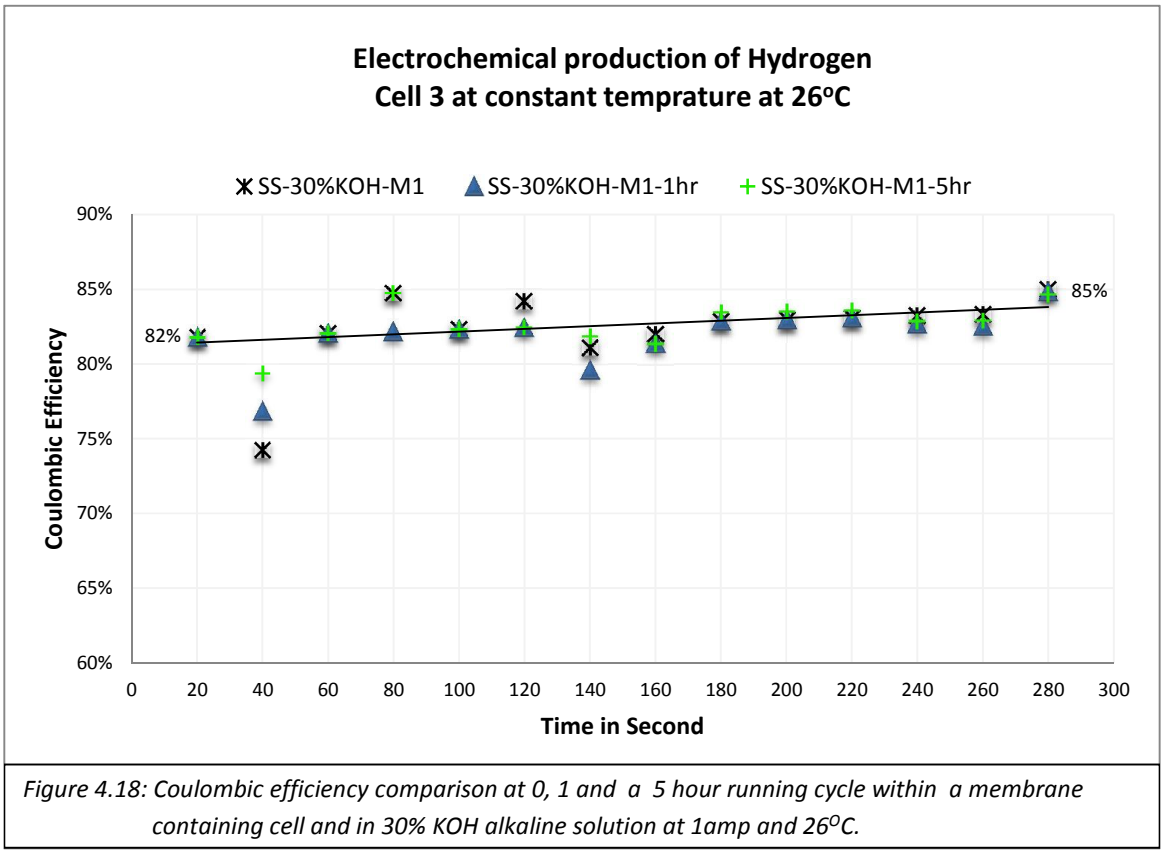

Figure 4.18: Coulombic efficiency comparison at 0, 1 and a 5 hour running cycle within a membrane containing cell and in 30% KOH alkaline solution at 1amp and 26°C.

The graphs shown in figure 4.18 give a comparison between the results found at: 0 hour (the start of the experiment), represented with a black star, 1 hour (into the experiment), represented with a blue triangle, and a 5 hours into the experiment,

represented with a green cross. The 5 hour result showed the best performance in the first 60 seconds. The results in figure 4.18 prove that the hydrogen generation cell becomes stable over time. The performances of hydrogen generation after 60 seconds are found to be almost the same within a small range. Therefore the 30% KOH alkaline solution performed well with the stainless steel electrode and membrane. Further explanation about the pressure balance and how the space between electrodes affects the hydrogen generation efficacy will be given in section 4.4 'Device Designs'.

4.3) Electrode

An electrochemical cell requires at least two electrodes to split water into hydrogen and oxygen. To obtain the highest performance from the electrodes, focus is required on two major areas, the first is electrode durability and the second is electrode conductivity. Many researchers have reported improvements in the conductivity of the electrode materials [89], [9-11]. There are many methods to improve conductivity; one of the favoured approaches is to aim for a higher surface area. This can be achieved by an expensive nano-materials deposition method [89] [43] [90].

The experiments in this section of the work were aimed at finding the best electrode material for the cells. Figure 4.19-A presents a comparison of copper and stainless steel electrodes. Copper is widely used as an electrical conductor because it is cost effective and has excellent conductivity compared to stainless steel. The brown line (copper electrode at 25°C) in Figure 4.19-A graph shows that the start point of experiment is much better than green line (stainless steel electrode at 26°C) [49] [47], but the performance of the copper electrode is seen to behave in a somewhat chaotic manner showing an overall reduction in the timescale of the experiment but with many fluctuations (see figure 4.19-B) which

was because of corrosion as shown in Figure 4.20. In contrast, the green line in figure 4.19-A showing the variation in the performance of the stainless steel electrode is less chaotic and verifies the stability in the electrochemical production of hydrogen that can be achieved with it.

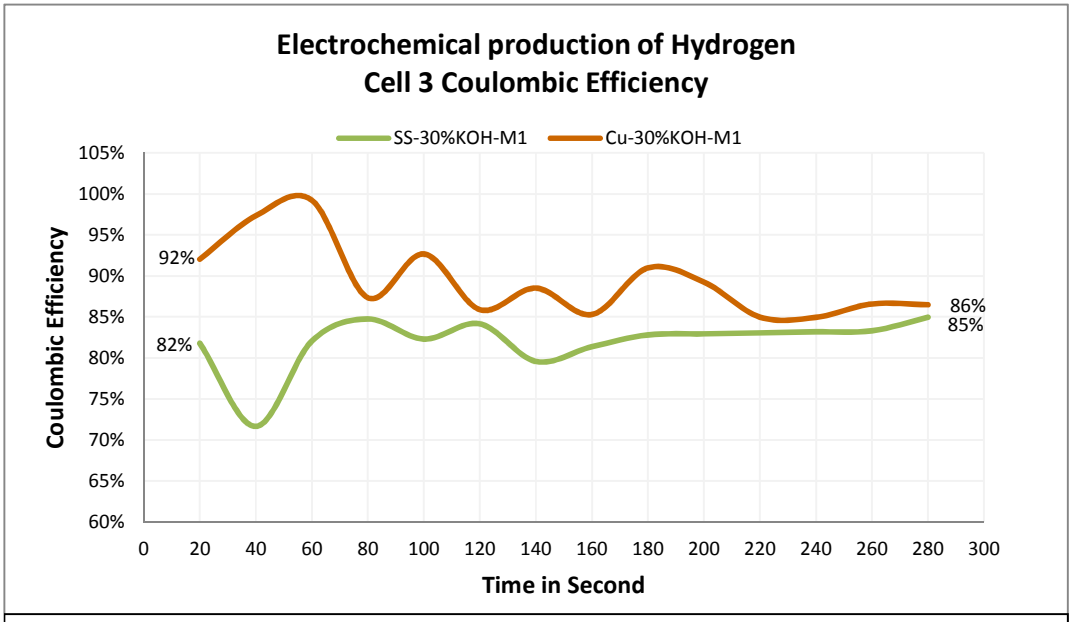

Figure 4.19-A: Transition metal electrode coulombic efficiency comparison at 1amp in 30% KOH.

Figure 4.20: Corrosion effects on copper electrode.

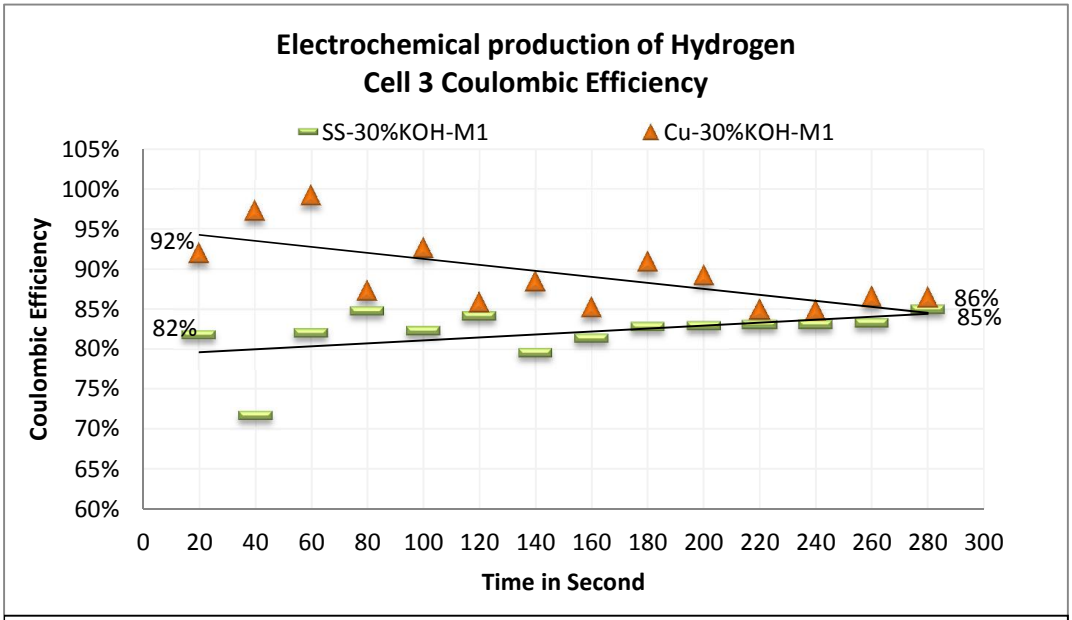

Figure 4.19-B: Transition metal electrode coulombic efficiency linear trend comparison.

Based on above results the stainless steel electrode was selected for the electrode and tested with some nano-material deposition as compared in figure 4.21 graph. The objective of figure 4.21 illustration was to compare the nano-deposit electrode efficiency with stainless steel electrode efficiency of hydrogen generation via water electrolysis.

Three different cathodes were tested. The first was stainless steel, the second was stainless steel sputter coated with 70nm of gold. The third was stainless steel sputter coated with 70nm of platinum. Sputter coating is the easy way of nano deposition and each electrode was monitored for 10 minutes under identical conditions. The first four minutes of each run were ignored as in this time ionic diffusion layers formed near the electrode surface. The succeeding minutes showed that these layers then performed with time as seen in figure 4.21. From the results

presented in figure 4.21, it appears that there is no noticeable advantage in using the sputter coated samples, as plain stainless steel gains the best result.

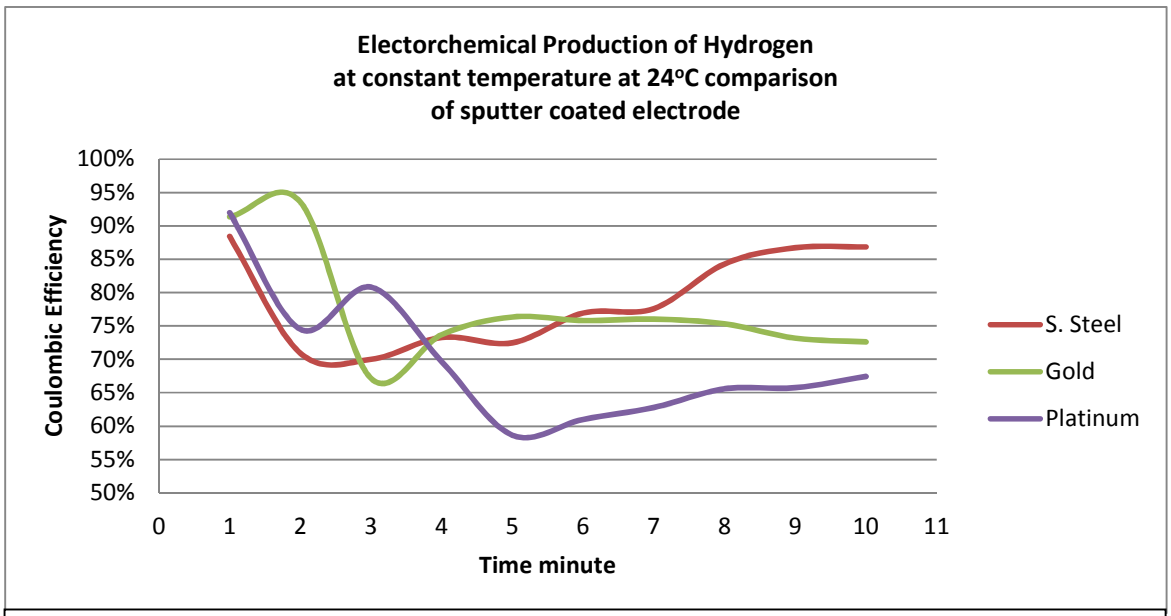

Figure 4.21: 70nm Sputter coated electrode coulombic efficiency comparison. [34]

There are many other methods of nano-deposition which may improve the efficiency but our project objective achieved the desired performance. Having consideration for completing the project in time, we moved forward to the next stage of the device design with the selection of stainless steel electrode.

4.4) Device Design

Having chosen the best electrode material and the cell membrane along with the optimisation of the KOH concentration the next step is to optimise the cell design in which they will be used. As the new cells were developed the KOH concentration was again varied as discussed in this section.

This section will explain the on-demand electrochemical hydrogen generation third generation cell design (cell-3) and additional factors that affected it. In addition the cell-3 performance boost compared with cell-1 (which as explained in chapter-3 section 3.1.3-Results and discussion cell-1, had a 46% (highest) performance at 3 amps in 30% KOH electrolyte). The shortcomings found from the work on cell 1 lead to the design of the second generation cell in which some additional problems were encounter, as explained in chapter 3 sections 3.2. Those problems were eliminated in the third generation electrochemical cell design (cell-3), as explained in the drawing in chapter 3.3.

Figures 4.2.13 and 4.2.14 illustrate the coulombic efficiency results of the third generation electrochemical hydrogen production cell and compare the effect of variation in the applied current with and without a membrane with different concentrations of KOH in the water.

It should be noted that the lines presented in the following figures:- (4.2.13 to 4.2.18, 4.2.20 to 4.2) are formed by joining multiple data points. Each data point was collected at 20 second intervals. To aid the eye in understanding the trends the lines are given alone and the data point are not identified in many of the figures.

To understand the performance of the cells it is useful to consider the influence of four factors:-

1. The presence or absence of a cell membrane;
2. The concentration of the electrolyte;
3. The presence or absence of turbulent flow in the electrolyte;
4. The current flow applied to the cell.

4.4.1) The presence or absence of a cell membrane

Firstly the presence and absence of a membrane on the performance in the cell will be considered. To help explain the results shown in figures 4.2.13 and 4.2.14, **"M"** means membrane, and this was positioned in the cell to separate the hydrogen and oxygen bubbles to provide pure hydrogen, and thus provide protection from fire/explosion.

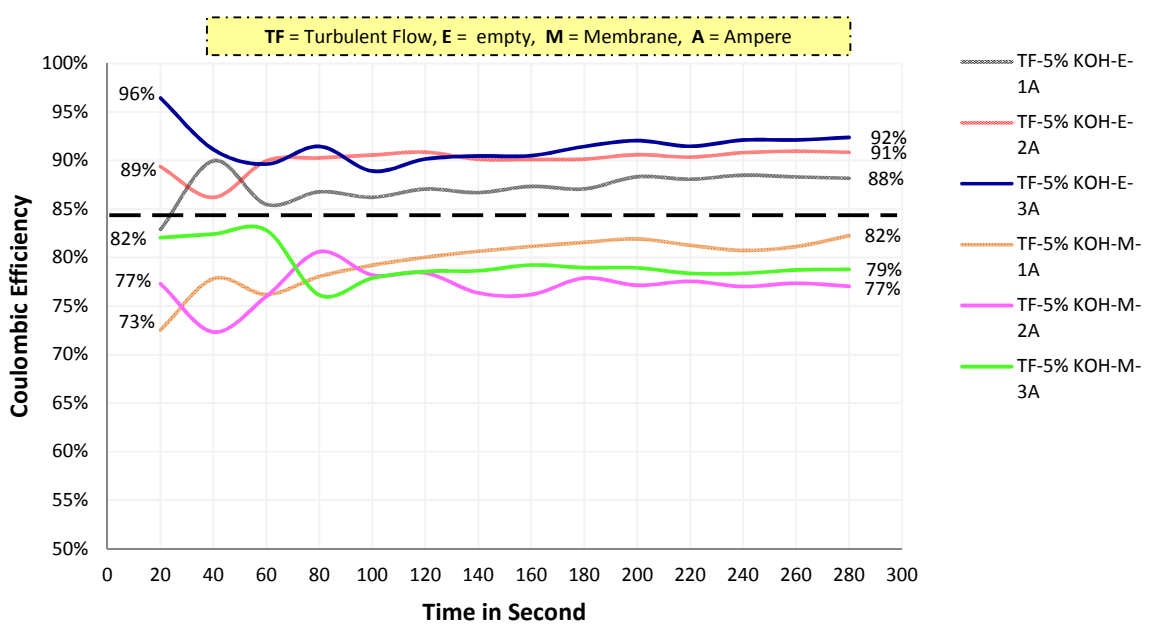

Figure 4.22: Coulombic efficiency comparison with and without a membrane in the cell at 5% KOH concentration for three different currents.

The **"E"** represented an empty cell, meaning no membrane was placed in the cell; in this case therefore hydrogen and oxygen are mixed in the cell and such cells can

cause an explosion in the case of generation of a spark or fire. The lines above the black dashed separation line in figure 4.22 graph represent the performance of the empty cell (no membrane). Here the highest performance of 96% was achieved at 3 ampere (A) (blue line), and over the timescale of the experiment a 92% stable performance was achieved. On the lower side of the black separator line, performance with a membrane cell is represented. Here an 82% at 1A was the highest performance achieved (light brown line).

4.4.2) The concentration of the electrolyte

Secondly the KOH concentration was varied and its effect on cell performance was studied.. Four different concentrations of 5%, 10%, 15%, and 30% KOH were studied. The graph in figure 4.22 is based on the 5% KOH alkaline solution and figures 4.2.14(A, B, C) give a comparison between cells with and without a membrane for the results at 10% in graph 'A', 15% in graph 'B' and 30% in graph 'C' at 1A, 2A and 3A respectively are presented. In all cases coulombic efficiency is greater towards the higher KOH concentrations, which makes 30% KOH alkaline solution the most reliable concentration as illustrated in graph 'C'. The experiment results of 30% KOH concentration also represent the best activation point among all concentrations at 1A, 2A and 3A as illustrated in figure 4.23.C.

The best performances obtained are presented in figure 4.23.C using a current of 3A (represented with blue and green lines), where the turn on efficiencies for cells without and with a membrane was 95%. The blue line gives an overall acceptable efficiency during the experiment but as the gases could mix this was not the approach of choice. In contrast the green line displays a rapid drop in performance because of electrode deactivation [91] [92]. The continuous performance drop displayed by the green line from 60sec to 140sec is because of the pressure imbalance and electrode deactivation [93] [94].

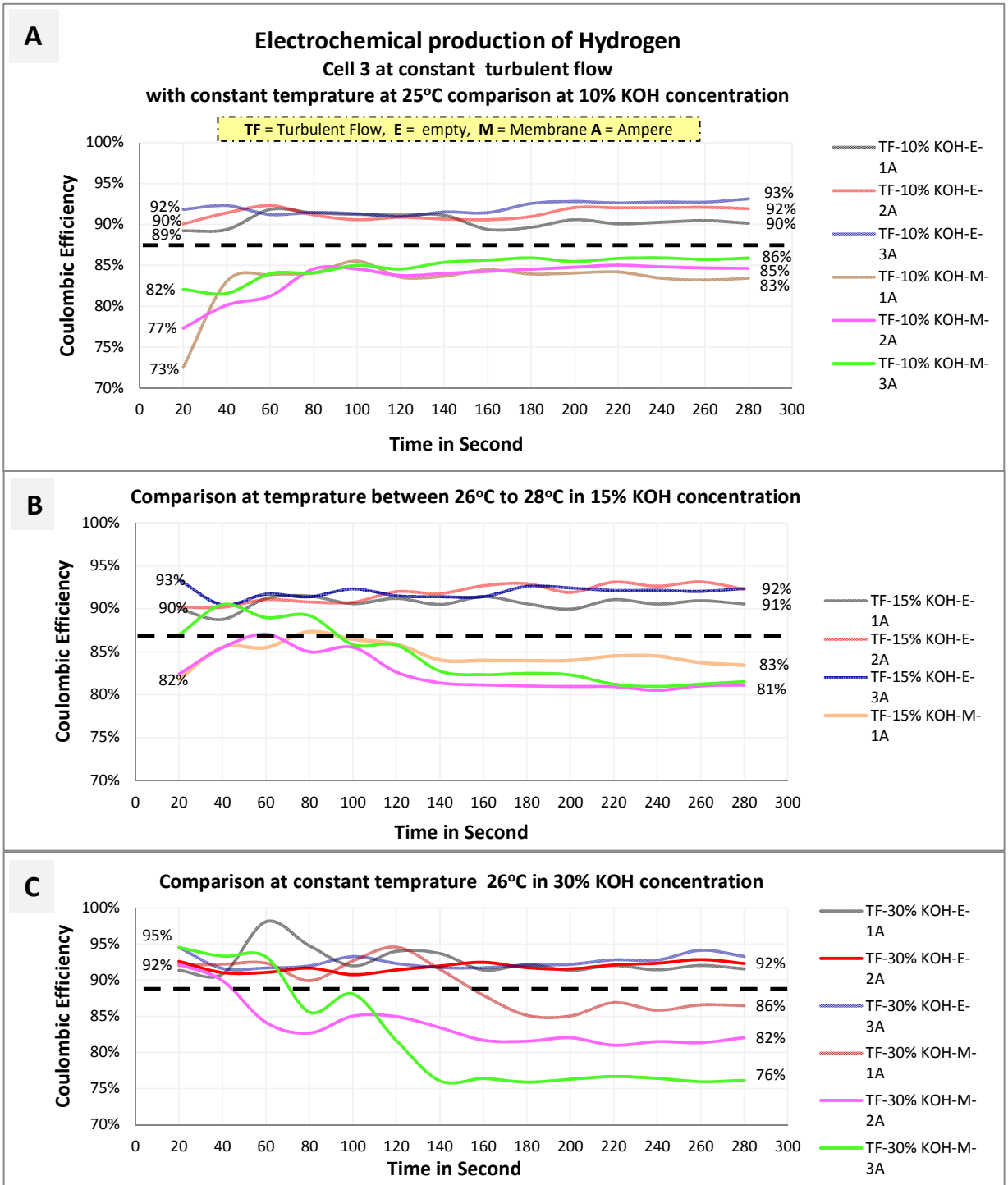

Figure 4.23: Coulombic efficiency comparison with and without a membrane cell at 10%, 15% and 30% KOH concentration for three different currents.

A 76% stable efficiency was achieved from 140sec, which was the point where the device reached a stable pressure and the deactivation of the electrode was stabilised. However, this problem can be overcome by increasing the space between the electrode and the membrane. The blue line is evidence of overcoming the deactivation behaviour, because more space was available to evacuate the bubbles in the absence of the membrane.

4.4.3) The presence or absence of turbulent flow in the electrolyte

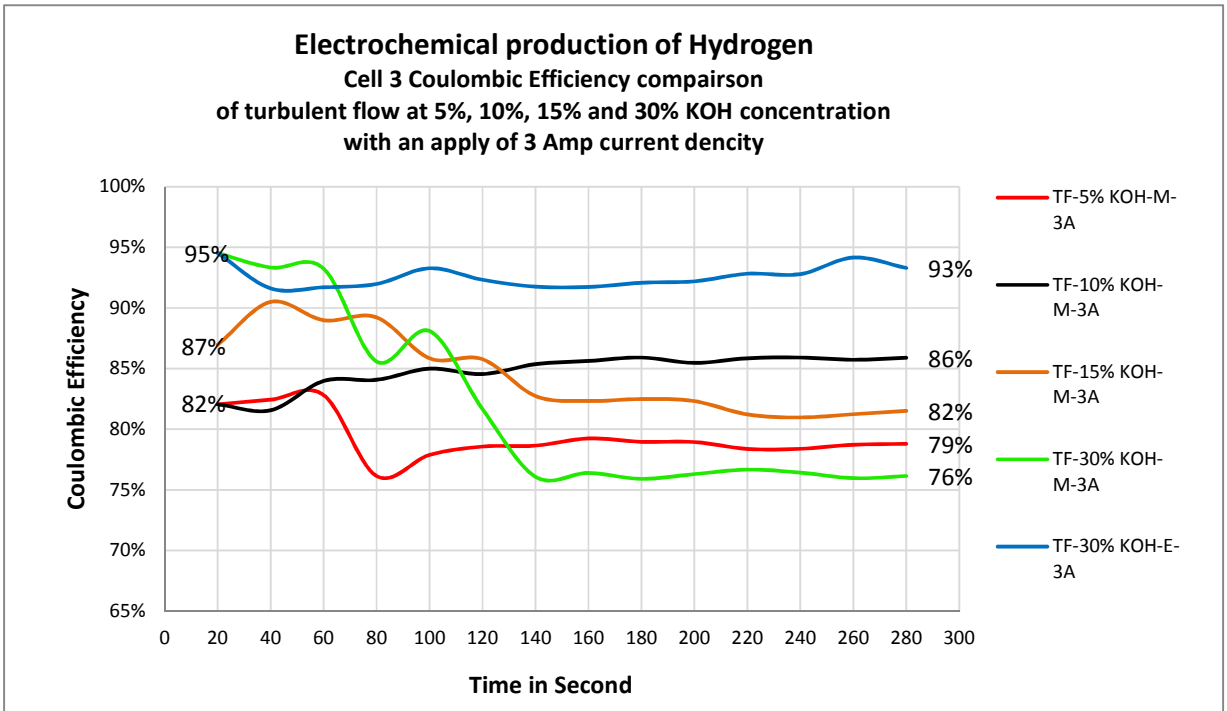

Figure 4.24: Coulombic efficiency comparison of turbulent flow at 5%, 10%, 15% and 30% KOH concentration.

In figure 4.24 graph displays a comparison of the results from the 5%, 10%, 15% and 30% KOH electrolyte concentrations at a current of 3 amps. The most stable performance was achieved in 30% KOH alkaline solution. The blue line represents 30% KOH electrolyte in the cell without a membrane, where the 95% coulombic

efficiency fell to the stable efficiency of 93% at the end of the experiment. Although the green line results are for a cell with a membrane at 3A and 30% KOH electrolyte, the 95% efficiency at the activation point is the same as the blue line.

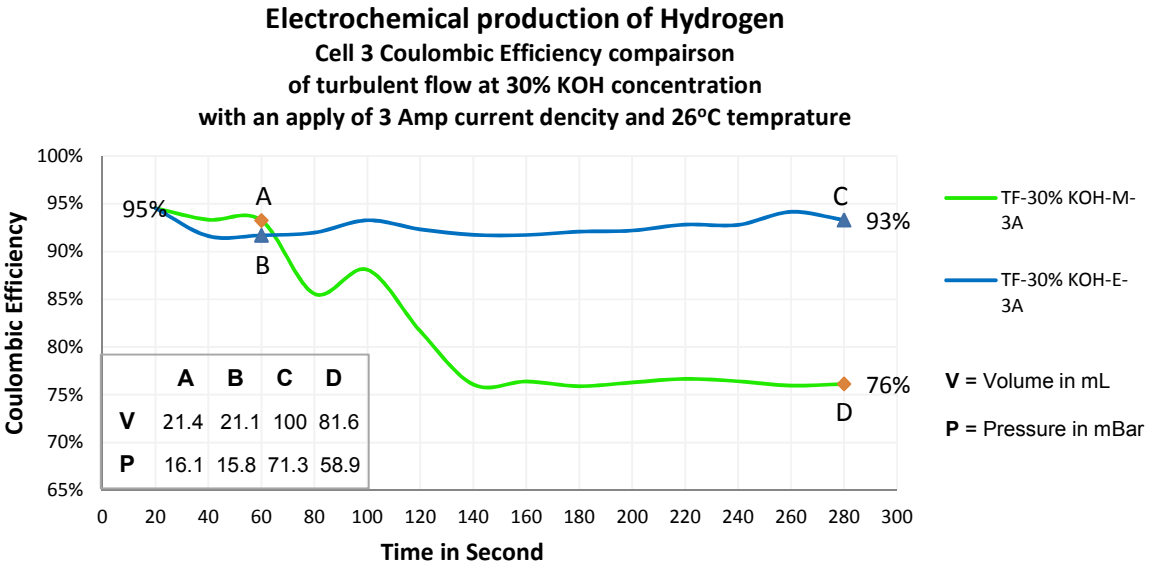

Figure 4.25: Coulombic efficiency comparison of turbulent flow at 5%, 10%, 15% and 30% KOH concentration.

Thus to emphasise this Figure 4.25 illustrates the efficiency comparison between the membrane cell and a cell without a membrane at a 3 amps supplied current, in 30% KOH concentration. The blue line is nearly linear over most of the time range studied; it represents a stable performance of 93%. This is because the combined chamber containing both hydrogen and oxygen results in a balanced pressure in the system. In contrast, the green line represents the cell containing a membrane; here the cell displayed an efficiency drop from 95% to 76%. One reason for the deactivation of the electrode is that a 2:1 ratio of hydrogen and oxygen was generated from the water. The hydrogen chamber holds two hydrogen molecules, for every oxygen molecule present in the other chamber. Therefore

space is needed to balance/maintain the pressure in the system. The space between the membrane and each electrode is 12.8cm^3, whereas in the cell without a membrane the space available to evacuate the bubbles is 26.6cm^2. Hence the blue line represents both a stable performance and a homogenous pressure because of mixing the hydrogen and oxygen.

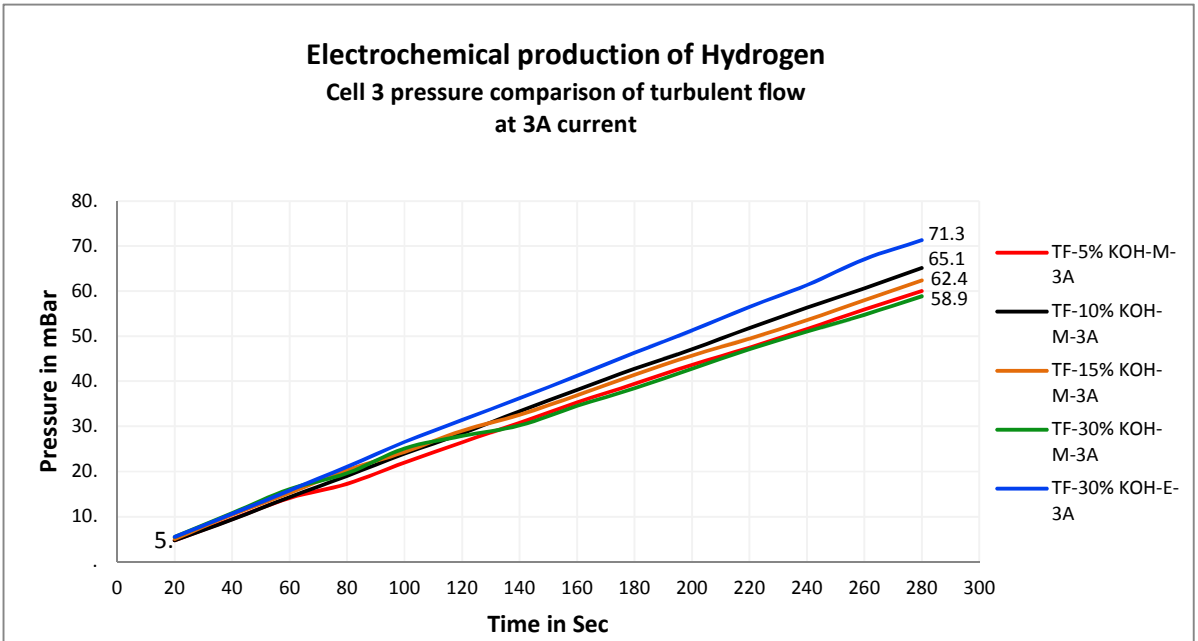

Figure 4.26: Pressure comparison of turbulent flow at 5%, 10%, 15% and 30% KOH concentration.

The pressure and volume data as a function of time for the experiments displayed in figures 4.2.15 and 4.2.16 are presented in figures 4.2.17 and 4.2.18 respectively. The graphs presented in figure 4.26 illustrate the pressure comparison of 5%, 10%, 15% and 30% KOH concentration at a 3 ampere current flow. All the pressure time graphs are fairly linear with only a small variation. From these graphs it is possible to verify that the device performance is proportional to the system pressure. The volume time graphs displayed in figure 4.27 show the same trend as

the pressure time graphs in figure 4.26. Thus from these results it is easy to understand how the initial 95% device efficiency (displayed in figures 4.2.15 and 4.2.16) can be maintained throughout the working period of the cell. What is needed is to provide more distance/volume between the electrodes.

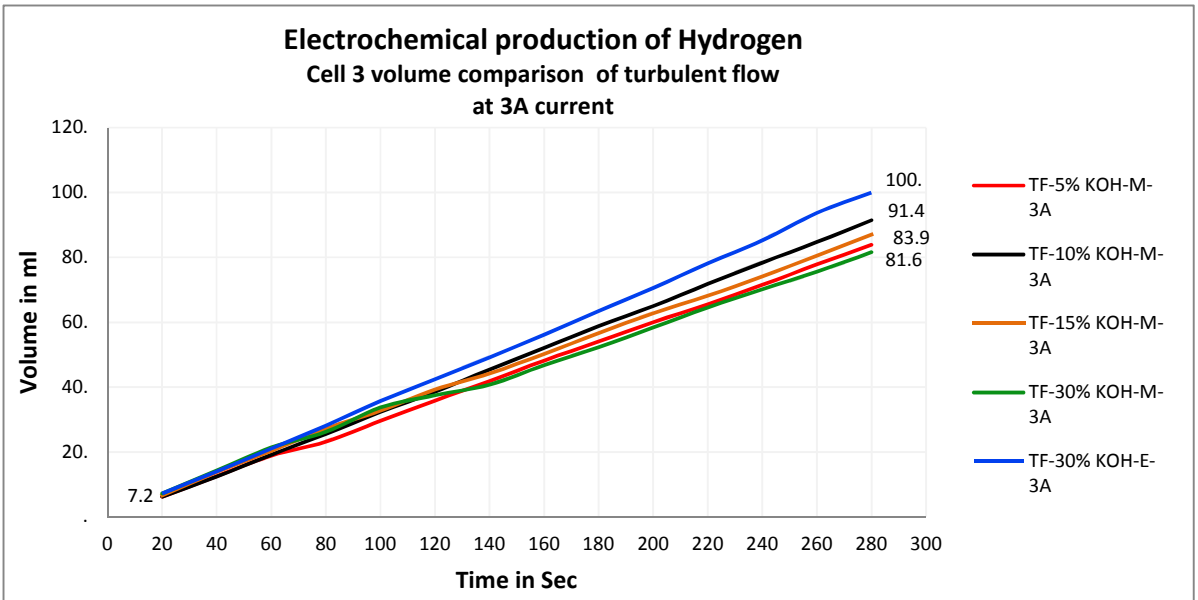

Figure 4.27: Volume comparison of turbulent flow at 5%, 10%, 15% and 30% KOH concentration.

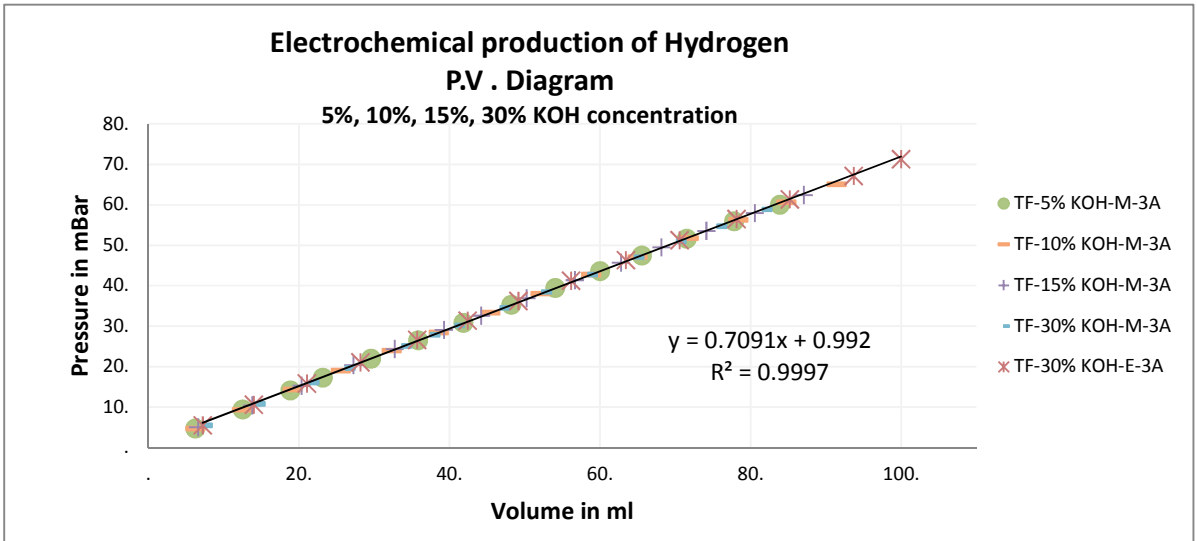

Figure 4.28: Pressure Volume comparison of turbulent flow at 5%, 10%, 15% and 30% KOH concentration with and without membrane cell.

The graph in Figure 4.28 illustrates the comparison between volume and pressure. A perfect linear regression relationship is found at all concentrations. For example, figure 4.28 relates the volume of gas to the pressure of gas using a linear regression model. Hence the graph projects the efficiency stability behaviour and proves that the results are reliable, with a fitting error that is very small (R^2 = 99.997%).

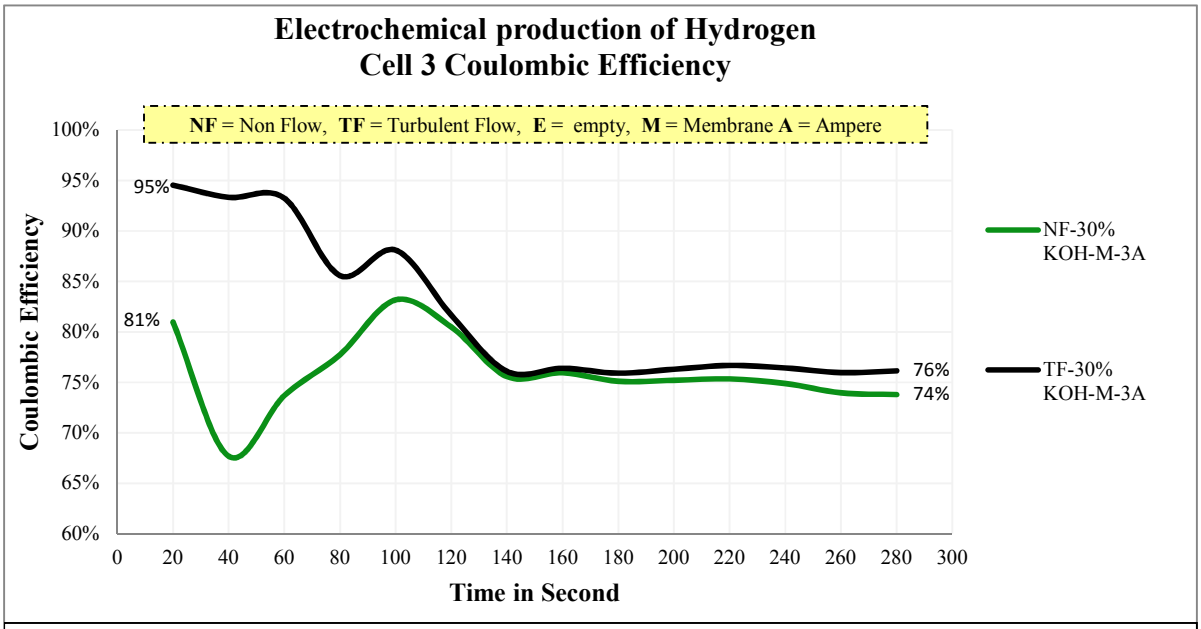

Figure 4.29: Coulombic efficiency compression of turbulent flow and non-flow at 3A current.

The third variable that needs to be considered is the electrolyte flow. The experimental results were based on two values for flow: non flow (NF) and turbulent flow (TF) (that is the flow is on or off). The highest performance with the membrane cell was 95% at 3A, and the most stable performance is 76% with turbulent flow represented in figure 4.29 with black line. The dark green line represents the result when there is no flow:- Here an 81% performance is observed that settles to a stable performance of 74%.

The graph for the membrane cell results is also presented in figure 4.29; clearly this shows the performance boost caused by the turbulent flow. The black line

manifests a 13% boost from the dark green line of 82% to 95% at the activation point and the boost in stability is 2%. Similarly, in figure 4.30, the 2A results illustrated by the pink line, show a value of 82% at the activation point and 80% stability. The green line shows a 92% activation point was achieved (which is a 10% boost) and 2% boost in stability.

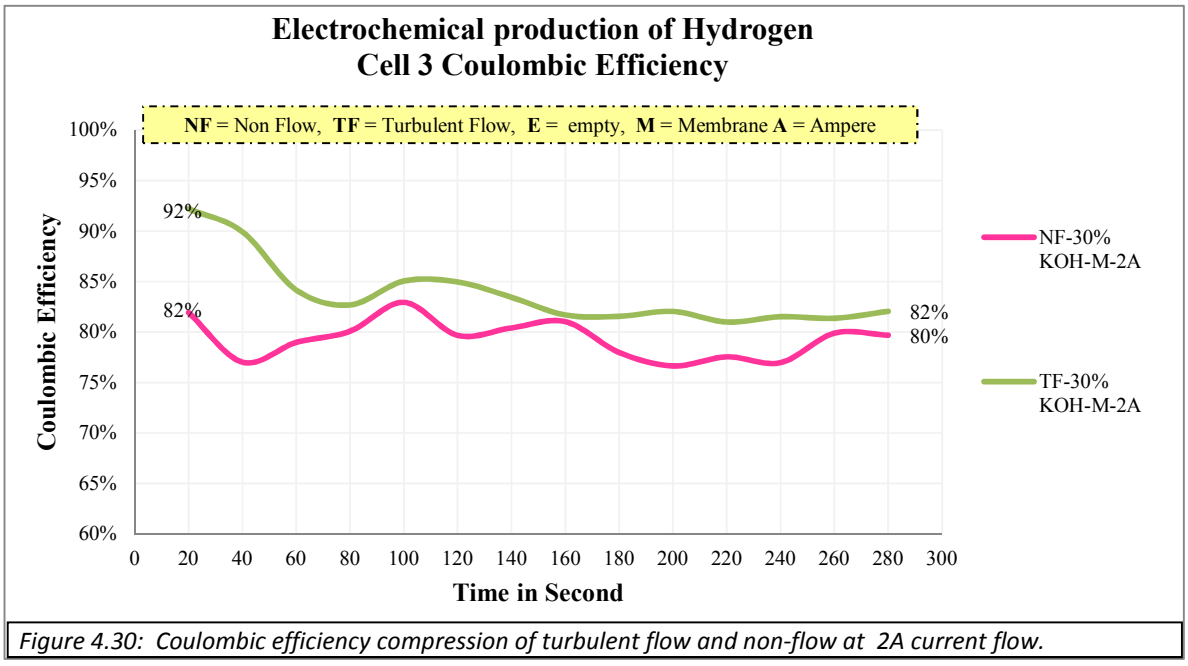

Figure 4.30: Coulombic efficiency compression of turbulent flow and non-flow at 2A current flow.

A comparison between flow and non-flow at 1A current flow is presented in figure 4.31 with a brown line representing the flow condition and a red line the absence of flow. The results were not very different from those obtained at 2A and 3A current flow. The only difference was the stability in performance was better at the lower current. The latter finding also explained why the deactivation of the electrode is less at 1A; this is due to a slower gas generation followed by a faster gas release.

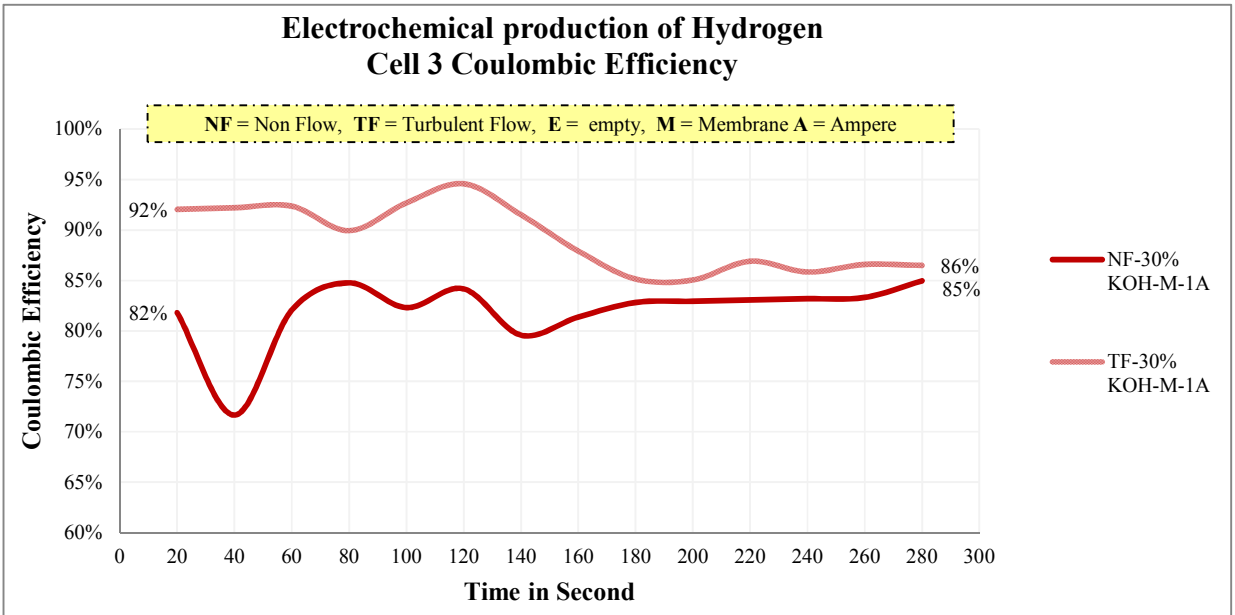

Figure 4.31: Coulombic efficiency compression of turbulent flow and non flow at 1A current flow.

The learning outcome from the presence of flow and its absence studies is that the flow results provide better performance and stability in the system [95]. The 3A current flow in 30% KOH alkaline solution result displayed the fastest establishment of the electrochemical reaction formation, in comparison to both the 2A and 1A current flow. As it is now apparent that turbulent flow is demonstrable beneficial, it was thus decided that the next study would be based on turbulent flow in a cell containing a membrane.

4.4.4) The current flow applied to the cell

The fourth property that is fundamental to running an efficient cell is the control of the current supplied to the system. To study this property experiments were conducted at three different current flow 1amp, 2amp and 3amps respectively. The behaviour of different concentrations of electrolyte at different current flow is reported below.

Figure 4.32 - 1A illustrates the electrolyte behaviour at 1 ampere current, 2A shows 2 ampere current and 3A is 3 ampere current. The expected behaviour of the electrochemistry was that greater current consumption along with a higher KOH concentration will generate higher production of hydrogen.

Figure 4.32 demonstrates the expected behaviour, where the 1A graph shows 30% KOH providing the best performance, then 15% KOH, 10% KOH and the lowest performance was found for the 5% KOH solution. Surprisingly in graphs 2A and 3A the expected behaviour found in graph 1A was not observed after the first 110 seconds. The graphs 2A and 3A shows a more complicated behaviour which was an interesting finding and relates to the discussion in sections of this chapter.

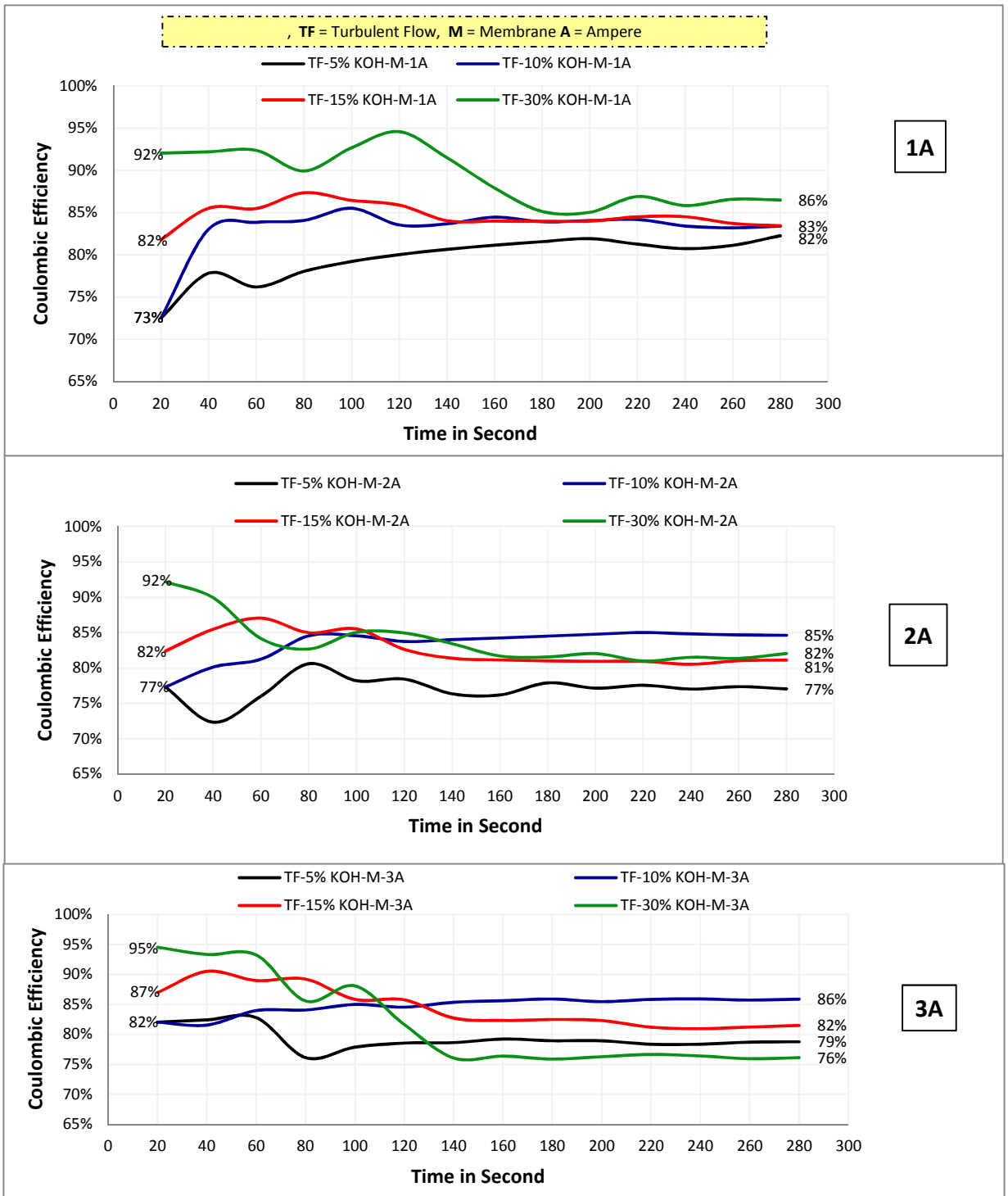

Figure 4.32: Coulombic efficiency comparison of 5%, 10%, 15% and 30% KOH concentration at 1A, 2A and 3A current.

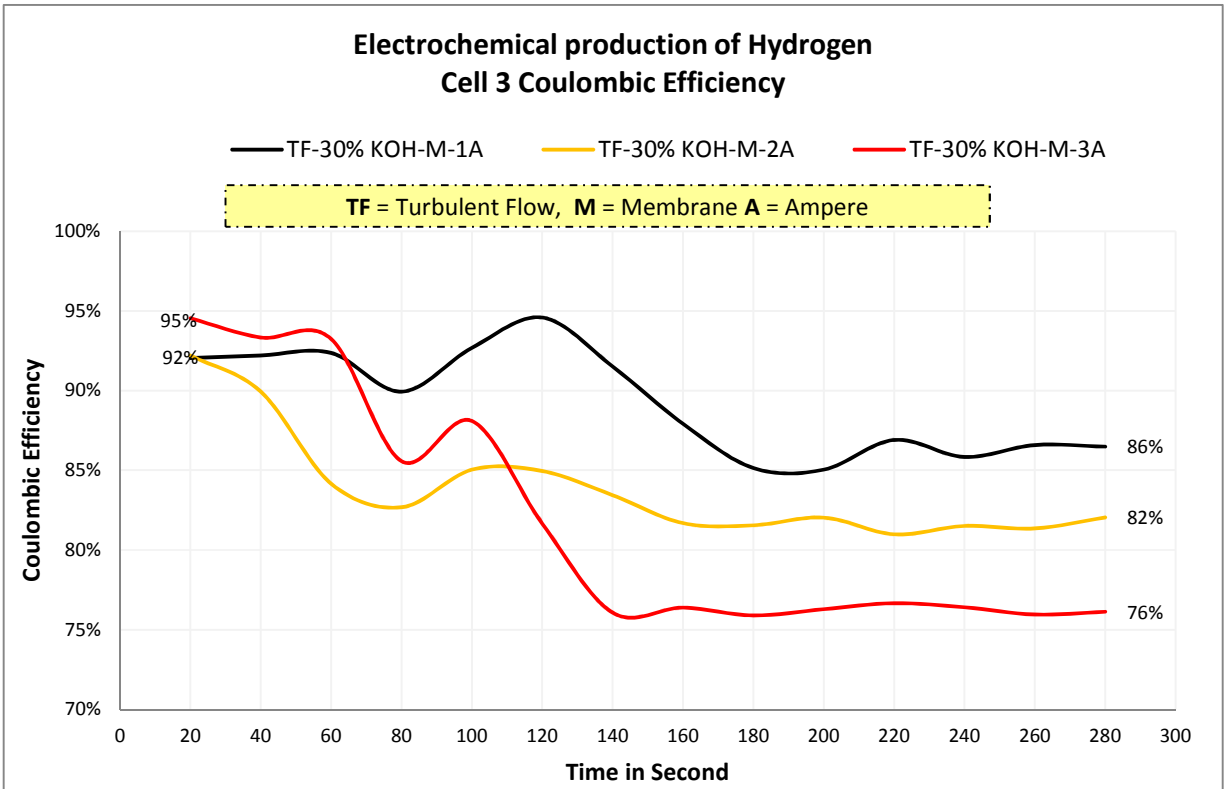

Figure 4.33: Coulombic efficiency comparison of 1, 2 and 3 ampere current flow in 30% KOH alkaline solution.

Figure 4.33 presents a comparison of the 30% KOH concentration at 1, 2, and 3 ampere current flow. The activation phase performance at 3amp in 30% KOH solution was higher than those for the 1 and 2amp, but the performance fall was faster than the others. Therefore, it can be deduced from figure 4.32 and 4.2.24 that the trend of performance is that at higher current flow and higher KOH concentrations higher initialisation values are recorded. Clearly the higher current flow cause greater gas production but this is a drawback if the gas cannot be efficiently removed at a fast pace. Here it is apparent that the behaviour and fall in performance for the 2Amp and 3Amp currents the gas production speed was a problem. Thus for the 2Amp and 3Amp applied currents because of bubble formation at the electrode deactivating the electrode the steady state performance

(after 110 seconds) was much lower than expected. Therefore, the selection of current flow and electrolyte concentration is dependent on the application requirements of running time and production rate.

4.5) Conclusions

The purpose of this project was to design and develop on-demand electrochemical production of hydrogen for portable applications. The main applications are for use with internal combustion(IC) engines and PEM fuel cells [96]. The reason behind designing this device was to provide an alternate or supplementary fuel solution for these existing technological systems. For example, the hydrogen on demand electrochemical cell could be used as an additional fuel cell for current automobiles [96]. Hence the results shown in this chapter explain the phases of device optimisation for such uses.

The first phase was to select the best gas defusing membrane to keep hydrogen and oxygen apart, to ensure that the risk from explosion in the case of flashback is minimised [97]. The best membrane was 1010 for this purpose.

The second aim was to make the right composition of KOH for this device to achieve higher ion exchange for better electrochemical hydrogen generation and less oxidation to protect the electrode: thus ensuring low maintenance and generator durability [3-5]. The best KOH concentration for this purpose was found to be a 30% KOH concentration.

The third aim was to find the best electrode in terms of durability, cost effectiveness and conductivity to get the best overall performance. Stainless steel

was found to be the best electrode material for this purpose and 95% is the best efficiency, achieved from the cell-3 device design.

Fourthly, the design of the first generation cell design was derived from Stephen Barrie Chambers' [51] patent; the result of the test of his device was 46% with stainless steel electrode. The nanostructured electrode research reports 73% efficiency [38]. This work has demonstrated substantial improvements to these figures. The On-Demand Hydrogen Generation cell-3 design described in this thesis gave about 49% efficacy improvements as compared to the stainless steel electrode, and was 22% better than the nano structured electrode. The achievement of such high efficiencies paves the way for more research in the areas of space management, electrode surface structure and flow control based on application requirement (see chapter 5 on suggested future work).

Chapter 5

Overview and Future Work

5) Objectives

The objective of the research reported in this thesis was to design an on-demand high performance electrochemical hydrogen generator. The design also considered low cost manufacturing, maintenance, durability and hazard free production of hydrogen. To produce hydrogen the following four areas were considered in this thesis in order to optimise the objective as discussed above.

4.1) Membrane : To find the best possible membrane to keep the generated hydrogen and oxygen separate. Membrane 1010 was found to be the best for this project.

4.2) Electrolyte : To make the best possible composition of electrolyte material to get a higher ion exchange and optimized performance. The best was found at 30% KOH concentration.

4.3) Electrode : To find the best electrode material to generate hydrogen. The stainless steel electrode satisfied the requirements relatively with the following attributes:- low cost, long life, low maintenance and high performance.

4.4) Device Design : To optimise the equipment design to facilitate facile breakup of water molecules into hydrogen and oxygen.

The Cell-3 design was found to be the best prototype for hydrogen generation.

5.1) Membrane

The purpose of membrane in the cell is to keep the hydrogen and oxygen apart for safe on-demand electrochemical production of hydrogen for portable applications. Stephen Barrie Chambers patented a hydrogen generator, which produces hydrogen and oxygen in the same chamber [51]. The drawback with this design is it has the potential for an explosion hazard in case of flashback [97] [98].

The main applications are for use with internal combustion(IC) engines and PEM fuel cells [96]. Hydrogen fuelled cars required a hydrogen cylinder, which holds pure hydrogen that feeds into the PEM fuel cell to generate electrical energy to drive the electric motor [96] as illustrated figure 5.1. Hydrogen cannot burn without oxygen, therefore pure hydrogen is theoretically safe to store [99].

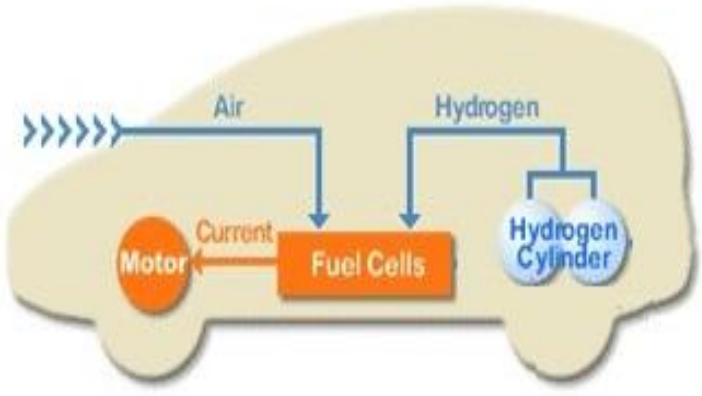

Figure 5.1: Flow diagram of hydrogen powered cars. Hydrogen cylinder stores hydrogen in the car and filled by the fuel station. Fuel cells take hydrogen from the cylinder and oxygen from air intake to produce electrical power. Motor drives the car by using electrical power generated from fuel cell.

Figure 5.2 displays the test result conducted by the Ford hydrogen safety team, which represents that pure hydrogen is safest among all the fuel types they tested. The hydrogen fuelled car survived due to the flame reducing over time, whereas a petrol car flame begins small and then increases till the car is completely burnt out [100] [101]. The graph in figure 5.3 demonstrates the risk of fire comparison between a numbers of different fuels. The values near to the origin (0,0,0) represent a greater risk of fire, and a lower risk is proportional to the values away from the origin. The highest level of safety from fire was reported as hydrogen [101]. Therefore a membrane is required to have safe generation of hydrogen from water.

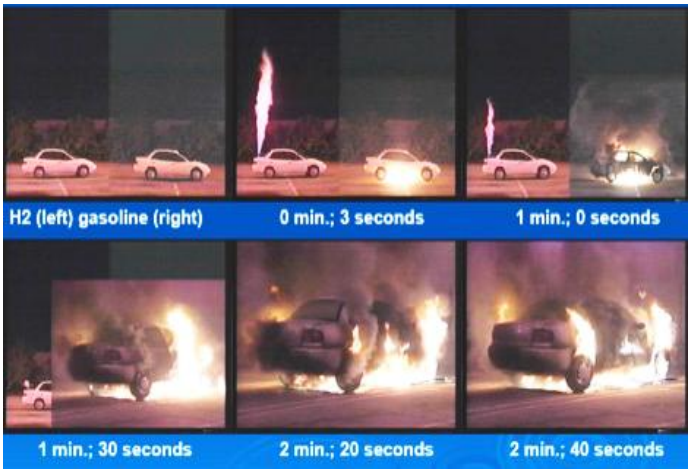

Figure 5.2 [100] [101]*: Hydrogen safety test. Left hand car contains hydrogen fuel and right hand car contains petrol. Experiment duration was 2 minute 40 seconds and found hydrogen is safer than petrol.*

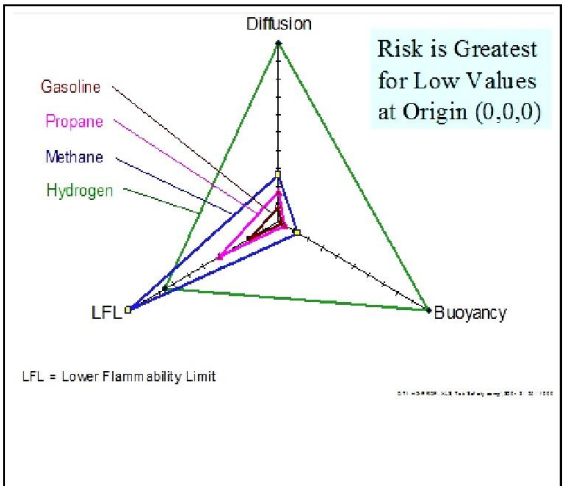

Figure 5.3 [100]*: Risk of fire result shows the hydrogen fuel had lowest level of risk.*

In this theses the first phase was to select the best gas defusing membrane to keep hydrogen and oxygen apart, thus making the device secure from explosion in the case of flashback. The best membrane was found to be 1010. This provided pure hydrogen while retaining its high strength and was also a low cost membrane

solution. In the future further work could be done on the membrane hardness and strength. Hardness can provide more stability over a higher pressure.

5.2) Electrolyte

The objective here was to establish the right composition of KOH to achieve higher ion exchange for better electrochemical hydrogen generation and less oxidation to protect the electrode, thus ensuring low maintenance and generator durability [8-12]. The best KOH concentration for this purpose was found to be 30% KOH. A major problem with using 30% KOH is that this is a highly destructive material that tends to dissolve or permeate many surrounding materials. Therefore the material properties of KOH storage need improvement such as lighter in weight; cost; non-conductive properties and also, need to be strong to resist higher pressures of gas. A second area for future work regarding the use of electrolyte is to design a system to maintain the level of the electrolyte in the cell and its concentration.

5.3) Electrode

In the quest to find the best electrode in terms of durability, cost effectiveness and conductivity to get the best overall performance; stainless steel was established to be the most fit electrode material for this purpose. There are many other electrode materials available, for example silver, copper, gold and aluminium [102]that have higher conductivity and surface area than stainless steel; however stainless steel has been found to offer long life, as well as being less expensive and having a higher resistance to oxidation. Hence more research is required to find

others materials which combine all the positive properties identified with stainless steel for hydrogen generation.

5.4) Device design

The design of the first generation cell design was derived from Stephen Barrie Chambers' [51] patent; his result from testing his device was 46% efficiency for hydrogen production with a stainless steel electrode and with a nanostructured electrode 73% efficiency was last reported in 2008 as a common industrial and commercial electrolysers [38] [103]. However, after 2008 most of the research on electrolysis of hydrogen production is derived from PEM fuel cell technology. The hydrogen production efficiency improvement stopped due to the problems in PEM fuel cell technology (as discussed in section 1.6) such as controlled pore size of electrode, membrane permeability, life and stability. The work in this thesis has demonstrated substantial improvements in these figures due to using conventional electrode and method in the new system design by keeping the idea of free nature (let nature move freely in the system). Hence problems from the conventional production of hydrogen being reduced and managed achieve subnational improvement. [104] [105]

In this research an On-Demand Hydrogen Generation cell-3 achieved a 95% hydrogen generation coulombic efficiency, which is about a 49% efficiency improvement as compared to the stainless steel electrode [51], and was 22% better than the nano structured electrode [38]. The achievement here of such high efficiencies paves the way for more research in the areas of space management, electrode surface structure and flow control (based on the application requirement).

The immediate need for more research is to develop device controls that combine the hydrogen generator to its required application. For example, introducing hydrogen into internal combustion engines (cars, automotive), where the engine control unit (ECU) is required to control safe use of and balance hydrogen production and injection in the engine. To ensure the expected safety and control properties, for example in the alternator and battery safety a number of factors need to be studied in future work. These include limiting the hydrogen generation into car to the use of excess current and not run-down the battery. So a system to regulate this is required. In addition leak detection of hydrogen and controlled shutdown if the leak is detected, is a further necessary refinement.

Also the control production and injection of hydrogen depending on demand (speed of vehicle and load) is a problem for future ECU. Further the level of electrolyte and its concentration needs to be regulated and this will need to include a water top-up system that is intelligently controlled.

However if all the above could be achieved, then on demand hydrogen generation could be a low cost and effective way of reducing carbon emission and using less carbon based fuels (either petroleum based or bio-based).

Bibliography

[1] D-Y. Wu, R. D. Mathews, E. T. Popova, and C. Mock, "The Texas Project, Part 4 - Final Results: Emissions and Fuel Economy of CNG and LPG Conversions of Light-Duty Vehicles," *SAE Technical Paper*, vol. 982446, 1998, doi:10.4271/982446.

[2] Ryoichi Komiyama and Yasumasa Fujii, "Analysis of energy saving and environmental characteristics of electric vehicles in regionally disaggregated world energy model," *Electrical Engineering in Japan*, vol. 186, no. 4, pp. 20–36, March 2014, DOI: 10.1002/eej.22373.

[3] Stanislav Beroun and Jorge Martins, "The development of gas (CNG, LPG and H2) engines for buses and trucks and their emission and cycle variability characteristics," *SAE Technical Papers*, vol. 1, 2001, 0144.

[4] Ersus auto gas equipments. (2014, Fab) Versusgas. [Online]. http://www.versusgas.com/

[5] Lpgmycar. (2014, March) Lpg my car. [Online]. http://www.lpgmycar.co.uk/aboutourlpg/how-does-lpg-work/

[6] David E. Bennett, Devlin A. Hunt, and Ronald H. Roche, "Fuel injector valve for liquified fuel," U.S. Patent 5,823,446, Oct 20, 1998.

[7] Zhan-Yi Wu, Horng-Wen Wu, and Cheng-Han Hung, "Applying Taguchi method to combustion characteristics and optimal factors determination in diesel/biodiesel engines with port-injecting LPG," *Fuel*, vol. 117, pp. 8-14, Jan 2014.

[8] Richard Stone, *Introduction to internal combustion engines*, 4th ed. United Kingdom: Palgrave Macmillan, 2012, ISBN:9780230576636.

[9] S. R. Ovshinsky, M. A. Fetcenko, and J. Ross, "A nickel metal hydride battery for electric vehicles," *Science*, vol. 260, no. 5105, pp. 176-181, 1993.

[10] George R Parsons, Michael K. Hidrue, Willett Kempton, and Meryl P. Gardner, "Willingness to pay for vehicle-to-grid (V2G) electric vehicles and their contract terms," *Energy Economics*, vol. 42, pp. 313-324, March 2014.

[11] Z. Q. Zhu and David Howe, "Electrical machines and drives for electric, hybrid, and fuel cell vehicles," *Proceedings of the IEEE*, vol. 95, no. 4, pp. 746-765, 2007.

[12] Farouk Odeim, Jürgen Roes, Lars Wülbeck, and Angelika Heinzel, "Power management optimization of fuel cell/battery hybrid vehicles with experimental validation," *Journal of Power Sources*, vol. 252, pp.

333-343, April 2014.

[13] Albert Stwertka, *A guide to the elements*. New York: Oxford University Press, 1996, ISBN: 0195080831.

[14] Pradyot Patnaik, *A comprehensive guide to the hazardous properties of chemical substances*, 3rd ed. USA: John Wiley & sons Inc., 2007, ISBN: 0471714585.

[15] Peter Anstey and Michael Hunter, "On the boyles," *A newsletter of work in progress on Robert Boyle (1627-91)*, vol. 5, March 2002, ISSN 1465-4970.

[16] Isaac Asimov, *A short history of chemistry*. London, UK: Greenwood Press, 1972, ISBN:0435550608.

[17] Chris Acott, "The diving "Law-ers": A brief resume of their lives," *South Pacific Underwater Medicine Society*, vol. 29, no. 1, pp. 39-42, October 1999, ISSN 0813-1988.

[18] Cavendish Henry, *The scientific papers of the honourable henry cavendish, F. R. S*, illustrated, reprint ed., James Clerk Maxwell, Sir Edward Thorpe, and Sir Joseph Larmor, Eds. Cambridge, UK: Cambridge University Press, February 2011, vol. 2, ISBN: 9781108018210.

[19] Antoine Laurent Lavoisier, *Elements of chemistry*. Mineola, NY, USA: Dover Publications, 1984, ISBN: 0486646246.

[20] Frank C. Walsh, *A first course in electrochemical engineering*. Portsmouth, UK: Electrochemical Consultancy, 1993, ISBN:0951730711.

[21] John Petrovic and George Thomas, "Reaction of aluminum with water to produce hydrogen," U.S. Department of Energy, DOE Version.1, 2008.

[22] David W. Oxtoby and Norman H. Nachtrieb , *Principles of modern chemistry*, 5th ed., H.Pat Gillis and Johathan Shui Rutland, Eds. California, USA: Brooks Cole, 2002, ISBN: 0030353734.

[23] Julius Scherze and A.J. Gruia, *Hydrocracking science and technology*, 1st ed. New York, USA: CRC Press, 1996, ISBN: 0824797604.

[24] Matthias Block, "Hydrogen as tracer gas for leak detection," in *16th WCNDT 2004. Sensistor Technologies.*, Montreal, Canada:, 2004.

[25] (2008, Aug.) Long Course Runs. [Online]. http://www.scta-bni.org/Bonneville/SpeedWeek_08/down_22.htm

[26] OHIO State University. (2008, Aug.) Buckeye bullet. [Online]. http://engineering.osu.edu/studentorgs/buckeye-bullet

[27] Ballard Power Systems Inc. (2010, March) Ballard. [Online]. http://www.ballard.com/about-ballard/fuel-cell-education-resources/how-a-fuel-cell-works.aspx

[28] Ram B. Gupta, *Hydrogen fuel : production, transport, and storage*. Boca Raton: CRC Press, 2009, ISBN: 9781420045758.

[29] Peter Whoriskey, "The Hydrogen Car Gets Its Fuel Back," *Washington Post,* October 17, 2009.

[30] Ford motor company, "Ford motor company business plan," http://online.wsj.com/public/resources/documents/Ford_Motor_Company_Business_Plan122008.pdf, December 2, 2008.

[31] Lyle Dennis, "Nissan swears off hydrogen and will only build electric cars," *All Cars Electric*, February 2009.

[32] F. Gutiérrez-Martín, J.M. García-De María , A. Baïri, and N. Laraqi, "Management strategies for surplus electricity loads using electrolytic hydrogen," *International journal of hydrogen energy*, vol. 34, no. 20, pp. 8468–8475, 2009.

[33] Approved by: Sunita Satyapal, "Well-to-wheels greenhouse gas emissions and petroleum use," DOE Hydrogen Program Record, 2009.

[34] Syed K. Raza, "On Demand Electrochemical Production of Hydrogen for Alternative Energy Applications," in *POGEE conferance*, Karachi, Pakistan, May, 2010.

[35] Edmond Amouyal, "Photochemical production of hydrogen and oxygen from water: A review and state of the art," *Solar Energy Materials and Solar Cells*, vol. 38, no. 1-4, pp. 249-276, 1995.

[36] Z.W. Tian and Y. Cao, "Photochemical and Photoelectrochemical Conversion and Storage of Solar Energy," in *Int. Conf. on Photochemical Conversion and Storage of Solar Energy, International Academic Publishers*, Beijing, 1993.

[37] Jean-Marie Lehn, "Photoinduced generation of hydrogen and oxygen from water," *Photochemical Conversion and Storage of Solar Energy*, pp. 161-200, 1981.

[38] John Turner et al., "Renewable hydrogen production," *INTERNATIONAL JOURNAL OF ENERGY*

RESEARCH, vol. 32, no. 5, pp. 379 - 407, 2008, ISSN 0363-907X.

[39] M. Conte, A. Iacobazzi, M. Ronchetti, and R. Vellone, "Hydrogen economy for a sustainable development: state-of-the-art and technological perspectives," *Journal of Power Sources*, vol. 100, no. 1-2, pp. 171-187, Nov. 2001.

[40] Stanislaw P. Wach, Michael B. Leven, and Prematilaka W. Kalubowila, "Electronic conductor and a method of manufacturing it," Patent : 4,549,043, October 22, 1985.

[41] C.M. Rangel, V.R. Fernandes, Y. Slavkov, and L. Bozukov, "Integrating hydrogen generation and storage in a novel compact electrochemical system based on metal hydrides," *Journal of Power Sources*, vol. 181, no. 2, pp. 382-385, July 2008.

[42] C. R. Hammond, *The elements, in handbook of chemistry and physics*, 81st ed., David R. Lide, Ed.: CRC press, 2000, ISBN: 0849304814.

[43] John T. Arms, William D. K. Clark, Dale E. Hall, and Vance R. Shepard, "Electrolytic production of hydrogen," Patent: 4,737,249, April 12, 1996.

[44] Martin Klein, "Electrolytic hydrogen storage and generation," Patent: 5,540,831, July 30, 1996.

[45] J. O'M Bockris and Amulya K. N Reddy, *Modern aspects of electrochemistry*, 2nd ed. London UK: Plenum Pub. Corp, 1998, ISBN:0306455544.

[46] George Boxer, *Work out engineering thermodynamics*.: Macmillan Education Ltd., 1987, ISBN 0333436644.

[47] Louis A. Bloomfield, *How things work : the physics of everyday life*, 3rd ed. Virginia: John Wiley & Sons, Inc., 2006, ISBN:047146886X.

[48] Ira. N. Levine, *Physical chemistry*.: McGraw Hill: University of Brooklyn, 1978, ISBN:007037418X.

[49] Louis A. Bloomfield, *How things work: the physics of everyday life*, 4th ed. Virginia: John Wiley & Sons, Inc., 2010, ISBN: 0470223995.

[50] Daniel V. Schroeder, *An introduction to thermal physics*, 1st ed.: Addison Wesley, 2000, ISBN:0201380277.

[51] Stephen Barrie Chambers, "Apparatus for producing orthohydrogen and/or parahydrogen," US6126794, Oct 3, 2000.

[52] Stanley A. Meyer , "Method for the production of a fuel gas," US4936961 A, Jun 26, 1990.

[53] Mark. (2014, March) HHO Generator Design.What do yoy think. [Online]. http://www.hhoforums.com/showthread.php?7279-HHO-Generator-Design.What-do-yoy-think

[54] Wu Xu and Keith Scott, "The effects of ionomer content on PEM water electrolyser membrane electrode assembly performance," *International Journal of Hydrogen Energy*, vol. 35, no. 21, pp. 12029–12037, November 2010.

[55] K.B. Kokoh et al., "Efficient multi-metallic anode catalysts in a PEM water electrolyzer," *International Journal of Hydrogen Energy*, vol. 39, no. 5, pp. 1924–1931, Feb 2014.

[56] Joshua M. Spurgeona and Nathan S. Lewis, "Proton exchange membrane electrolysis sustained by water vapor," *Energy & Environmental Science*, vol. 4, no. 8, pp. 2993-2998, Feb 2011.

[57] F. Arbabi et al., "Feasibility study of using microfluidic platforms for visualizing bubble flows in electrolyzer gas diffusion layers," *Journal of Power Sources*, vol. 258, pp. 142-149, July 2014.

[58] Marcelo Carmo, David L. Fritz, Jürgen Mergel, and Detlef Stolten, "A comprehensive review on PEM water electrolysis," *International Journal of Hydrogen Energy*, vol. 38, no. 12, pp. 4901–4934, April 2013.

[59] L. J. Nuttall, "Conceptual design of large scale water electrolysis plant using solid polymer electrolyte techonology.," *Internation Jurnal of Hydrogen Energy*, vol. 2, pp. 395-403, 1977.

[60] S. Litster and G. McLean, "PEM fuel cell electrodes," *Journal of power sources*, vol. 130, no. 1, pp. 61 - 76, 2004, ISSN 0378-7753.

[61] M.S. Wilson, J.A. Valerio, and S. Gottesfeld, "Low platinum loading electrodes for polymer electrolyte fuel cells fabricated using thermoplastic ionomers," *Electrochimica Acta*, vol. 40, no. 3, pp. 355–363, Feb 1995.

[62] G.S. Kumar, M. Raja, and S. Parthasarathy, "High performance electrodes with very low platinum loading for polymer electrolyte fuel cells," *Electrochimica Acta*, vol. 40, pp. 285–290, 1995.

[63] Mahlon S. Wilson, "Membrane catalyst layer for fuel cells," 5234777, Oct 08, 1993.

[64] "Bulk and contact resistances of gas diffusion layers in proton exchange membrane fuel cells," *Journal of Power Sources*, vol. 256, pp. 449-456, June 2014.

[65] Aimy Bazylak, "Oxygen bubble nucleation modeling in a PEM electrolyzer electrode.," *In 225th ECS Meeting*, pp. 11-15, May 2014.

[66] Sundar Pethaiah Sethu, Sasikumar Gangadharan, Siew Hwa Chan, and Ulrich Stimming, "Development of a novel cost effective methanol electrolyzer stack with Pt-catalyzed membrane," *Journal of Power Sources*, vol. 254, pp. 161-167, May 2014.

[67] P Milleta et al., "Electrochemical performances of PEM water electrolysis cells and perspectives.," *International Journal of Hydrogen Energy*, vol. 36, no. 6, pp. 4134–4142, March 2011.

[68] Guoying Chen, Chad C. Waraksa, Hungoo Cho, Digby D. Macdonald, and Thomas E. Mallouk, "EIS studies of porous oxygen electrodes with discrete I. impedance of oxide catalyst supports," *Journal of The Electrochemical Society*, vol. 150, no. 9, pp. E423-E428, 2003.

[69] S.J. Lee et al., "Effects of Nafion impregnation on performances of PEMFC electrodes," *Electrochimica Acta*, vol. 43, no. 24, pp. 3693–3701, Aug 1998.

[70] Khalfan Abdulla Said, Ibrahim Saana Amiinu, Haining Zhang, and Mu Pan, "Functionalized Polysulfones as an Alternative Material to Improve Proton Conductivity at Low Relative Humidity Fuel Cell Applications," *Chemistry and Materials Research*, vol. 6, no. 2, pp. 19-29, 2014.

[71] Oliver J. Murphy, G.Duncan Hitchens, and David J. Manko, "High power density proton-exchange membrane fuel cells," *Jurnal of Power Sources*, vol. 47, no. 3, pp. 353–368, Jan 1994.

[72] E.A. Ticianelli, C.R. Derouin, A. Redondo, and S. Srinivasan, "Methods to advance technology of proton exchange membrane fuel cells," *Journal of the Electrochemical Society*, vol. 135, no. 9, pp. 2209-2214, Sep 1998.

[73] Kai Zeng and Dongke Zhang, "Recent progress in alkaline water electrolysis for hydrogen production and applications," *Progress in Energy and Combustion Science*, vol. 36, no. 3, pp. 307-326, 2010, ISSN 0360-1285.

[74] A.T. Marshall, S. Sunde, M. Tsypkin, and R. Tunold, "Performance of a PEM water electrolysis cell using IrxRuyTazO2 electrocatalysts for the oxygen evolution electrode," *International Journal of Hydrogen Energy*, vol. 32, no. 13, pp. 2320–2324, Sep 2007.

[75] Miguel Lopez-Haro et al., "Atomic-scale structure and composition of Pt3Co/C nanocrystallites during real PEMFC operation: A STEM–EELS study," *Applied Catalysis B: Environmental*, vol. 152-153, pp. 300–308, Jun 2014.

[76] Faraz Arbabi et al., "Visualizing bubble flows in electrolyzer GDLs Using microfluidic platforms," *ECS Transactions*, vol. 58, no. 1, pp. 907-918, 2013.

[77] F. Baron, "European space agency fuel cell activities," *Journal of power sources* , vol. 29, no. 1, pp. 207-221, 1990.

[78] D. Lj. Stojić, T. D. Grozdić, B. Umićević, and A. D. Maksić, "A comparison of alkaline and proton exchange membrane electrolyzers," *Russian journal of physical chemistry*, vol. 82, no. 11, pp. 1958-1960, 2008, ISSN 0036-0244.

[79] Morris Hein and Leo R. Best, *College chemistry*. California, USA: Dickenson Publishing Company, 1976, ISBN:0822101629.

[80] E Juzeliunas, "ChargeTransfer at Electrochemical Interfaces "Two Hundred Years of Electrlysis"," *Electrochimica Acta*, vol. 51, no. 27, pp. 5997 - 5998, 2006, ISSN 0013-4686.

[81] Stephen Barrie Chambers, "Apparatus for producing orthohydrogen and/or parahydrogen," US Patent 6,126,794, October 3, 2000.

[82] J BARGON, J KANDELS, and K WOELK, "Orthohydrogen and parahydrogen including nuclear-spin polarization," vol. 180, pp. 65-93, 1993, SICI:09429352.

[83] K. Walasek and A. L. Kuzemskii, "Theory of nuclear spin-lattice relaxation in solid orthohydrogen," *Theoretical and Mathematical Physics*, vol. 4, no. 3, pp. 383-393, 1970.

[84] Jin-Cherng Shyu and Cheng-Ling Huang, "Characterization of bubble formation in microfluidic fuel cells employing hydrogen peroxide," *Journal of Power Sources*, vol. 196, no. 6, pp. 3233 - 3238, 2011, ISSN 0378-7753.

[85] Ying Li, Yan-Yan Song, Chen Yang, and Xing-Hua Xia, "Hydrogen bubble dynamic template synthesis of porous gold for nonenzymatic electrochemical detection of glucose," *Electrochemistry Communications*, vol. 9, no. 5, pp. 981-988, 2007.

[86] Siemens. (2011) Siemens NX Software. [Online]. http://www.plm.automation.siemens.com/en_us/about_us/index.shtml

[87] Syed K. Raza, "On Demand Electrochemical Production of Hydrogen for Alternative Energy Applications," , Karachi, 2010.

[88] C. Brussieux, Ph. Viers, H. Roustan, and M. Rakib, "Controlled electrochemical gas bubble release from electrodes entirely and partially covered with hydrophobic materials," *Electrochimica Acta*, vol. 56, no. 20, pp. 7194-7201, 2011.

[89] Robert B. Dopp, "Hydrogen generation via water electrolysis using highly efficient nanometal electrodes," *Quantum Sphere, Inc*, 2007.

[90] Bockris, J. O'M., *Modern Aspects of Electrochemistry*, 2nd ed., J. O'M. Bockris, Ed. London UK: Butter Worrths, 1959.

[91] Daniel M. Zeitler et al., "The effects of cochlear implant electrode deactivation on speech perception and in predicting device failure.," *Otology & Neurotology*, vol. 30, no. 1, pp. 7-13, Jan 2009.

[92] Cynthia G. Zoski, Ed., *Handbook of Electrochemistry*, 1st ed.: Elsevier, Dec 2006, ISBN:9780444519580.

[93] Pingyu Wan and X. Jin Yang, "Electrolysis of water and common salt solutions," *ChemSusChem*, vol. 5, no. 8, pp. 1381-1382, August 2012.

[94] Edward Furimskya and Franklin E. Massoth, "Deactivation of hydroprocessing catalysts," *Elsevier B.V*, vol. 52, no. 4, pp. 381 - 495, 1999, ISSN 0920-5861.

[95] T. Bewer, T. Beckmann, H. Dohle, J. Mergel, and D. Stolten, "Novel method for investigation of two-phase flow in liquid feed direct methanol fuel cells using an aqueous H2O2 solution," *Journal of Power Sources*, vol. 125, no. 1, pp. 1-9, 2004.

[96] David L. Trimma* & Z. Ilsen Önsanb , "Onboard fuel conversion for hydrogen-fuel-cell-driven vehicles.," *Catalysis Reviews*, vol. 43, no. 1-2, pp. 31-84, 2001.

[97] L. M. DAS, "Hydrogen-oxygen reaction mechanism and its implication to hydrogen engine combustion," *International Journal of Hydrogen Energy*, vol. 21, no. 8, pp. 703 - 715, 1996, ISSN 0360-3199.

[98] Viatcheslav Osipov et al., "Explosion hazard from a propellant-tank breach in liquid hydrogen-oxygen rockets," *Journal of Spacecraft and Rockets*, vol. 50, no. 4, pp. 860-871, August 2013.

[99] C. E. Thomas, "Direct hydrogen fueled proton exchange membrane fuel cell system for transportation applications: Hydrogen vehicle safety report," Ford Motor Co., Dearborn, MI (United States); Argonne National Lab., IL (United States), DOE/CE/50389-502, 1997.

[100] Thomas. (2001) Hydrogen vehicle safety report. [Online]. http://www.cleancaroptions.com/html/hydrogen_safety.html#DTI-FordSafetyreport

[101] M.R. Swain, "Fuel leak simulation," *In Proceedings of the 2001 US DOE Hydrogen Program Review*, pp. 17-19, 2001.

[102] Yoon-Seok Choi , Yun-Ha Yoo, Jung-Gu Kim, and Sang-Ho Kim, "A comparison of the corrosion resistance of Cu–Ni–stainless steel multilayers used for EMI shielding," *Surface and Coatings Technology*, vol. 201, no. 6, pp. 3775-3782, Dec 2006.

[103] Kaveh Mazloomi, Nasri b. Sulaiman, and Hossein Moayedi, "Electrical Efficiency of Electrolytic Hydrogen Production," *International Journal of Electrochemical Science*, vol. 7, pp. 3314-3326, April 2012.

[104] Robert B. Dopp, "High-rate and high efficiency 3D water electrolysis whitepaper," DoppStein Enterprises, Marietta, GA, 770-649-1933, 2011.

[105] Bjørnar Kruse, Sondre Grinna, and Cato Buch, "hydrogen—status and possibilities," Bellona's co-operation , B7 2002.

[106] Y. A. Cengel and M. A. Boles, *Thermodynamics : An engineering approach*, 2nd ed. USA: McGraw-Hill, Inc., 1994, ISBN:007113249X.

[107] Wikipedia. (2009, October) Wikipedia®. [Online]. http://en.wikipedia.org/wiki/Hydrogen_vehicle

[108] William Leffler, *Petroleum refining in nontechnical language, fourth Edition*.: PennWell Corp., Oct. 2008, ISBN: 1593701586. [Online]. http://en.wikipedia.org/wiki/Hydrogen

[109] Liviu Oniciu, *Fuel cells*. Tunbridge Wells, KENT: Abacus Press, 1976, ISBN:0856260142.

[110] Wikipedia®. (2009, Oct.) Wikipedia. [Online]. http://en.wikipedia.org/wiki/Antoine_Lavoisier

[111] Wikipedia®. (2009, October) Wikipedia. [Online]. http://en.wikipedia.org/wiki/Paracelsus

[112] Wikipedia®. (2009, October) Wikipedia. [Online]. http://en.wikipedia.org/wiki/Henry_Cavendish

[113] K. McGrath. (2011) High concentration direct methanol fuel cell using QI-Nano Pd., 714-545-6266. [Online]. http://www.qsinano.com/white_papers/2008_07_03_dmfc.pdf

[114] M.S. Ismail, D.B. Ingham, L. Ma, and M. Pourkashanian, "The contact resistance between gas diffusion

layers and bipolar plates as they are assembled in proton exchange membrane fuel cells," *Renewable Energy*, vol. 52, pp. 40-45, 2013.

[115] N. D. Brinkman, E. E. Ecklund, and R. J. Nichols, *Fuel Methanol : A Decade of Progress*. Warrendale, PA: Society of Automotive Engineers, Inc, 1990, ISBN:1560910119.

[116] Julius Scherzer and A. J. Gruia, *Hydrocracking science and technology*. New York: Marcel Dekker, 1996, ISBN: 0824797604.

[117] Yang-Liu Zhou, Xin-Sheng Zhang, Ying-Chun Dai, and Wei-Kang Yuan, "Studies on chemical activators for electrode I: Electrochemical activation of deactivating cathode for oxalic acid reduction," *Chemical engineering science*, vol. 58, no. 3-6, pp. 1021 – 1027, March 2003.

[118] A. D. McNaught and A. Wilkinson , *Compendium of chemical terminology: IUPAC recommendations*, 2nd ed.: Wiley-Blackwell, 1997, ISBN: 0865426848.

Appendix – 1

1. Carl Zeiss Axioskop 2 MAT optical microscope fitted with a camera Axiocam MR-5

2. SEM Operation Guide

Appendix – 2

Data Sheets

Appendix-2 present current research electrochemical hydrogen generator data sheets, which represent the raw data and calculated data. Data represent flow result, non-flow results, pressure, PH, amps, volt, temperature and efficiency. It also present previous research data.

Appendix-2, Page-1: Data sheet represent displacement of water (Δh) values

Appendix-2, Page-2: Data sheet represent calculated result of all hydrogen generator cell, where theoretical production of hydrogen (VSTP), experimental pressure (Pexp), experimental production of hydrogen (VEXP), and efficiency of hydrogen production (%).

Appendix-2, Page-3: Data sheet represent hydrogen production cell-3 calculated results.

Appendix-2, Page-4: Data sheet represent hydrogen production pressure results.

Appendix-2, Page-5: Donghao Ye et al provide comprehensive comparison between carbon cloth and carbon paper.

Donghao Ye et al provide comprehensive comparison between carbon cloth and carbon paper.

Table 1.

Compression of carbon cloth and carbon paper GDL materials.

Pressure (MPa)	Thickness (t_{GDL}, μm) ±10 μm	
	Carbon paper initial thickness: 370	Carbon cloth initial thickness: 397
Initial compression	301	320
0.27	281	298
0.38	267	267
0.54	261	247
0.8	256	241
1.08	248	234
1.6	239	220
2.16	229	211

Table 2.

Resistivities of catalyst layer and GDL materials.

Material	ρ_{bulk} (mΩ cm)	$\rho_{contact}$ (mΩ cm^2)
Catalyst layer	90	50
Carbon cloth GDL	10	25
Carbon paper GDL	6	13